

1-1-2007

Complexation and electrode effects on the electrochemical behavior of the cerium(IV)/cerium(III) redox couple

Sandra Elias Elkouz
University of Nevada, Las Vegas

Follow this and additional works at: <https://digitalscholarship.unlv.edu/rtds>

Repository Citation

Elkouz, Sandra Elias, "Complexation and electrode effects on the electrochemical behavior of the cerium(IV)/cerium(III) redox couple" (2007). *UNLV Retrospective Theses & Dissertations*. 2101.
<http://dx.doi.org/10.25669/06zo-41dn>

This Thesis is protected by copyright and/or related rights. It has been brought to you by Digital Scholarship@UNLV with permission from the rights-holder(s). You are free to use this Thesis in any way that is permitted by the copyright and related rights legislation that applies to your use. For other uses you need to obtain permission from the rights-holder(s) directly, unless additional rights are indicated by a Creative Commons license in the record and/or on the work itself.

This Thesis has been accepted for inclusion in UNLV Retrospective Theses & Dissertations by an authorized administrator of Digital Scholarship@UNLV. For more information, please contact digitalscholarship@unlv.edu.

COMPLEXATION AND ELECTRODE EFFECTS ON
THE ELECTROCHEMICAL BEHAVIOR OF THE
CERIUM(IV)/CERIUM(III) REDOX COUPLE

by

Sandra Elias Elkouz

Associate of Science
Community College of Southern Nevada
2001

Bachelor of Science
University of Nevada, Las Vegas
2004

A thesis submitted in partial fulfillment
of the requirements for the

Master of Science Degree in Chemistry
Department of Chemistry
College of Sciences

Graduate College
University of Nevada, Las Vegas
May 2007

UMI Number: 1443749

INFORMATION TO USERS

The quality of this reproduction is dependent upon the quality of the copy submitted. Broken or indistinct print, colored or poor quality illustrations and photographs, print bleed-through, substandard margins, and improper alignment can adversely affect reproduction.

In the unlikely event that the author did not send a complete manuscript and there are missing pages, these will be noted. Also, if unauthorized copyright material had to be removed, a note will indicate the deletion.

UMI[®]

UMI Microform 1443749

Copyright 2007 by ProQuest Information and Learning Company.

All rights reserved. This microform edition is protected against unauthorized copying under Title 17, United States Code.

ProQuest Information and Learning Company
300 North Zeeb Road
P.O. Box 1346
Ann Arbor, MI 48106-1346



Thesis Approval
The Graduate College
University of Nevada, Las Vegas

April 6, 2007

The Thesis prepared by

Sandra Elias Elkouz

Entitled

Complexation and Electrode Effects on the Electrochemical Behavior
of the Cerium(IV)/Cerium(III) Redox Couple

is approved in partial fulfillment of the requirements for the degree of

Master of Science in Chemistry

Examination Committee Chair

Dean of the Graduate College

Examination Committee Member

Examination Committee Member

Graduate College Faculty Representative

ABSTRACT

**Complexation and Electrode Effects on the Electrochemical
Behavior of the Cerium(IV)/Cerium(III)
Redox Couple**

by

Sandra Elias Elkouz

Dr. David W. Hatchett, Examination Committee Chair
Associate Professor of Chemistry
University of Nevada, Las Vegas

The electrochemistry of the Ce(IV)/Ce(III) redox couple was investigated as a function of working electrode composition and solution environment. Optimum redox couple resolution in aqueous sulfuric acid was achieved at an acid concentration of 0.1 M. A decline in redox couple resolution and reversibility was observed as acid concentration was increased to 2.0 M. The influence of pH was illustrated using sulfate solutions of increasing pH and constant ionic strength. Results indicated that a pH greater than 2 was detrimental to redox couple resolution. The glassy carbon electrode provided the widest potential window and was least affected by changes in pH. Studies were conducted in aqueous NTA, citrate, and EDTA, but redox couple resolution was successful only at the Pt electrode in EDTA. Complexation with EDTA resolved cerium electrochemistry from background currents by shifting the redox couple to less positive potentials, and allowed its observation across a wide pH range.

TABLE OF CONTENTS

ABSTRACT.....	iii
LIST OF FIGURES	v
LIST OF TABLES.....	vi
ACKNOWLEDGEMENTS.....	vii
CHAPTER 1 INTRODUCTION.....	1
1.1 The Nuclear Fuel Cycle	1
1.2 Separation of Curium and Americium.....	3
1.3 The Lanthanide Elements	8
1.4 Present Work.....	20
CHAPTER 2 BACKGROUND.....	23
2.1 Electrochemical Theory.....	23
2.2 Experimental Considerations.....	29
CHAPTER 3 MATERIALS AND METHODS	34
3.1 Equipment and Experimental Setup.....	34
3.2 Solution Preparation and Experimental Procedures	37
CHAPTER 4 RESULTS AND DISCUSSION.....	41
4.1 Acid Study	41
4.2 pH Study	61
4.3 Complexation Study.....	73
CHAPTER 5 CONCLUSIONS	98
REFERENCES	103
VITA.....	110

LIST OF FIGURES

Figure 1.1	Reduction Reactions of Am(IV) and Cm(IV)	5
Figure 1.2	The Ce(IV)/Ce(III) Redox Couple	10
Figure 1.3	The Oxidation of Water	11
Figure 1.4	Proposed Ce(IV)/Sulfate Complexation at Low pH.....	12
Figure 1.5	Reduction Reactions of Ce(IV) in Perchloric Acid.....	17
Figure 2.1	The Triangular Potential Waveform Used in Cyclic Voltammetry.....	27
Figure 2.2	Three-Electrode Setup for a CV Experiment	28
Figure 2.3	Experimental Difficulties in Ce(IV)/Ce(III) Investigations	31
Figure 4.1	CV obtained for Ce at the Au Electrode in 0.1, 1.0, and 2.0 M H ₂ SO ₄	43
Figure 4.2	Peak Ce (IV) Reduction Current vs. Scan Rate ^{1/2} at the Au Electrode	46
Figure 4.3	Peak Ce(III) Oxidation Current vs. Scan Rate ^{1/2} at the Au Electrode.....	47
Figure 4.4	CV obtained for Ce at the Pt Electrode in 0.1, 1.0, and 2.0 M H ₂ SO ₄	49
Figure 4.5	Peak Ce(IV) Reduction Current vs. Scan Rate ^{1/2} at the Pt Electrode.....	52
Figure 4.6	Peak Ce(III) Oxidation Current vs. Scan Rate ^{1/2} at the Pt Electrode	52
Figure 4.7	CV obtained for Ce at the GC Electrode in 0.1, 1.0, and 2.0 M H ₂ SO ₄	54
Figure 4.8	Peak Ce(IV) Reduction Current vs. Scan Rate ^{1/2} at the GC Electrode.....	56
Figure 4.9	Peak Ce(III) Oxidation Current vs. Scan Rate ^{1/2} at the GC Electrode	56
Figure 4.10	CV obtained for Ce at the GC, Au, and Pt Electrodes in 0.1 M HNO ₃	59
Figure 4.11	CV obtained for Ce at the GC, Au, and Pt Electrodes in 0.1 M K ₂ SO ₄	63
Figure 4.12	CV obtained for Ce at the Au Electrode at pH values of 1.0, 3.4, 4.7	65
Figure 4.13	CV obtained for Ce at the Pt Electrode at pH values of 1.0, 3.4, 4.7.....	66
Figure 4.14	CV obtained for Ce at the GC Electrode at pH values of 1.0, 3.4, 4.7.....	68
Figure 4.15	Speciation of Sulfuric Acid as a Function of pH.....	71
Figure 4.16	Structures of EDTA, NTA, and Citric Acid	73
Figure 4.17	CV of the Ce/NTA Complexation Study at Au (pH 2, 4, 6, 8, 10)	76
Figure 4.18	CV of the Ce/NTA Complexation Study at GC (pH 2, 4, 6, 8, 10).....	77
Figure 4.19	CV of the Ce/NTA Complexation Study at Pt (pH 2, 4, 6, 8, 10).....	79
Figure 4.20	Speciation of NTA as a Function of pH	80
Figure 4.21	CV of the Ce/Citrate Complexation Study at Pt (pH 2, 4)	81
Figure 4.22	CV of the Ce/Citrate Complexation Study at Au (pH 2, 4, 8, 10, 12).....	83
Figure 4.23	CV of the Ce/Citrate Complexation Study at GC (pH 2, 4, 6, 8, 10, 12)...	84
Figure 4.24	CV of the Ce/EDTA Complexation Study at GC (pH 2, 4, 6, 8, 10, 12) ..	86
Figure 4.25	CV of the Ce/EDTA Complexation Study at Pt (pH 2.5, 4, 6, 8, 10, 12) ..	87
Figure 4.26	CV at Pt of EDTA with Ce(III) concentrations of 2, 6, 10, 14, 24 mM.....	90
Figure 4.27	CV at Pt showing the Ce/EDTA system with increasing pH (2.5 to 3.0) ..	92
Figure 4.28	Speciation of EDTA as a Function of pH.....	93
Figure 4.29	CV of EDTA/Ce, EDTA/Sm, EDTA/Eu, EDTA/Ce/Sm/Eu at Pt.....	94

LIST OF TABLES

Table 4.1	Data Obtained at the Au Electrode for Ce in 0.1, 1.0, and 2.0 M H ₂ SO ₄	45
Table 4.2	Data Obtained at the Pt Electrode for Ce in 0.1, 1.0, and 2.0 M H ₂ SO ₄	50
Table 4.3	Data Obtained at the GC Electrode for Ce in 0.1, 1.0, and 2.0 M H ₂ SO ₄ ...	55
Table 4.4	Data Obtained at the GC, Au, and Pt Electrodes for Ce in 0.1 M HNO ₃	58
Table 4.5	Data Obtained at the Pt Electrode for Ce in EDTA at pH 2, 4, 6, 8, 10	88

ACKNOWLEDGEMENTS

To my advisor, Dr. David Hatchett for everything he has taught me, starting with my first day at UNLV in his Quantitative Analysis class. Thank you for all the encouragement, advice, and support you have given me all these years and for always letting me feel that you had faith in me and that I could succeed in whatever path I chose. Working for you has been a wonderful experience and a great pleasure. I am also very grateful to my committee members Dr. Spencer Steinberg, Dr. Kenneth Czerwinski, and Dr. Shawn Gerstenberger for their advice, and for all of the time they have invested in helping me to put this project together and to complete this thesis. My deepest thanks go to Dr. Vernon Hodge for all of his advice and encouragement, and for the many hours he spent reviewing this thesis in the middle of a very busy semester.

Funding for this project was made available through the U.S. Department of Energy Advanced Fuel Cycle Initiative/Transmutation Research Program (AFCI/TRP).

Many thanks go to my fellow Hatchett-Lab researchers John Kinyanjui, Nicole Millick, and Jade Morgan for their support, encouragement, and all the great times that we've had in the lab all these years. Your company every day is something that I will miss very much. To Ranmali Wijeratne and Sujanie Gamage, who have gone on to pursue their Ph.D. degrees, for their kindness, friendship, and warm welcome to me when I was a new graduate student just starting in Dr. Hatchett's lab. A great deal of credit and gratitude go to Patrick Houlihan, who worked as an undergraduate researcher on this

project, and is now pursuing a Ph.D. in Pharmacology. Thank you so much, Pat, for the long hours, your dedication, and all of the excellent work you did on this project. I appreciate it very much. To Carolyn Hatchett for all the good times in the stockroom, and the Harry Potter discussions that have yet to be resolved. To Mark Miyamoto and Debbie Masters in the chemistry office for helping me with every problem and question I've had ever since I came here. Their dedication and absolute kindness are a wonderful part of what makes this department such a great place to be.

I am very grateful to my parents Elias and Jacquie, my sister Natalie, and my brother Mark for their love and encouragement all of my life, and especially throughout this long college experience.

In these 6 years I've spent in the chemistry department, I've had the pleasure of spending every day with a wonderful group of people and I've had the best and most rewarding time of my life. This department has done a lot for me...and it will always mean a great deal to me. Do I really have to graduate?

CHAPTER 1

INTRODUCTION

1.1. The Nuclear Fuel Cycle

1.1.1. Constituents of Nuclear Waste

The “once-through” or “open” fuel cycle for the commercial processing and production of energy from nuclear fuels is one that does not implement any fuel recycling or reprocessing procedures. Thus, it is technically not a true cycle but rather a direct path from initial, unprocessed uranium ore to the waste remaining after energy has been extracted (National Research Council, 1996). Spent nuclear fuels are first stored at the reactor site for several years to “decay cool” or release heat from short-lived radionuclides, then stored temporarily in monitored retrievable storage (MRS) facilities where they await shipment to permanent geological repositories, such as the one proposed at the Yucca Mountain site in Nevada. One major concern in this scheme is the high-level radioactivity of this waste, since it contains long-lived radioisotopes including the major actinides uranium (U) and plutonium (Pu), as well as technetium 99 (^{99}Tc), iodine 129 (^{129}I), and the minor actinides neptunium (Np), curium (Cm) and americium (Am) (National Research Council, 1996). The technetium and iodine have been evaluated as more potentially harmful, due to their aqueous solubility and consequent propensity for travel through adjacent groundwaters. The actinides are water insoluble in

conditions favoring reduced species at storage sites, and are considered somewhat less of a projected health risk (National Research Council, 1996). There are, however, other considerations that render undesirable the disposal of these minor actinides as constituents of the bulk of spent waste.

1.1.2. The Need for Efficient Separation Methods

The need for long-term storage that will maintain its integrity over millennia is based on ~1% of the total waste that is composed of long-lived radionuclides such as the actinides (Schultz and Horwitz, 1994). If separation of this small fraction from the bulk waste could be accomplished, the remainder would be left more innocuous, therefore minimizing the amount of waste requiring high-level storage facilities. The separation and recycling of these long-lived species would also alleviate concerns regarding future tampering with wastes stored at permanent repositories. Finally, long-lived radionuclides such as the actinides are potential sources of energy remaining unreacted within the waste form (Broeders *et al.*, 1997). Proven processes such as UREX (URanium EXtraction) and PUREX (Plutonium URanium EXtraction) are currently in use at all fuel reprocessing facilities. The PUREX process accomplishes the separation of Pu and U through the dissolution of the waste matter in nitric acid and subsequent solvent extraction steps. The recovered Pu can then be used directly as a fuel source, and the U enriched prior to its use in fuel fabrication. A modification of the PUREX process allows for the separation and recovery of the minor actinides Np, Am, and Cm. These elements can then be subjected to transmutation through pyroprocessing. In this way, the amount of high-level components of the nuclear waste can be minimized, the unused fuel sources in the waste are salvaged, and the remaining radioactive elements are transmuted to

shorter-lived, albeit still high-level, radioactive species. The requirements for these procedures, however, are twofold: an effective recovery process, which is capable of removing all significant levels of the target elements; and an efficient method of separation, so that each separated species can be subjected to its appropriate transmutation protocol.

1.2. Separation of Curium and Americium

1.2.1. Chemical Separation Methods

The separation of Cm from Am, as well as the separation of these actinide elements from the rare earths, is a problem of significant interest and focus. As early as the 1960's, the separation of these elements was reported through the utilization of displacement complexing chromatography (DCC). This technique accomplished the separation of Cm and Am from the lanthanides, followed by the gram-scale recovery of Cm through the use of diethylenetriaminepentaacetic acid (DTPA) and nitrilotriacetic acid (NTA) as the respective eluent solutions (Wheelwright *et al.*, 1968). Subsequent efforts accomplished similar results with only one DTPA ion-exchange cycle, by employing faster flow rates in pressurized columns (Hale and Lowe, 1969). Although these techniques proved capable of yielding relatively large fractions of high purity Cm, they resulted in incomplete separations of Am and lanthanides. Chuveleva and coworkers refined the DCC approach through the introduction of separating ions, such as Cd^{2+} , to improve the separation of Cm and Am present at trace levels in samples. This method employed an eluent solution of NTA (pH 4); with sorption occurring on a cation exchange resin (Chuveleva *et al.*, 1999). Modifications of this technique yielded an

improvement in separation efficiency as a result of increased Cd^{2+} concentrations. The mode of introduction of both the actinides and the separating ions was also found to affect separation, with optimum results obtained through the initial sorption of Cd^{2+} onto the column resin, and the subsequent introduction of Cm and Am into the system (Chuveleva *et al.*, 1999b). In both studies, measurements of γ -activity were used to quantitate actinide content. Although these modified DCC techniques have shown the ability to achieve near-complete separation of Cm and Am, they are somewhat impractical for large-scale use.

1.2.2. Electrochemical Separation Methods

The fundamental electrochemical properties of chemical species result in innate differences in their oxidation/reduction behavior. These intrinsic energetic and kinetic characteristics can be manipulated to provide a powerful means of accomplishing their separation from one another in aqueous solution. By taking advantage of each species' distinct complexation and speciation behavior at a given set of solution conditions, these differences in redox potential can further be enhanced to achieve improved separations between particular species present in solution. In order to accomplish an electrochemical separation, it is first necessary to obtain a thorough understanding of the electrochemical behavior of the species whose separation is desired, as well the effects of their environment, which is comprised of the solution conditions in which they exist. Figure 1.1 shows the standard reduction potentials for Cm(IV) and Am(IV), referenced vs. the Standard Hydrogen Electrode (SHE) and tabulated in the 82nd Edition of the CRC Handbook of Chemistry and Physics (2001).

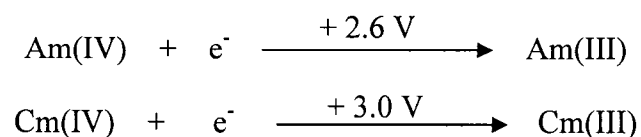


Figure 1.1. Reduction reactions of Am(IV) and Cm(IV).

It should be noted that, in aqueous solution, the existence of a divalent state of Am is not known (Penneman and Keenan, 1960; Aspinall, 2001). The trivalent oxidation state is prevalent in aqueous solution for Ac, the prototype for the series, as well as for the later actinides such as Am and Cm, with the exception of Lr (Aspinall, 2001). The trivalent cation is the only Cm species known to exist in either acidic or basic aqueous media (Penneman and Keenan, 1960). It is clear from the comparison of Am(IV) and Cm(IV) in Figure 1.1, that these two cations possess sufficiently different reduction potentials to render them candidates for separation by electrochemical means. It is of further interest to note that the *chemical* characteristics of these elements are quite analogous, and it is these similarities that render the pursuit of electrochemical separation techniques so valuable.

Experiments devised to exploit these inherent electrochemical dissimilarities, particularly with regard to the separation of actinide and lanthanide elements, can be found in the literature. In many instances, these separations have been accomplished by means of techniques such as cathodic stripping voltammetry (Bouissieres and Legoux, 1965; Maly, 1969). This method allows for the separation of metal ions in solution through the application of an initially positive potential to a mercury pool working electrode, followed by an incremental potential scan in the negative (cathodic) direction.

The ions are consequently reduced out of solution by amalgamation with the working electrode. Individual species can thus be separated by their intrinsic differences in reduction potential. The requirement, however, on which the success of this method depends, is a difference in reduction potentials sufficient to obtain efficient separation of the target species. Since the interaction of a species with its solution environment (*i.e.* hydrolysis, complexation, and precipitation) has a profound effect on the nature of its behavior at an electrode, these solution variables can be manipulated in order to optimize separation. For example, work by Bouissieres and Legoux (1965) demonstrated that the reduction of divalent rare earth elements such as Eu, Sm, and Yb from lithium citrate solutions at a mercury pool electrode was kinetically more favorable than the reduction of elements in the same group possessing, instead, a trivalent oxidation state. Since the trivalent actinide Cf was similar to the divalent lanthanides in its propensity to form mercury amalgams, an intermediate oxidation state of +2 was proposed in its reduction pathway from +3 to the metallic state. In a similar fashion, Maly (1969) was able to separate the heavier actinides (Cf to No) from their lighter counterparts via cathodic stripping in sodium acetate medium. The proposed rationalization for this effect was the influence of the acetate complexing environment on the stabilization of a divalent state for the late actinides. Thus, electrochemical methods not only provide the means of separating elements within a group that may possess very similar chemical properties, but they can often serve as powerful tools for probing reaction mechanisms as well. Problems with these stripping voltammetry efforts, however, included limited potential windows due to dissolution of the mercury electrode, generally poor separation between individual solution species, and very low recoveries of elements from the amalgams as a

result of irreversibility of the reduction process (David and Bouissieres, 1968; David *et al.*, 1990).

The usefulness of the technique of cyclic voltammetry, in conjunction with a controlled complexing environment, can be demonstrated by the work of Morris (2002), who investigated the electrochemical behavior of the uranyl redox couple using cyclic voltammetry. Electrochemical values such as the redox potential ($E_{1/2}$) of the $\text{UO}_2^{2+}/\text{UO}_2^+$ couple were evaluated, in addition to kinetic parameters such as the rate constant for electron transfer (k^0) and the electron transfer coefficient (α). The effect of complexation on the electrochemical behavior of the uranium species was also examined, with $E_{1/2}$ values of -0.396, -0.065, -0.169, -0.927, and -0.820 V obtained for the acetate, chloride, water, hydroxide, and carbonate complexes, respectively. Complexation was found to significantly alter the kinetic aspect of the electrode reaction as well, with the voltammetry for the uranyl/acetate system yielding an average redox peak separation of 73 mV, close to the Nernstian value of 59 mV for a single-electron transfer process. In contrast, the uranyl/carbonate system exhibited kinetically-limited electron transfer and asymmetric redox peaks, which revealed an inequality in the barriers to the oxidation and reduction reactions (Bard and Faulkner, 2001). As these studies clearly revealed, the manipulation of the complexing environment can afford a means of selectively tuning the behavior of electroactive solution species, allowing their potential separation by electrochemical methods.

1.3. The Lanthanide Elements

1.3.1. The Lanthanides and Actinides in Aqueous Solution

The lanthanides, or rare earth elements, make up the $4f$ block of the periodic table. These elements are, in many respects, similar to their $5f$ analogues, the actinides. Much similarity can be observed in the speciation and complexation behavior of the two groups in aqueous solution. Like Cm and Am, the lanthanides most commonly exist as trivalent cations in solution. Both the lanthanides and actinides are classified as hard Lewis acids, denoting their affinity for complex formation with hard Lewis bases such as ligands possessing O, F, or N lone pairs. Anions such as Cl^- , Br^- , I^- , NO_3^- , ClO_3^- , and ClO_4^- form only outer sphere complexes with the actinides and lanthanides, due to their inability to displace the hydration spheres about the metal cations. Inner sphere complexes are formed with F^- , SO_4^{2-} , IO_3^- , and CH_3COO^- (Aspinall, 2001). Coordination with multidentate ligands, such as the aminopolycarboxylates (*e.g.* EDTA^{4-} , DTPA^{5-}) results in the most stable solution complexes for both the actinides and lanthanides. Am and Ce, for example, possess stability constants with DTPA^{5-} of $10^{22.9}$ and $10^{20.33}$, respectively (Martell and Smith, 1974-1989). Hydrolysis is a significant solution phenomenon for both the actinide and lanthanide elements at $\text{pH} > 6$. For the lanthanides at $\text{pH} = 7$, and in the absence of any stabilizing ligands, the species Ln^{3+} and $\text{Ln}(\text{OH})^{2+}$ appear to coexist at near equal concentrations. At higher pH , the species $\text{Ln}(\text{OH})^{2+}$, $\text{Ln}_2(\text{OH})_2^{4+}$, and $\text{Ln}_3(\text{OH})_5^{4+}$ predominate; with the eventual appearance of $\text{Ln}(\text{OH})_3$ in the form of a precipitate (Aspinall, 2001). One important conclusion that can be drawn from this information is that the aqueous chemistry of the actinide and lanthanide elements can be seen as a competition between stable complexation in solution or loss to hydrolysis and

precipitation. The above comparisons between the two groups of elements also reveal their very similar properties in aqueous solution. This is a conclusion which possesses very powerful implications for experimental design using the lanthanide elements as a non-radioactive, cost-effective, and easily-obtained *model system* for actinides such as Cm and Am.

1.3.2. The Ce(IV)/Ce(III) Redox Couple

The rare earth element cerium is anomalous among the other elements in its group with regard to its ability to exist as a tetravalent solution species, in addition to its more common trivalent form. This Ce(IV) cation is quite stable, remaining several weeks in aqueous solution before gradual conversion to Ce(III) occurs. These two cerium species possess different complexation stabilities with given ligands as well as differing pH thresholds for hydrolysis, with pH > 6 sufficient for Ce(III) hydrolysis and that of Ce(IV) occurring at even lower pH due to its higher charge and smaller ionic radius (Aspinall, 2001). The hydrolysis product constants for Ce(III) in the form of CeOH^{2+} , $\text{Ce}_2(\text{OH})_2^{4+}$, and $\text{Ce}_3(\text{OH})_5^{4+}$ have been estimated at $10^{-9.7}$, $10^{-15.6}$, and $10^{-35.75}$, respectively, in 3 M LiClO_4 (Baes and Mesmer, 1976). Similar constants for the Ce(IV) hydrolysis products CeOH^{3+} , $\text{Ce}(\text{OH})_2^{2+}$, $\text{Ce}_2(\text{OH})_2^{6+}$, $\text{Ce}_2(\text{OH})_3^{5+}$, $\text{Ce}_2(\text{OH})_4^{4+}$, and $\text{Ce}_6(\text{OH})_{12}^{12+}$ have been measured at $10^{1.1}$, $10^{0.3}$, $10^{3.6}$, $10^{4.1}$, $10^{3.5}$, and $10^{15.4}$, respectively, also in 3 M LiClO_4 (Baes and Mesmer, 1976). These values reflect the greater propensity for the hydrolysis of Ce(IV) over that of Ce(III). The $\text{Ce}(\text{OH})_3$ and $\text{Ce}(\text{OH})_4$ precipitates have solubility product constants of $10^{-20.2}$ and $10^{-50.4}$, respectively (Sillén and Martell, 1964).

Electrochemically, cerium is of interest because of the highly positive potential at which Ce(IV) reduction takes place (Figure 1.2).

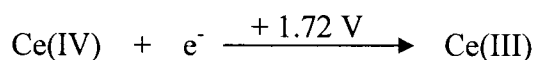


Figure 1.2. The Ce(IV)/Ce(III) redox couple.

The highly positive reduction potential of the Ce(IV)/Ce(III) redox couple has resulted in numerous accounts in the literature regarding its electrochemical behavior. Much of the recent work has been conducted with a view towards exploitation of the couple's highly anodic reduction potential for application in redox flow battery technology (Paulenova *et al.*, 2002; Liu *et al.*, 2004), as well in the field of electro-organic synthesis, and the oxidation of organic waste compounds and contaminants (Morita *et al.*, 1995; Nzikou *et al.*, 1995; Vijayarathi *et al.*, 1999; Chung and Park, 2000; Vijayarathi *et al.*, 2001; Abbaspour and Mehrgardi, 2005). It has been shown in the literature that the electrochemical, kinetic, and chemical speciation properties of the Ce(IV)/Ce(III) aqueous redox system are comparable to the corresponding IV/III couples of the transuranium elements such as Cm and Am (Stokely *et al.*, 1972; Hobart *et al.*, 1982; Morris and Hobart, 1987). These similarities make the electrochemistry of cerium profoundly interesting to the pursuit of actinide separations, by allowing the cerium system to act as an especially appropriate and useful model for the more expensive and highly radioactive actinides of interest.

The remarkably positive potential at which ceric/cerous redox activity occurs creates difficulties in the investigation of this redox couple using conventional electrochemical techniques. Since Ce(IV)/Ce(III) electrochemistry is typically examined in aqueous solution, one serious complication that arises is interference from the oxidation of water (Figure 1.3), which occurs in a similar potential range to the oxidation of Ce(III) to

Ce(IV). An examination of the literature reveals the great deal of experimental effort that has been devoted to the elucidation of cerium redox chemistry and its resolution from O₂ evolution.

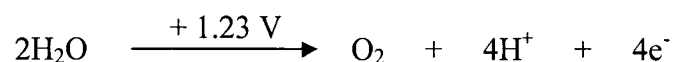


Figure 1.3. The oxidation of water.

The parameters that can be adjusted to accomplish these goals are: 1) the material, structure, and reactivity of the working electrode and 2) the solution characteristics, complexing ability, and stabilization provided by the aqueous environment.

Although the standard redox potentials (*i.e.* thermodynamics) of the Ce(IV)/Ce(III) and O₂/H₂O couples are inconveniently close to one another, their kinetics can be adjusted by using working electrodes of various composition. This effect exerted by the material of the working electrode is a result of the *overpotential* that a particular electrode has for a specific reaction of interest. This overpotential means that a redox reaction will occur at a more extreme potential value than its E^0 due to kinetic limitations imposed by the electron-transfer process at the working electrode surface. Thus, for the cerium system, a working electrode that has a high overpotential for oxygen evolution will provide a wider potential window through which cerium electrochemistry can be observed, as well as better separation of the cerium current peak from that of water oxidation. Events that modify the electrode surface, such as adsorption of solution species, have the capacity to alter the reactions that can take place. At sufficiently positive potentials, the formation of oxide layers on noble metal electrodes such as

platinum and gold can significantly affect the kinetics of electron transfer at their surfaces.

1.3.3. Influence of Working Electrode on Ce(IV)/Ce(III) Electrochemistry

The challenges encountered in the investigation of Ce(IV)/Ce(III) electrochemistry can be seen in the early literature, where only Ce(IV) reduction was examined at conventional electrodes such as platinum due to the difficulties associated with observing the oxidation process (Bauer and Glaessner, 1903; Kunz, 1930). The study of Ce(III) oxidation remained elusive even with the use of the dropping mercury electrode; a consequence of the propensity of mercury for easy oxidation (Noddak and Bruckl, 1937; Goffart, 1948). Desideri (1961) examined the reduction of Ce(IV) in H₂SO₄ solutions using polarography at a bubbling platinum electrode. It was found that lower acid concentrations moved the reduction to less positive potentials. However, this desirable effect was counteracted by extensive hydrolysis of cerium species in solution. From his results, Desideri reported that reversibility of Ce(IV) → Ce(III) was attainable only at sulfuric acid concentrations greater than 7 M. This reversibility was attributed to the redox reaction of a Ce(IV) solution complex formed at low pH and shown in Figure 1.4.



Figure 1.4. Proposed Ce(IV)/sulfate complexation at low pH.

A comprehensive investigation into the effects of platinum oxide formation was conducted by Greef and Aulich in 1968, and yielded the following conclusions: 1) oxide formation was not affected by the presence of either Ce(III) or Ce(IV) 2) oxide formation

affected redox currents, especially inhibiting the reduction of Ce(IV) 3) the inhibition was more pronounced in perchloric than in sulfuric acid and 4) the retardation of the cathodic reaction by the oxide was not solely due to blockage of the electrode surface. Thus, the oxide film on the Pt working electrode affected the reduction of tetravalent cerium. Furthermore, this was a variable effect that could not be corrected for, since the oxide continued to grow for the duration of the experiment and never truly reached a steady state. This finding was in contradiction to earlier work by Galus and Adams (1963) who obtained values of the heterogeneous rate constant k_s for the reduction of Ce(IV) at both platinum and carbon paste rotating disk electrodes (RDEs) and found them to be identical, challenging the concept of a Pt oxide effect. Attempts to standardize Pt oxide films have met with mixed success (Randle and Kuhn, 1983). Investigation of the effects of oxygen adsorption on gold similarly determined that oxide formation occurred independently of cerium concentration in solution (Bonewitz and Schmid, 1970). Contrary to the behavior of platinum oxide, however, the gold oxide layer was found to behave as a good electronic conductor, and no retardation of Ce(IV) reduction was observed in its presence.

Miller and Zittel (1964) made use of pyrolytic graphite; an ordered, planar allotrope of carbon; in an attempt to avoid the difficulties associated with the use of noble metal electrodes. Polarography experiments showed reversibility of the cerium redox couple at this electrode in 1 M H₂SO₄. The pyrolytic graphite working electrode also provided a wide potential window as a result of its high overpotential for water oxidation. This was especially true when either sulfuric or sulfuric/phosphoric acids were used as the supporting electrolytes, reflecting the stabilization of cerium species in these media. The

electrode dependence of Ce(IV)/Ce(III) electrochemistry was clearly demonstrated by Kiekens *et al.* (1981) in their comparison of gold, glassy carbon, and iridium RDEs. These researchers observed a non-Nernstian displacement of the redox peaks, which was especially pronounced at the metal electrodes, and was attributed to oxide formation at their surfaces. Similar to the results at pyrolytic graphite, those obtained at glassy carbon (GC); an inert, amorphous carbon allotrope; showed optimum redox couple reversibility. In interesting contrast to the results of Bonewitz, a retardation of Ce(IV) reduction was observed at gold. The reactivation of the gold surface was accomplished through the use of potential cycling between experiments.

A landmark comparison conducted by Bishop and Cofré in 1981 examined the oxidation of Ce(III) at Au, Pt, and GC RDEs. While Au showed the highest overpotential for oxygen evolution, it was observed to corrode in the presence of Ce(IV). The GC electrode, however, remained inert and yielded redox behavior in accordance with the Nernst equation. Oxidation of the aqueous background solution proved to be an issue at Pt, a possible result of Pt oxide catalysis of this reaction. These results were in contrast to earlier work, which found that Pt oxide effectively inhibited O₂ evolution (Gilroy, 1977). The paradoxical nature of the literature on cerium electrochemistry was further demonstrated by a subsequent work reporting Au as the optimum working electrode for the cerium redox system. In fact, GC has been labeled “inefficient” due to irreversibility of the couple and insufficient separation from the background oxidation current (Sacchetto *et al.*, 1992). Recent studies have attempted to evade the working electrode enigma through the use of novel electrode materials such as boron-doped diamond (Maeda *et al.*, 1999; Ferro and De Battisti, 2002). Although the claim of superior results

is made for these electrodes, the voltammetry at their surfaces does not differ significantly from that observed at the more conventional electrodes, and suffers from the same shortcomings with regard to overpotential and the exploitable potential window. Uncertainty exists in the literature regarding the “optimum” working electrode for Ce(IV)/Ce(III) investigations, in spite of the large amount of literature that exists for this redox system. However, the choice of the working electrode remains just one element in the design of that optimum electrochemical experiment that remains so elusive.

1.3.4. Influence of Solution Conditions on Ce(IV)/Ce(III) Electrochemistry

The speciation of cerium has long been known to play an integral role in the information obtainable from a particular electrochemical experiment. This is a reflection of the stability and electroactive characteristics of the solution complexes of tetravalent or trivalent cerium present in the electrochemical cell. Noyes and Garner (1936) suggested complexation effects as an explanation for significant variations in redox potential observed for the cerium system in different acidic media, noting that the less positive redox potential obtained in sulfuric compared to nitric acid reflected a greater degree of Ce(IV) complexation with either SO_4^{2-} or HSO_4^- anions. It was further concluded that these variations ruled out hydrolysis as the major mechanism in these solutions, and that the change in redox potential with increasing acid concentration suggested the existence of electroactive cerium *complexes*, rather than the redox of the free cations (Smith and Getz, 1938). These researchers measured redox potential values of +1.70, +1.61, +1.44, and +1.28 V (vs. SHE) for the Ce(IV)/Ce(III) couple at a Pt electrode in 1 M HClO_4 , HNO_3 , H_2SO_4 , and HCl , respectively. This order of decreasing redox potential was, in general, considered a consequence of increased stabilization of cerium species by means

of complexation. The value obtained in HCl was called into question, however, due to the generally poor complexing ability of the chloride anion (Wadsworth *et al.*, 1957), and has recently been re-evaluated at +1.47 V employing the same experimental conditions (Maverick and Yao, 1993).

Both Ce(III) and Ce(IV) have been found to be strongly complexed in basic carbonate medium, existing primarily as $\text{Ce(IV)(CO}_3)_6^{8-}$ and $\text{Ce(III)(CO}_3)_4^{5-}$, with no mixed carbonate-hydroxide species due to the much greater stabilization offered by the carbonate anion (Salvatore and Vasca, 1990). The precipitation of cerium carbonates, however, presented a problem for the carbonate system. A further demonstration of the remarkable complexation behavior of cerium cations was the determination of the predominance of Ce(IV) trimers of the form $\text{Ce}_3\text{O}_3(\text{HOAc})^{6+}$ in aqueous acetic acid (Wiberg and Ford, 1968). The weak complexation affinity of anions such as nitrate, chloride, and perchlorate for trivalent rare earth elements such as cerium has been attributed to an outer sphere interaction of these ligands with Ce(III) through a “monomolecular shell” of water molecules in which the rare earth cation is encased (Spedding and Jaffe, 1954b).

The poor complexing ability of the perchlorate anion was further demonstrated by Sherrill and coworkers in 1943, when they observed a redox potential independent of perchlorate ion concentration, and described the predominant speciation of cerium in perchloric acid solutions to consist of two hydrolyzed forms of the ceric cation shown in Figure 1.5. Ce(III) was presumed to exist in free cationic form, although a later study suggested the existence of a CeClO_4^{2+} complex (Heidt and Berestecki, 1955).

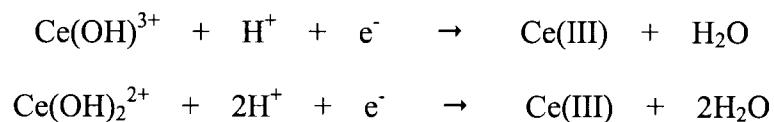


Figure 1.5. Reduction reactions of Ce(IV) in perchloric acid.

It is interesting to note the absence of perchlorate ion interaction with the cerium cations in this solution environment, which is a demonstration of the instability of such complexes. This failure of the perchlorate anion to stabilize the electroactive species is manifested by the highly anodic redox potentials observed for the cerium couple in this system. The complexity of the cerium/perchloric acid system has been further demonstrated by both spectral and radioactive ^{144}Ce tracer studies providing evidence of a hydrolyzed Ce(IV) dimer of the form $(\text{Ce} - \text{O} - \text{Ce})^{6+}$, $(\text{HO} - \text{Ce} - \text{O} - \text{Ce})^{5+}$, or $(\text{HO} - \text{Ce} - \text{O} - \text{Ce} - \text{OH})^{4+}$ (Hardwick and Robertson, 1951; Duke and Parchen, 1956). Despite the low fraction (0.5 to 2.5%) of this species in solution, the further suggestion was made that the redox couple activity observed for cerium in perchlorate medium was indeed solely due to this hydrolyzed Ce(IV) dimer undergoing reduction, followed by the reoxidation of the mixed Ce(IV)/Ce(III) dinuclear species (Fronæus and Östman, 1956). Some disagreement with these conclusions was shown by Bilal and Müller (1992), who attributed electroactivity in perchloric acid (0.02 to 7.45 M concentration of acid) to uncomplexed Ce(IV) alone.

A survey of the literature, from the earliest studies to the present, reveals a general preference for aqueous sulfuric acid as the medium in which to investigate the electrochemistry of the Ce(IV)/Ce(III) redox couple. Early investigators, in their efforts to measure the standard potential of Ce(IV) reduction, observed a shift toward less

positive potentials concurrent with an increase in sulfate ion concentration (Kunz, 1931; Noyes and Garner, 1936; Smith and Getz, 1938). These workers conjectured the presence of electroactive cerium-sulfate complexes, although they were unable to specify their precise stoichiometries. Spectroscopic studies of tetravalent cerium in sulfate solutions indicated that CeSO_4^{2+} , $\text{Ce}(\text{SO}_4)_2$, and $\text{Ce}(\text{SO}_4)_3^{2-}$ were formed successively as sulfate concentration increased, with $\text{Ce}(\text{SO}_4)_3^{2-}$ as the predominant cerium species in concentrated sulfate solutions (Hardwick and Robertson, 1951b). Importantly, these studies also concluded that neither H^+ nor OH^- was a component of the sulfate complexes (in conflict with Desideri's work described above), and that ceric complexes with greater than three sulfate anions did not form. These conclusions also indicated that Ce(IV)/bisulfate complexes were not present to any significant extent in the sulfate solution environment. Similar investigations, using spectrophotometric and conductance methods, yielded the information that CeSO_4^+ was the dominant complex for Ce(III) in sulfate solutions (Connick and Mayer, 1951; Newton and Arcand, 1953; Spedding and Jaffe, 1954).

The result of varying sulfuric acid concentration on the electrochemistry of Ce(III) \rightarrow Ce(IV) was investigated by Bishop and Cofré (1981), who determined that an increase in the rate of Ce(III) oxidation was observed with increasing concentrations of H_2SO_4 . They were also able to show a decrease in reaction rate for the background solution (O_2 evolution), which they ascribed to the lowered fraction of water in the bulk solution. A decrease in the mass transport coefficients was measured as acid concentration was increased, due to the higher viscosity of the supporting electrolyte. In 2002, Fang and coworkers calculated cerium ion speciation in sulfuric acid solutions and determined that

the trivalent species existed in predominantly complexed form (CeSO_4^+ , $\text{Ce}(\text{SO}_4)_2^-$) at acid concentrations greater than 0.5 M. For Ce(IV), an even lower concentration of 0.15 M was necessary to complex the bulk of solution cations in the form of CeSO_4^{2+} , $\text{Ce}(\text{SO}_4)_2$, and $\text{Ce}(\text{SO}_4)_3^{2-}$. They also found that sulfuric acid medium at 0.1 M concentration yielded the most Nernstian behavior for the redox couple via cyclic voltammetry at a GC working electrode, although they classified the couple as irreversible. Increasing temperature was also found to exert a favorable effect, as far as reduced peak potential separation and increased redox peak currents, but unfortunately moved the redox couple to more positive potentials. Contradictory results were reported by Paulenova *et al.* (2002), who reported increased redox peak separations at low concentrations of sulfuric acid. Their work also differed from previous studies when they cited the history of the GC electrode as a factor in the electron transfer reaction. Rather than observing a beneficial effect of higher temperatures, they remarked on the degradation of the supposedly inert GC surface, resulting in an attenuation of the Ce(IV) reduction current. Even the most recent literature on the cerium/sulfuric acid electrochemical system is beset with contradictions, with reports of inhibited reaction of Ce(III) at the oxidized Pt electrode surface, and the claim of increased reversibility of the redox couple at higher (2 M) sulfuric acid concentrations (Liu *et al.*, 2004). Clearly, significant amounts of work have been conducted in the search for “optimum” solution conditions for resolution of the Ce(IV)/Ce(III) redox couple. However, similar to the debate over the choice of the “optimum” working electrode, significant ambiguities remain as to the exact nature of the ideal solution environment.

1.4. Present Work

1.4.1. Purpose

As we have seen, the electrochemical study of the Ce(IV)/Ce(III) redox couple; demonstrated throughout the literature as an intricate balance between working electrode material, temperature, concentration, and complexing environment; is one which presents many challenges to the investigator. With the ultimate goal of electrochemical separation of actinide elements built on the Ce(IV)/Ce(III) model, a thorough understanding of the electrochemistry of aqueous cerium systems was desired. It was thus the purpose of the present work to attempt the elucidation of optimum conditions for the observation of this redox couple, as defined by minimum reaction inhibition (high redox peak currents), reversibility (near-Nernstian peak potential separation), and resolution (sufficient separation from the background currents caused by the oxidation of water). The electrochemical technique implemented was that of cyclic voltammetry, allowing the repeated survey of a particular potential range in search of electroactive species. Clarification of the electrochemical effects of several experimental parameters was sought. These were the concentration and identity of the acid supporting electrolyte, the ionic strength of the medium, the solution pH, and the presence of multidentate complexing ligands together with the pH of the medium in which they exist. Finally, due to the pivotal role which the working electrode composition has been shown to play in the ability to observe electrochemical phenomena, all experiments were conducted at Pt, Au, and GC working electrodes as a comparison of their relative performance.

1.4.2. Acid Study

In view of the conflicting literature reports regarding the beneficial or detrimental effect of increasing acid concentration, an acid study was conducted to determine optimum acid concentration for resolution of the Ce(IV)/Ce(III) redox couple. Aqueous sulfuric acid was chosen as the medium for this study, since it has long been utilized for such electrochemical experiments due to its stable complex formation with both trivalent and tetravalent cerium species. The experiment was then repeated using nitric acid, at the optimum concentration determined from the H₂SO₄ study, in order to examine the effect of varying the nature of the anionic species in solution. Each experiment was conducted at three different working electrodes: GC, Au, and Pt. This practice was implemented to allow observation of the cerium redox couple resolution achievable at each particular electrode.

1.4.3. pH Study

Studies of the Ce(IV)/Ce(III) redox couple have traditionally been carried out in acidic medium. This convention has been variously ascribed to the avoidance of hydrolysis, to which both oxidation states of cerium are known to succumb quite readily, or alternatively to the need for acid as an oxidizing medium for metal electrodes, providing a proposed “activation” effect (Ferro and De Battisti, 2002). However, optimum acid concentration, once determined, will necessarily correspond to some particular, optimum value of solution ionic strength. Although the effects of varying acid concentration have frequently been examined in the literature, those of the ionic strength solution characteristic have not received particular scrutiny. The investigation of cerium electrochemistry as a function of increasing acid concentration raises questions about the

nature of the observed effects on the redox couple. As acid concentration is raised, a concurrent increase in ionic strength occurs, together with a parallel lowering of solution pH. Separation of these related variables from one another may potentially yield a greater understanding of the role played by each parameter in observed experimental results. With this objective in mind, a pH study was outlined and conducted on the Ce(IV)/Ce(III) redox couple, through the use of sulfate solutions of incrementally increasing pH and constant ionic strength.

1.4.4. Complexation Study

The known propensity for lanthanide and actinide elements to undergo highly stable complex formation with multidentate ligands, particularly members of the aminopolycarboxylates, allows a potentially effective method for their electrochemical separation in aqueous solution. An understanding of the changes in redox potential resulting from such coordination events with the cerium system can provide a foundation on which such electrochemical separation schemes can be built. To this end, the electrochemistry of the Ce(IV)/Ce(III) redox couple was investigated in strongly complexing ligand environments such as aqueous NTA, citrate, and EDTA. The initial pH of each cerium-ligand solution was incrementally increased by means of base titration, and voltammograms were obtained at each increment of the experimental pH range. Speciation profiles for the ligands under investigation were also constructed to more efficiently identify the predominant form of the ligand available for complex interaction at each particular solution pH probed in the course of the experiment.

CHAPTER 2

BACKGROUND

2.1. Electrochemical Theory

2.1.1. A Description of Electrode Processes

The types of electrochemical reactions that can occur at the interface between a metal electrode and the solution with which it is in contact can generally be classified either as *faradaic* or *nonfaradaic*. Faradaic processes are those that take place through the transfer of electrons from the electrode metal to the solution, or from solution species to the electrode. These reactions show behavior that is in accordance with Faraday's law, which states that the number of moles of species electrochemically reacted at an electrode is directly proportional to the number of moles of electrons transferred at that electrode surface. The resulting rate of this faradaic process, using the appropriate sign convention for the current, can be expressed by the following equation:

$$\text{Rate (mol / s)} = \frac{i}{nF}$$

where i is the current, n is the number of moles of electrolyzed species, and F is the Faraday constant (9.64853×10^4 C).

It is the direction of electron transfer that dictates the nature of the reaction taking place at the electrode surface; with electron transfer from electrode to solution resulting in a reduction, or *cathodic* (+) current flow, and the reverse process yielding an *anodic* (-)

current due to oxidation of the electroactive species. Thus, the working electrode, in a technique such as cyclic voltammetry, has the propensity to function as either the cathode or the anode in the electrochemical cell, depending on the energy of the electrons in the electrode relative to their energy in the solution. It is through this experimental control of the applied electrode potential that a reaction is driven in one direction or the other, as a result of electron transfer across the metal/solution interface to the phase of more favorable (lower) energy.

In contrast to faradaic processes, those classified as nonfaradaic result from changes to the electrode surface caused by such occurrences as sorption and desorption, or non-specific interactions such as the formation of the double layer. Such events give rise to nonfaradaic currents as the metal/solution interface and solution characteristics are altered, although no charge transfer across the interface occurs. It is very important to take such processes into account, since any modification of the electrode surface may exert significant effects on faradaic processes taking place through charge transfer across that interface.

Electrode reactions described as *Nernstian* are those governed by thermodynamic rather than kinetic considerations at the electrode surface, and whose behavior is in accordance with the predictions of the *Nernst* equation:

$$E = E^0 + \frac{RT}{nF} \ln \frac{a_O}{a_R}$$

The above is the Nernst equation for an electrode reaction of the following form:



The observed experimental reduction potential E is thus expressed as a function of the standard reduction potential E^0 for the reaction vs. a reference (usually the standard

hydrogen electrode), the gas constant R , the experimental temperature T , the number of moles of electrons n transferred in the reduction process, as well as the activities a_O and a_R of the oxidized and reduced species, respectively.

The Nernst equation is applicable when kinetic effects can be ignored. This is the case when electron transfer is not kinetically limited and occurs as rapidly as species reach the electrode surface. For this reason, the reaction rates of such Nernstian processes are governed by the efficiency of the various mass transfer mechanisms operating in the experimental system. There are three possible modes of mass transfer by which electroactive species are brought to the electrode surface. The first of these is diffusion, which is the movement of species from regions of higher concentration to those of lower concentration due to the presence of a concentration gradient; the second is migration, which describes the movement of charged species under the influence of an electric field. Finally, convection is a mode of mass transfer that can be externally applied through stirring or vibration of the solution in the electrochemical cell. The mathematical description of this mass transport-controlled flux J_i of species i to the electrode surface is contained in the *Nernst-Planck* equation, shown below for a linear (one-dimensional) system:

$$J_i(x) = -D_i \frac{\partial C_i(x)}{\partial x} - \frac{z_i F}{RT} D_i C_i \frac{\partial \phi(x)}{\partial x} + C_i v(x)$$

where the three equation terms represent the contributions of diffusion, migration, and convection, respectively. It is clear from this expression that the flux of species i , which in turn dictates the rate at which reduction/oxidation at the electrode surface can occur, is dependent on its diffusion coefficient D_i (in cm^2/s), its charge z_i and solution

concentration C_i (in $\text{mol}\cdot\text{cm}^{-3}$), the volume flow rate (in units of cm/s) along the x -axis $v(x)$, as well as the concentration and potential gradients $\frac{\partial C_i(x)}{\partial x}$ and $\frac{\partial \phi(x)}{\partial x}$.

The concurrent effects of all three of these mass transport modes would yield an inconvenient complexity in the treatment and interpretation of experimental results. For this reason, measures can be taken in the design of an electrochemical experiment to minimize or eliminate the effects of one or more of these mechanisms. An inert “working” electrolyte, such as K_2SO_4 or KNO_3 at sufficiently high concentration minimizes the effects of migration. Avoiding stirring and minimizing the vibrations applied to the system allow the convection term to be ignored as well. Thus, we can reduce the dependence of the flux to the electrode surface simply to the effects of a single mode of mass transport, leaving us with a process that can be treated as solely diffusion-controlled and can be described by the simplified mass transport equation:

$$J_i(x) = -D_i \frac{\partial C_i(x)}{\partial x}$$

2.1.2. Cyclic Voltammetry

Cyclic voltammetry (CV) is a widely used electrochemical technique of practical importance in the elucidation of the kinetics and thermodynamics of redox processes, and ultimately the potential for separation of solution species based on these properties. Through the application of a triangular waveform of potential vs. time (Figure 2.1), cyclic voltammetry provides an experimental window through which the reaction behavior of existing electroactive species can be examined as observations of current generated at characteristic applied electrode potentials.

Thus, cyclic voltammetry provides a convenient and effective means of assessing the effects of changing solution characteristics such as complexation, hydrolysis, precipitation, pH, and ionic strength on an electrochemical system. The technique provides several parameters which can be adjusted to optimize the experiment; these include the initial and final potentials (E_i and E_f), potential scan rate (v), as well as the number of complete potential cycles performed on the system. In general, a *steady-state*

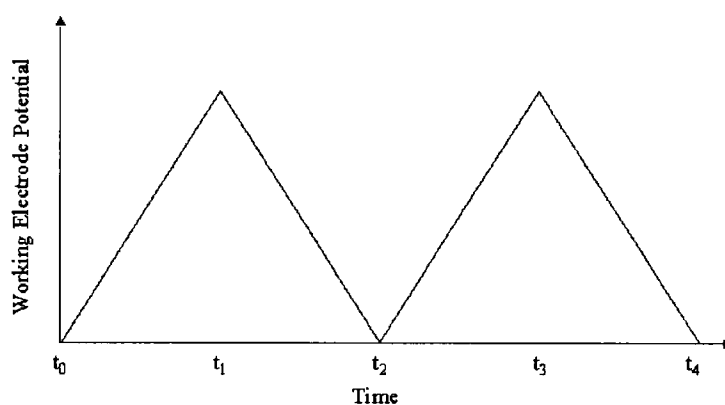


Figure 2.1. The triangular potential waveform used in cyclic voltammetry.

voltammogram is desired, or one in which the current response for a particular cycle is identical to that of the previous cycle, indicating an electrochemical system that has reached its equilibrium current values.

2.1.3. The Three-Electrode System

Electrochemical experiments conducted using the technique of cyclic voltammetry make use of a three-electrode system that consists of a working electrode of conductive material (*e.g.* Au, Pt, GC), a reference electrode (*e.g.* calomel, Ag/AgCl) and a counter electrode of some conductive metal, usually Pt. Figure 2.2 shows the three-electrode

system in the context of a typical experimental setup. The redox reaction under investigation occurs at the surface of the working electrode. This is the electrode held under potential control by the potentiostat, and whose potential is the independent variable in the cyclic voltammetric experiment. It is not possible to obtain the “absolute” redox potential of any reaction. Thus, we can only measure potential values *relative* to some reference electrode of our choosing that is capable of maintaining constant potential throughout the course of the experiment. The potential applied to the working electrode by the potentiostat is therefore, in reality, a potential *difference* between the working electrode and the constant-potential reference electrode.

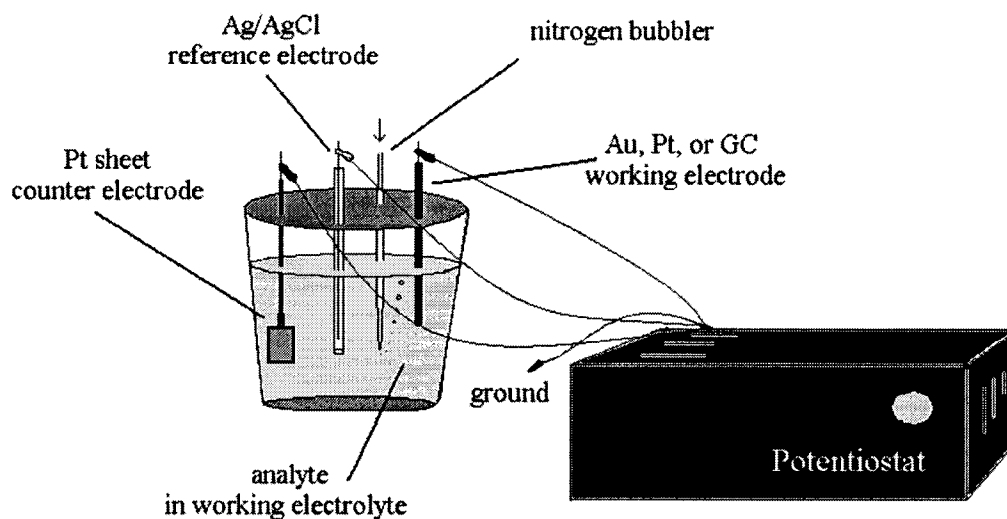


Figure 2.2. Three-electrode setup for a CV experiment.

Since any half-reaction (reduction or oxidation) must be accompanied by a second half-reaction (oxidation or reduction) of the appropriate stoichiometry, the use of only

two electrodes in an electrochemical experiment would result in the inevitable reaction of the reference electrode and the loss of stable potential for one half-cell. This would lead to undesirable changes in its composition, and consequent potential fluctuations detrimental to both the accuracy and precision of the experiment. The reference electrode must, in other words, be present in the cell without participating in the cell reaction. The purpose of a third, or counter, electrode is to serve as an electron source or sink, depending on the process occurring at the working electrode. Thus, the cell reaction is completed and current flows between the working and counter electrodes, while accurate potential measurement can take place between the working electrode and the reference. Additionally, the potentiostat has a high input impedance, which prevents current from reaching and affecting the potential of the reference electrode.

2.2. Experimental Considerations

2.2.1. Determination of Optimum Experimental Conditions

In order to investigate the effects of changing experimental parameters and determine optimum conditions for a particular redox couple, it is necessary to define the specific electrochemical characteristics by which we can identify the optimum experimental system. The realization of optimum conditions in this project was defined as the observation of a Nernstian or reversible Ce(IV)/Ce(III) redox couple. The behavior of such reversible systems is governed by the Nernst equation. The reversibility of a redox couple can be evaluated experimentally from the information contained in the voltammogram. The Nernst equation predicts a potential separation between peak anodic (oxidation) and peak cathodic (reduction) current potentials (E_{pa} and E_{pc}) of 59 mV per

electron transferred. Reversibility of the Ce(IV)/Ce(III) couple should be demonstrated by a peak potential separation of 59 mV since it is, in fact, a single-electron process. True reversibility also stipulates the symmetry of the oxidation and reduction current peaks. In other words, the ratio of the peak anodic to the peak cathodic current (i_{pa}/i_{pc}) should have a value of 1, indicating a balanced occurrence of the two electrode processes. These characteristics of reversibility should exist independently of the experimental scan rate.

Since all experiments in this project made use of a working electrolyte (to minimize migration effects) and did not involve stirring of the solution in the electrochemical cell (no convection), diffusion-controlled conditions were assumed to prevail in the system. Experimentally, we have the ability to identify such diffusion-controlled processes knowing that they are governed by the *Randles-Sevcik* equation:

$$i_p = 2.687 \times 10^5 n^{3/2} \nu^{1/2} D_i^{1/2} A C_i$$

Thus, the peak current i_p obtained from the electrochemical reaction of analyte i is expressed as a function of the number of moles of electrons n involved in the redox process, the scan rate ν , the area of the electrode surface (in cm^2), as well as the diffusion coefficient and concentration of species i . Since typical electrochemical techniques, such as cyclic voltammetry, allow for experimental control over the scan rate parameter, peak currents can be measured as a function of the applied scan rate. Experimental current values linear with the square root of the scan rate can, therefore, be used as confirmation of a diffusion-controlled electrode process. The agreement of experiment with this predicted linear model is thus another indicator of the reversibility of the redox couple under investigation.

The other experimental indicator used in this project as a measure of optimum results was the resolution of the redox couple from background currents. Figure 2.3 is a representation of the various interferences and limitations encountered in the cyclic voltammetric study of the Ce(IV)/Ce(III) redox couple. Several experimental difficulties exist, largely due to the positive potential at which the redox couple appears.

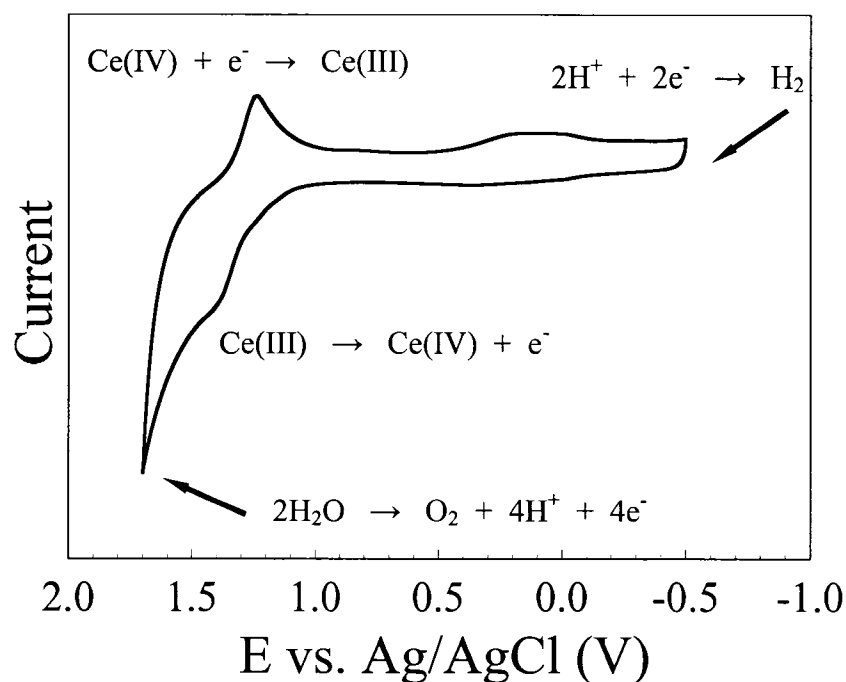


Figure 2.3. Typical CV showing the experimental difficulties encountered during investigation of the Ce(IV)/Ce(III) redox couple (voltammogram obtained using a Pt disk working electrode and a $\text{Ce}(\text{NO}_3)_3 \cdot 6\text{H}_2\text{O}$ concentration of 6.0 mM in 0.1 M HNO_3 working electrolyte).

In aqueous media, such as the 0.1 M HNO_3 used to obtain the data in Figure 2.3, there is a relatively narrow potential window across which we have the ability to scan in search

of electroactive species. This potential range is limited by the oxidation and reduction of the medium itself, with the oxidation of water occurring at sufficiently positive potentials, and currents from the evolution of H₂ appearing as potential is scanned in the negative direction (the two bold arrows in Figure 2.3 indicate these limits on the applied potential). Currents arising from the oxidation of water are of particular concern in investigations of the cerium system, due to the proximity of the potentials of these two redox processes. The sample voltammogram in Figure 2.3, for example, shows poor resolution (separation) of the Ce(III) oxidation peak from that of O₂ evolution. Because of this consideration, resolution of the cerium redox couple from background currents due to water oxidation was another indicator used to identify optimum conditions in this study.

2.2.2. Electrodes and Overpotential

A significant aspect of this research project was an assessment of the extent to which the working electrode material affected the redox reaction of cerium taking place at its surface. Each working electrode (*e.g.* Au, Pt, GC) has its own overpotential for any particular reaction. This overpotential is the difference between the thermodynamically predicted redox potential for a reaction at the given conditions and the observed experimental potential at which it occurs in the electrochemical cell. Overpotential describes the experimental observation of a redox reaction at more extreme potential values than those predicted by thermodynamics, due to kinetic limitations on electron transfer at the electrode surface. Thus, the material and reactivity of the working electrode can have a significant effect on the experimental redox potential because electron transfer may be kinetically hindered to a greater or lesser extent, depending on the nature of the surface. Any process that modifies the electrode surface (*e.g.* adsorption

of solution species, oxide formation) will likely affect electroactive species that must react through the transfer of electrons at this constantly changing interface. For the purposes of this project, the working electrode with the highest overpotential for water oxidation was desired, since such an electrode would afford the best resolution of the cerium redox couple from aqueous background currents. However, the usefulness of a specific working electrode as a probe for a particular redox system cannot be predicted, but rather must be determined experimentally.

CHAPTER 3

MATERIALS AND METHODS

3.1. Equipment and Experimental Setup

3.1.1. Instrumentation and Data Collection

All cyclic voltammetric investigations of the Ce(IV)/Ce(III) redox couple carried out in this project made use of a potentiostat of high input impedance. The specific instruments used to provide this potential control included the CHI660A potentiostat manufactured by CH Instruments (Austin, TX), as well as the CHI760B and CHI760C bipotentiostats obtained from the same manufacturer. The bipotentiostat is operated in an identical manner to the standard potentiostat but offers the ability to run two working electrodes simultaneously. This feature was not exploited in these studies due to the significant variation in potential range among the different electrodes. For this reason, it was necessary to run each electrode according to its particular experimental potential requirements. The software used was that provided by CH Instruments in the version appropriate to each instrument model. When running cyclic voltammetry, the instrument varies the potential applied to the working electrode (independent variable) and measures an experimental current value for each potential point applied. While the data are presented by the software in graphical form, the data points may be imported into Excel or another equivalent spreadsheet program and a figure constructed using Excel or some

comparable graphical utility. The data obtained in this project are presented in figures created using the Deltagraph software program.

3.1.2. Electrodes and Electrode Maintenance

Potential was measured in all experiments vs. a Ag/AgCl reference electrode (MF2052) manufactured by Bioanalytical Systems (West Lafayette, IN). This reference electrode has a potential of +0.197 V compared to the Standard Hydrogen Electrode (SHE), which is assigned a value of 0.0000 V. A conversion must be made between these two reference scales when comparing experimental values to those found in the literature. The Ag/AgCl electrode required regular restoration procedures in order to maintain a constant potential. These procedures included changing the membrane at the tip, due to possible leaks or corrosion by the solution environment; as well as periodically changing the filling solution, because of changes in internal concentration due to osmosis in either direction through the electrode membrane. The filling solution used was a 3 M aqueous solution of KCl (J. T. Baker, A.C.S. Reagent crystal, 7447-40-7). Reference electrodes were stored in a saturated solution of KCl between uses. The accurate potential measurement of the reference electrodes was verified periodically by running a 4 mM $\text{K}_3\text{Fe}(\text{CN})_6$ solution (J. T. Baker, A.C.S. Reagent, 13746-66-2). This compound undergoes reversible redox of Fe(III) \leftrightarrow Fe(II) at an E^0 value of +0.3610 V, and is widely used as a standard reference in electrochemical experiments.

The working electrodes used in these studies included 3 mm dia. glassy carbon (CHI104), 2 mm dia. Pt (CHI102), and 2 mm dia. Au (CHI101) disk working electrodes obtained from CH Instruments (Austin, TX). In addition to these disk electrodes, Au “bead” electrodes were prepared by flame melting the tip of a 0.5 mm dia. Au wire (Alfa

Aesar, 99.5%) so that a small ball of solid gold at the tip of the wire provided a larger surface for redox reaction. A Pt wire electrode was also prepared by coiling an approximately 30 mm length of 0.5 mm dia. Pt wire (Alfa Aesar, 99.95%) to provide a greater electrode surface area for a given depth of electrode immersion in the cell. Because of this larger surface area, these Au bead and Pt coil wire electrodes provide experimental currents of greater magnitude than those obtained using the disk electrodes. Thus, they were used for experiments that did not require a reproducible electrode surface area, such as evaluations of redox potentials under differing solution conditions. The disk electrodes were used in scan rate studies, because a constant electrode area was necessary for valid comparisons to be made of current as a function of changing scan rate. The counter electrode used for all experiments was a 2 cm² Pt sheet (Alfa Aesar, 99.99%, 0.2 mm thick). The immersed area of this electrode was always maintained at ~2.5 times that of the working electrode. This protocol was followed to ensure that the rate of any redox reaction occurring at the working electrode was not limited by current constraints at the counter electrode.

Metal electrodes were thoroughly flame cleaned using a butane torch prior to each analysis. This was done without exception so that each experiment was assumed to begin at a reproducibly clean electrode surface. The Au and Pt disk electrodes, which could not be flame-cleaned due to their Teflon casing, were cleaned by polishing for ~2 minutes with a 3 μM diamond polish, and then repeating the same procedure using a 0.3 micron alpha alumina powder polish. Finally, the electrodes were sonicated for ~10 minutes in distilled water, followed by a quick rinse with methanol. The same cleaning procedure was used for the GC disk electrodes, omitting the diamond polish step. This protocol and

the required equipment and solutions were obtained from an electrode cleaning kit (MF-2060) purchased from Bioanalytical Systems (West Lafayette, IN).

3.2. Solution Preparation and Experimental Procedures

3.2.1. General Solution Considerations

All solutions were purged of oxygen by means of a nitrogen bubbler. The solutions were degassed in this way for ~20 minutes prior to each analysis, and each subsequent time the cell was opened. A positive nitrogen pressure was maintained against the surface of the solution throughout all experiments to prevent the reentry of oxygen into the headspace of the electrochemical cell.

A considerable number of the studies on cerium electrochemistry found in the literature employ solutions where cerium concentrations lie in the millimolar range. Justifications for this practice include the avoidance of precipitation of insoluble hydroxides and the high sensitivity of electrochemical techniques such as cyclic voltammetry, which eliminates the need for high analyte concentrations. Early studies, which looked only at the reduction of Ce(IV) due to the background interferences described in Chapter 1, employed solutions containing only the tetravalent cation (Miller and Zittel, 1963; Greef and Aulich, 1968). Using mixtures of both cerium species is unnecessarily complicated and troublesome, since the ceric cation tends to convert over time to the trivalent form, and requires titration prior to each experiment to confirm Ce(IV) concentration. Cyclic voltammetry allows the use of Ce(III) solutions since a single positive potential scan will supply the other cation. This is convenient because the Ce(III) cation possesses long-term stability in aqueous solution and hydrolyzes less

readily than Ce(IV). For these reasons, millimolar concentrations of Ce(III) were employed in all studies.

3.2.2. Acid Study

The acid study was designed to compare the electrochemical behavior of Ce(IV)/Ce(III) at increasing concentrations of H₂SO₄, and also as a function of the electrode material. Aqueous solutions of sulfuric acid (Mallinckrodt, analytical reagent 96.0%, 7664-93-9) were prepared at 0.1, 1.0, and 2.0 M. Ce(III) solutions were then prepared at a concentration of 6.0 mM in each of these electrolytes using the Ce(NO₃)₃·6H₂O salt (Aldrich, 99.999%, 233-297-2). All analytical solutions were prepared using water obtained from a Barnstead E-pure filtration system (18.3 MΩ·cm), and sonicated for 30 minutes at room temperature to ensure complete reagent dissolution. Samples were analyzed by room temperature cyclic voltammetry using a scan rate of 100 mV/s, which is a standard scan rate used in electrochemical studies. This scan rate was maintained as a constant across experiments so that current comparisons would be possible (faster scan rates yield higher peak currents at a given set of conditions). Comparison experiments in nitric acid were conducted using 6.0 mM Ce(III) solutions in 0.1 M HNO₃ (Fisher, certified ACS *Plus* 69.4%, 7697-37-2).

3.2.3. pH Study

In the pH study, room temperature cyclic voltammetry was first conducted at Au, Pt, and GC working electrodes in a 0.1 M solution of K₂SO₄ (fine crystal, J. T. Baker, “Baker-analyzed reagent,” 99.9%, 7778-80-5). For the second part of the pH study, it was necessary to prepare sulfate solutions of increasing pH (~3 and ~5) at a fixed ionic strength. In order to meet these simultaneous requirements of pH and ionic strength,

solutions of the appropriate ionic strength were prepared using Na_2SO_4 (Mallinckrodt, 100% ACS grade, 7757-82-6), and the pH adjusted using concentrated HCl (EM Science, *OmniTrace*, 37.0-38.0%, 7647-01-0) and an approximately 10 M solution of NaOH (EM Science, ACS grade pellets, 97.0% min., 1310-73-2). These pH 3 and pH 5 solutions were prepared in volumes of 1 L each, so that the addition of a few drops of concentrated acid or base would not have a significant effect on the ionic strength of the solution. Solutions of 6.0 mM $\text{Ce}(\text{NO}_3)_3 \cdot 6\text{H}_2\text{O}$ (Aldrich, 99.999%, 233-297-2) were also prepared in each of these electrolytes and pH was adjusted again since it was slightly altered by addition of the metal. Solution pH was monitored using a Corning 240 pH meter, calibrated before each use using a 2-point calibration method (pH 7/4 or 7/10 depending on the experimental pH range) and operated according to procedures outlined in the user's manual.

3.2.4. Complexation Study

In the complexation study, investigations of Ce(IV)/Ce(III) electrochemistry were carried out in the strongly complexing solution environments provided by such ligands as citrate, NTA, and EDTA. Working electrolytes of 12.0 mM citric acid monohydrate (Fisher, certified ACS, 5949-29-1), Na_2NTA (Eastman, reagent grade, 15467-20-6), and $\text{Na}_2\text{EDTA} \cdot 2\text{H}_2\text{O}$ (Fisher, certified ACS, 6381-92-6) were prepared and 6.0 mM $\text{Ce}(\text{NO}_3)_3 \cdot 6\text{H}_2\text{O}$ (Aldrich, 99.999%, 233-297-2) solutions were prepared by dissolving the appropriate mass of the cerium salt in each 12.0 mM ligand solution. The resulting solutions had a ligand:metal ratio of 2:1, in order to ensure that the ligand was present in excess and all metal cations would be present in complexed form. For the pH titration studies, each metal/ligand or background ligand solution was adjusted to an initial pH of

2.0 using a strategic combination of concentrated HCl and 10 M NaOH, as described above for the pH study, together with $\frac{1}{2}$ dilutions of each for finer pH adjustment. The pH was then incrementally increased (2 points at a time) using the NaOH solutions. Concentrated solutions of acid and base were used in order to ensure that no significant dilution occurred during the course of the experiment. Solutions were degassed with N_2 after each pH adjustment and steady-state voltammograms obtained.

For the investigations of cerium electrochemistry in EDTA as a function of metal:ligand ratio, it was not possible simply to add cerium to a single EDTA solution since the EDTA concentration would then be changing simultaneously. Therefore, separate $Ce(NO_3)_3 \cdot 6H_2O$ solutions were prepared at concentrations of 2.0, 6.0, 10.0, 14.0, and 24.0 mM at a constant concentration of EDTA (12 mM). Thus, voltammograms were obtained showing the effects of varying the metal:ligand ratio from 1:6 to 2:1. For this study, solutions were maintained at a constant pH of 2.0 using the acid/base adjustment techniques outlined above.

Finally, comparative studies on various rare earths in the EDTA solution environment were carried out by preparing 6.0 mM solutions of $Ce(NO_3)_3 \cdot 6H_2O$ (Aldrich, 99.999%, 233-297-2), $Sm(NO_3)_3 \cdot 6H_2O$ (Aldrich, 99.99%, 13759-83-6), and $Eu(NO_3)_3 \cdot xH_2O$ (Aldrich, 99.99%, 10031-53-5) in 12.0 mM EDTA. An equal volume mixture of these three lanthanides (2.0 mM of each) was also prepared. The solutions in this study were maintained at a constant pH of 1.4, since the pH variable proved to have a significant effect on the number and magnitude of redox peaks observed in EDTA medium.

CHAPTER 4

RESULTS AND DISCUSSION

4.1. Acid Study

4.1.1. Introduction

A significant portion of the literature on cerium electrochemistry describes investigations into the role played by acid concentration, as well as the effect of the type of aqueous acid constituting the working electrolyte, on the ability to resolve the Ce(IV)/Ce(III) redox couple. However, an overview of the literature (given in Chapter 1) reveals a general lack of consensus regarding the nature of the “optimum” solution environment for electrochemical investigations of this system. The preference for aqueous solutions of sulfuric acid over those of other acids such as nitric and hydrochloric is widespread, due to increased stabilization of cerium cations with sulfate, resulting in a shift of the redox couple to less positive potentials more accessible to commonly available working electrodes such as Pt, Au, and graphite.

While this favorable view of aqueous sulfuric acid is nearly universal, conflicting data abounds in the literature regarding the preference of high vs. low acid concentration, with results and recommendations offered at both ends of the concentration range. The acid study was designed to evaluate cerium redox chemistry as a function of acid concentration and the type of acid employed as the working electrolyte. Knowing of the

uncertainties in the literature regarding the optimum working electrode at which to observe Ce(IV)/Ce(III) electrochemistry, all experiments were conducted at Au, Pt, and glassy carbon (GC) electrodes in order to assess the importance of working electrode material.

4.1.2. Acid Study at the Au Electrode

Since aqueous sulfuric acid is the widely preferred medium for electrochemical investigations of the Ce(IV)/Ce(III) redox couple, the acid study was designed to determine the optimum concentration of sulfuric acid for studies of this system. In order to accomplish this, Ce(NO₃)₃ solutions, prepared at a concentration of 6.0 mM, were examined electrochemically using the technique of cyclic voltammetry. The working electrolytes consisted of aqueous solutions of increasing H₂SO₄ concentration. Figure 4.1 shows cyclic voltammetry obtained at the Au working electrode using concentrations of 0.1, 1.0, and 2.0 M sulfuric acid as the electrolytic solutions. A scan rate of 100 mV/s was applied to the working electrode for all voltammograms in the figure. Potentials were measured vs. a Ag/AgCl reference electrode. A background voltammogram (electrolyte only, no cerium) was collected for each system under investigation. A direct comparison of each cerium voltammogram with its corresponding background clearly shows the net current peaks due to cerium electrochemical activity. These backgrounds are represented in Figure 4.1 as the dashed lines and are paired with the data obtained for cerium in the same system (solid lines). Since Figure 4.1 b and c have been shifted up along the y axis for the purpose of clear comparison, crosshairs have been drawn on each voltammogram indicating the zero point for both the potential and current axes. The

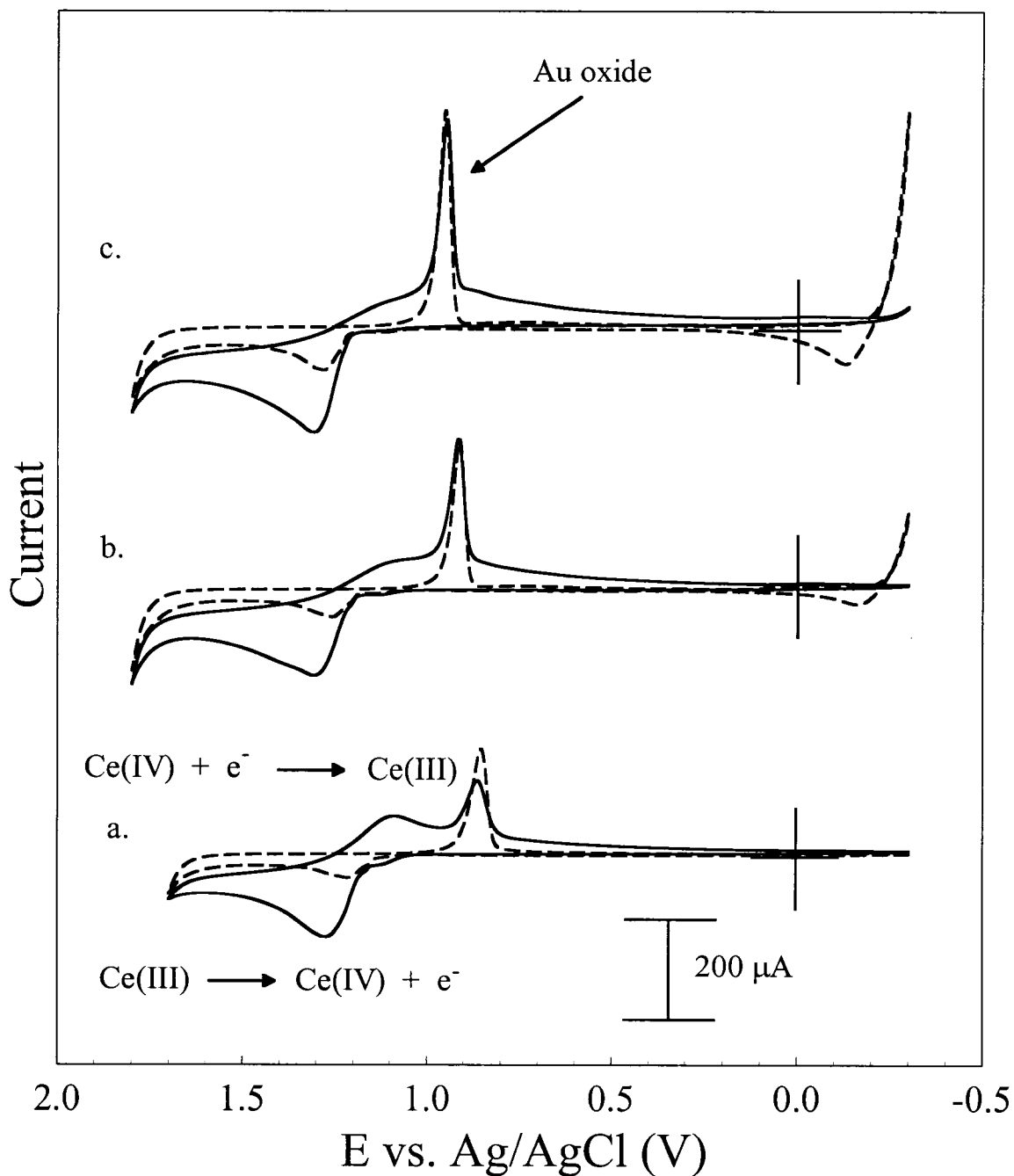


Figure 4.1. Steady-state voltammograms obtained at the Au working electrode for 6.0 mM $\text{Ce}(\text{NO}_3)_3 \cdot 6\text{H}_2\text{O}$ in a. 0.1 M H_2SO_4 b. 1.0 M H_2SO_4 and c. 2.0 M H_2SO_4 . ($\nu = 100$ mV/s, solid line = cerium solution, dashed line = background, no cerium).

current magnitude for the voltammograms in Figure 4.1 is defined by the 200 μA scale marking.

When evaluating the information contained in the figure, it is useful to consider again the definition and indicators of optimum experimental conditions. Reversible, or Nernstian, behavior for this system would yield a redox peak potential separation ($E_{pa} - E_{pc}$) of 59 mV, in accordance with the Nernst equation, since it is a single-electron transfer. Reversibility also requires a peak current ratio (i_{pa}/i_{pc}) of unity, signifying an equivalent incidence of oxidation and reduction at the electrode surface. Resolution from the background current arising from the oxidation of water was another characteristic evaluated in the determination of optimum experimental conditions. With these stipulations in mind, Figure 4.1 clearly shows a decrease in reversibility for the Ce(IV)/Ce(III) redox couple with increasing acid concentration. In contrast to the Ce(III) oxidation peak, which was not greatly affected throughout the entire concentration range employed in the experiments, the cathodic peak was not only decreased in magnitude, but also appeared to shift slightly in the negative potential direction. The increased oxidation of the gold electrode surface should not be expected to reduce peak magnitudes, since it has been shown to be a conductive extension of the electrode surface (Bonewitz and Schmid, 1970). The observed cathodic shift resulted in a Ce(IV) reduction peak that was not resolved from the gold oxide reduction peak located at approximately +0.9 V. Sufficient resolution was achieved between Ce(III) oxidation and the O_2 evolution background current for all three acid concentrations employed in the study. Thus, a visual assessment indicates that 0.1 M H_2SO_4 appears to yield more favorable voltammetry than the higher acid concentrations.

A more quantitative evaluation can be made using the data summarized in Table 4.1. Since the redox peaks rest on a non-zero background current, the peak current values reported in the table are *net* currents obtained by subtracting the existing background current at the potential of the cerium redox peak. From this information, it is clear that while none of these systems yielded completely reversible behavior ($\Delta E_p = 59$ mV), a significant decrease in reversibility was observed as H_2SO_4 concentration was increased from 0.1 to 2.0 M. This effect was demonstrated in the widening of the peak potential separation from 0.187 to 0.248 V and the further departure of the peak current ratio from unity, as it increased from 1.68 to 2.59.

Table 4.1. Electrochemical data obtained at the Au working electrode in increasing concentrations of H_2SO_4 ($\Delta E_p = E_{pa} - E_{pc}$ and $E_{1/2} = (E_{pa} + E_{pc})/2$). All peak current values (i_{pa} and i_{pc}) are net current values obtained through background subtraction.

	E_{pc} (V)	i_{pc} (μA)	E_{pa} (V)	i_{pa} (μA)	$E_{1/2}$ (V)	ΔE_p (V)	i_{pa}/i_{pc}
0.1 M H_2SO_4	1.089	71.38	1.276	-120.21	+1.183	0.187	1.68
1.0 M H_2SO_4	1.066	52.86	1.308	-119.27	+1.187	0.242	2.26
2.0 M H_2SO_4	1.061	48.18	1.309	-124.60	+1.185	0.248	2.59

While the results in 0.1 M H_2SO_4 do not conform to those characterizing a reversible system they are, nevertheless, the nearest to Nernstian results obtained at this electrode,

with a ΔE_p of 0.187 V and a peak current ratio of 1.68. These data place optimum sulfuric acid concentration at 0.1 M for the Au working electrode.

Having determined optimum sulfuric acid concentration for the Au electrode, it was also possible to determine whether the reduction and oxidation reactions of cerium in this medium were diffusion controlled. Because such processes demonstrate a linear correlation between reduction/oxidation peak currents and the square root of the experimental scan rate ($v^{1/2}$), a scan rate experiment was conducted in 0.1 M H₂SO₄ using a gold disk electrode (constant area) and yielded the data presented in Figures 4.2 and 4.3.

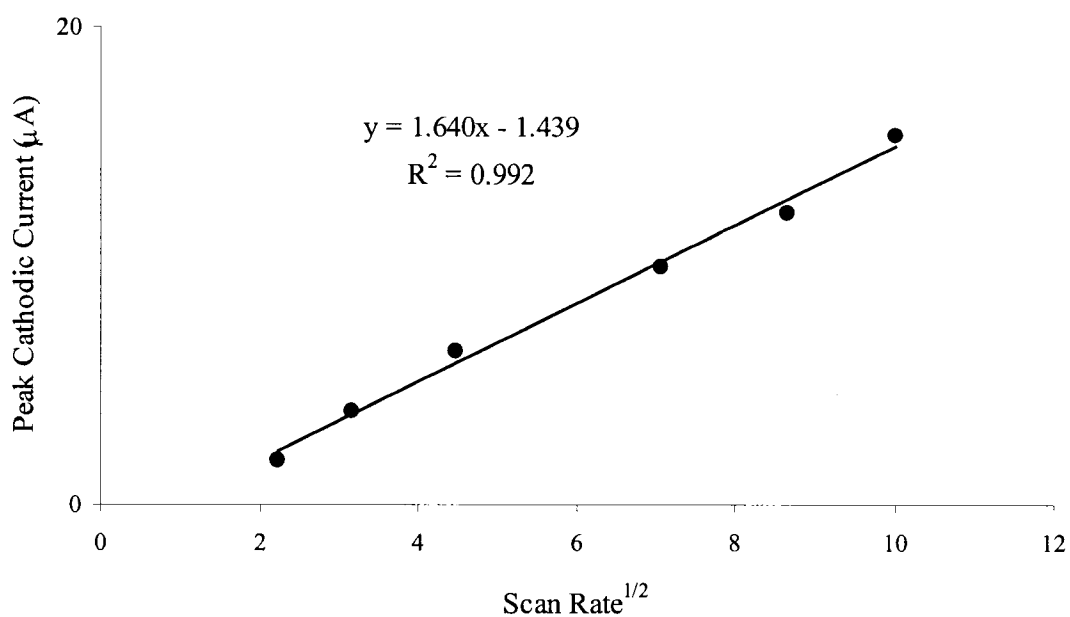


Figure 4.2. Peak Ce(IV) reduction current vs. $v^{1/2}$ at the Au disk working electrode in 0.1 M H₂SO₄ ($v = 5, 10, 20, 50, 75,$ and 100 mV/s, [Ce(III)] = 6.0 mM).

Figure 4.2 shows the peak cathodic (reduction) current response as a function of $v^{1/2}$. A strong linear relationship was demonstrated by the correlation coefficient (R^2) value of 0.992, which indicated that Ce(IV) reduction at a Au electrode is most likely diffusion controlled. The observation that this linear behavior was maintained over the entire range of experimental scan rates was also characteristic of a diffusion controlled process, since this linearity is predicted to be independent of v . The data presented in Figure 4.3 were obtained from the same scan rate experiments at a Au disk working electrode, this time plotting the peak oxidation current vs. $v^{1/2}$. Again, the marked linear correlation ($R^2 = 0.982$) indicated a diffusion-controlled electron transfer process for the oxidation of Ce(III).

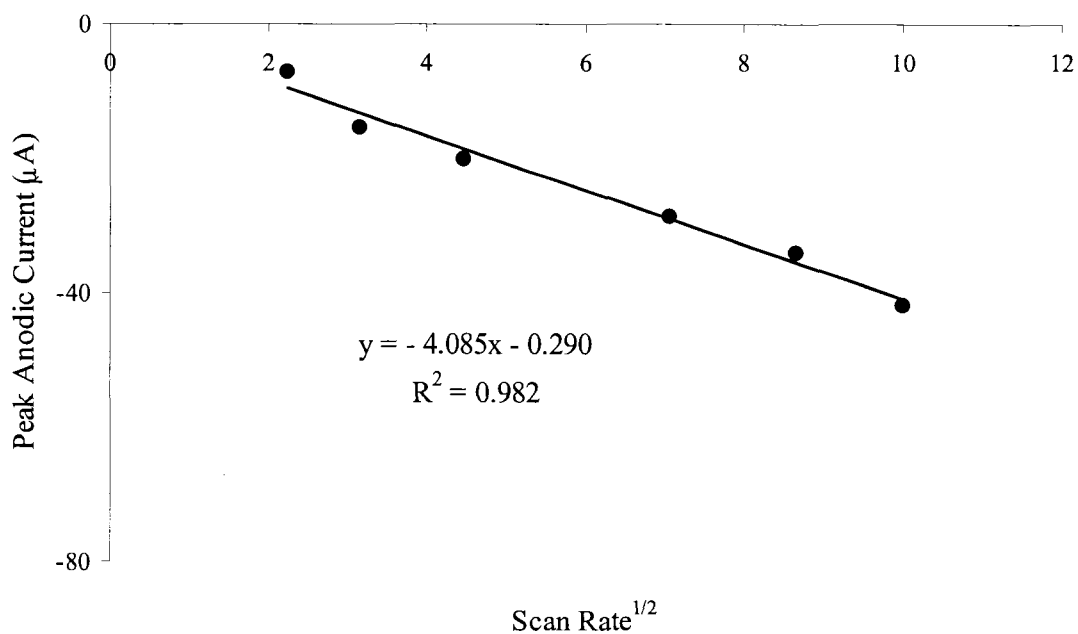


Figure 4.3. Peak Ce(III) oxidation current vs. $v^{1/2}$ at the Au disk working electrode in 0.1 M H₂SO₄ ($v = 5, 10, 20, 50, 75,$ and 100 mV/s, [Ce(III)] = 6.0 mM).

Taken together, the information contained in Figures 4.2 and 4.3 renders unlikely the suggestion of alternative electrode surface phenomena, such as the adsorption of electroactive cerium species, which has been suggested in the literature (Ferro and De Battisti, 2002). These workers also suggested the propensity of cerium species to block the gold electrode surface, and cited a significantly diminished reduction peak for Au oxide in the presence of cerium. While a slight attenuation of this peak can be observed for 0.1 M H₂SO₄, the data in Figure 4.1 do not conclusively support such a theory.

4.1.3. Acid Study at the Pt Electrode

In order to compare the relative abilities of the different electrodes to resolve cerium electrochemistry, an identical study using the same concentrations of aqueous sulfuric acid was carried out at the Pt electrode. The results of this study are shown in Figure 4.4. Once again, cerium voltammograms are presented with the corresponding background currents to allow for the confident assignment of peaks arising from cerium redox activity. It is useful first to identify those peaks characteristic of the reactions of the Pt electrode itself, since Pt electrodes oxidize readily in acidic solution environments (Hammond and Winograd, 1977; Shibata and Sumino, 1981; Benziger *et al.*, 1986; Kriksunov *et al.*, 1994). The two symmetric pairs of redox peaks located between -0.2 and 0 V arise from the reduction and oxidation of adsorbed hydrogen at different, energetically non-equivalent sites of the polycrystalline Pt (Loo and Furtak, 1980; Ross, 1981). The positive current peak observed at approximately +0.3 to +0.6 V, depending on the solution environment, is evidence of the reduction of a Pt oxide layer at the electrode surface. The accessible potential window for all working electrodes in aqueous systems is limited by the reduction and oxidation of the medium itself. For the Pt

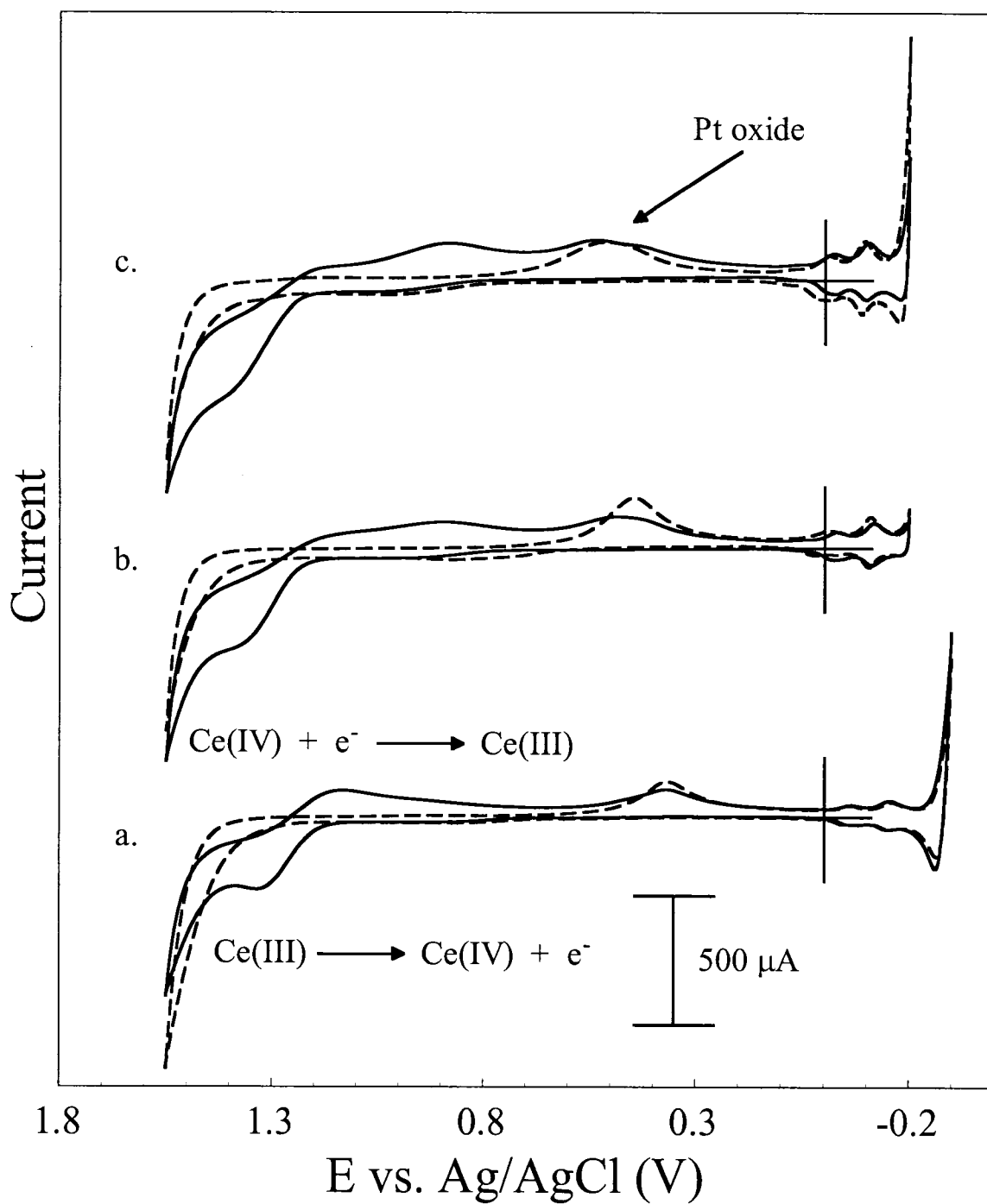


Figure 4.4. Steady-state voltammograms obtained at the Pt working electrode for 6.0 mM $\text{Ce(NO}_3)_3 \cdot 6\text{H}_2\text{O}$ in *a.* 0.1 M H_2SO_4 *b.* 1.0 M H_2SO_4 and *c.* 2.0 M H_2SO_4 ($\nu = 100$ mV/s, solid line = cerium solution, dashed line = background, no cerium).

electrode, this working range between the evolution of O₂ at the positive potential limit and the reduction of protons to H₂ at sufficiently negative potentials was about 1.8 V (+1.5 to -0.3 V). This potential window was slightly more restricted than the ~2.0 V window provided by the Au working electrode. The narrower potential range offered by the Pt electrode may indicate an exertion of a catalytic effect on water decomposition reactions at its surface. A summary of electrochemical data obtained from the acid study at Pt is contained in Table 4.2.

Table 4.2. Electrochemical data obtained at the Pt working electrode in increasing concentrations of H₂SO₄ ($\Delta E_p = E_{pa} - E_{pc}$ and $E_{1/2} = (E_{pa} + E_{pc})/2$). All peak current values (i_{pa} and i_{pc}) are net current values obtained through background subtraction.

	E_{pc} (V)	i_{pc} (μA)	E_{pa} (V)	i_{pa} (μA)	$E_{1/2}$ (V)	ΔE_p (V)	i_{pa}/i_{pc}
0.1 M H₂SO₄	1.133	98.15	1.335	-61.42	+1.234	0.202	0.63
1.0 M H₂SO₄	0.887	94.81	1.436	-137.67	+1.162	0.549	1.45
2.0 M H₂SO₄	0.881	125.84	1.442	-159.00	+1.162	0.561	1.26

At the Au electrode, the redox peak separation remained relatively constant, increasing by only ~60 mV over the acid concentration range employed in the study. Interestingly, the voltammetry obtained at Pt showed an increase in ΔE_p of ~350 mV when acid concentration was increased from 0.1 to 1.0 M, due mostly to the shift of the cathodic peak toward more negative potentials. The peak potential separation did not,

however, change significantly when the concentration was further increased to 2.0 M. This effect is perhaps best explained by the influence of the oxide layer, which forms on Pt electrode surfaces in acidic solution. The retardation of Ce(IV) reduction by platinum oxide has been suggested (Greef and Aulich, 1967), and would explain the observation of cerium reduction at more negative potentials when acid concentration is higher, and the electrode more extensively oxidized. The oxide can thus be described as increasing the electrode overpotential for the reduction of Ce(IV), considerably decreasing the reversibility of the cerium redox couple at this electrode at high acid concentrations. This effect presents considerable complications, and is difficult to address experimentally, since the oxide layer continues to grow throughout the duration of the experiment. Another outcome of increasing acid concentration at the Pt electrode was to shift the oxidation peak slightly in the positive direction, increasing interference from the O₂ evolution current. This undesirable effect was not observed at Au, and presented another drawback to the use of Pt as the working electrode material for investigations of the cerium system at high acid concentrations. Just as for the Au electrode, optimum conditions at Pt were also realized in 0.1 M H₂SO₄. The ΔE_p value of 0.202 V, obtained at this concentration, indicated a slightly less reversible redox reaction than that observed at Au ($\Delta E_p = 0.187$).

The possibility of adsorption effects at the electrode surface was investigated by means of a scan rate study carried out at a Pt disk electrode. Figures 4.5 and 4.6 show the peak cathodic and anodic current responses to increases in the experimental scan rate. The data shown in Figure 4.5 reveal the significance of the linear relationship between the peak Ce(IV) reduction current observed at Pt and the square root of the applied scan

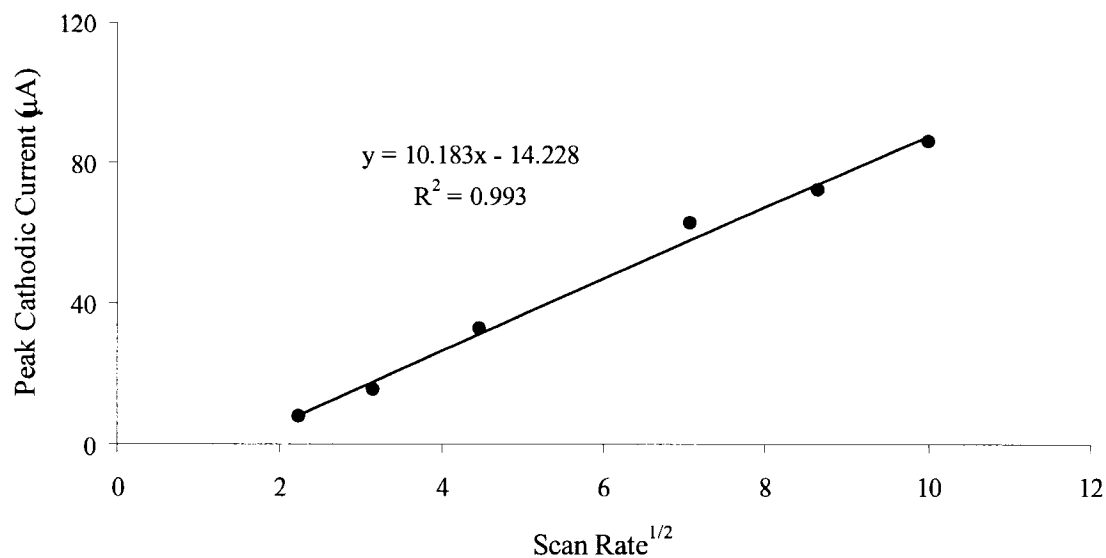


Figure 4.5. Peak Ce(IV) reduction current vs. $v^{1/2}$ at the Pt disk working electrode in 0.1 M H₂SO₄ ($v = 5, 10, 20, 50, 75,$ and 100 mV/s, [Ce(III)] = 6.0 mM).

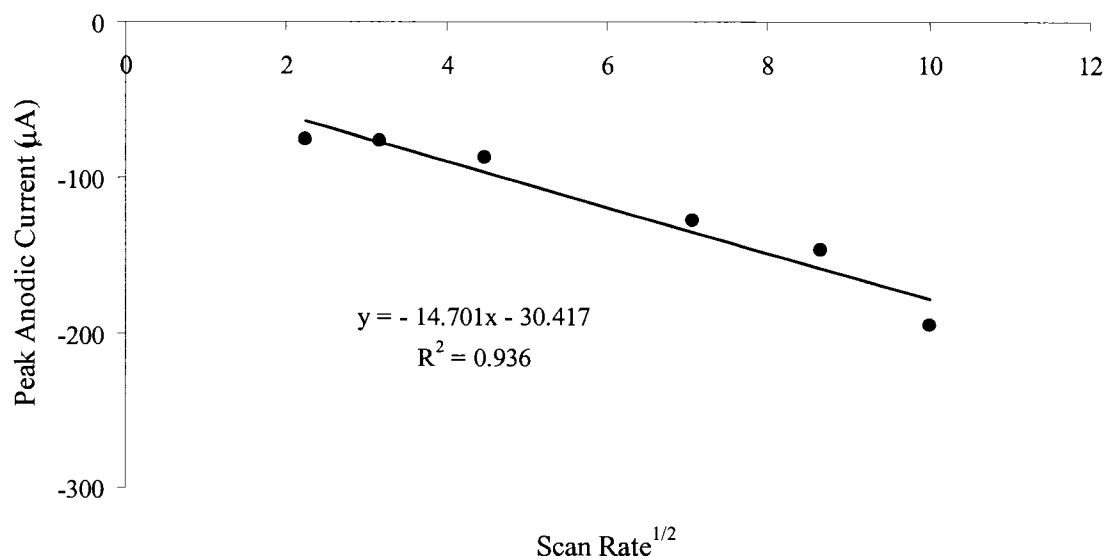


Figure 4.6. Peak Ce(III) oxidation current vs. $v^{1/2}$ at the Pt disk working electrode in 0.1 M H₂SO₄ ($v = 5, 10, 20, 50, 75,$ and 100 mV/s, [Ce(III)] = 6.0 mM).

rate ($R^2 = 0.993$). This relationship held throughout the scan rate range employed in the experiment. The trendline shown in Figure 4.6, obtained by plotting the peak Ce(III) oxidation current vs. the square root of the scan rate, demonstrates a somewhat less linear response, with an R^2 value of 0.936. This behavior of the oxidation peak currents approaching non-linearity may reflect some degree of adsorption phenomena at the electrode surface, possibly as a result of the interaction of cerium species with surface oxides. Such adsorption effects, if truly present, would also explain the slightly less reversible ΔE_p value at Pt compared to Au, since this would be a result of limitations on the diffusion of cerium species toward and away from the electrode. The less linear response of the Ce(III) oxidation peak at Pt may also simply be due to interference from the O_2 evolution current, since the oxidation peak at Pt occurred at more positive potentials than the corresponding peak at Au (+1.335 V compared to +1.276 V). Thus, our ability to obtain accurate current values from this peak may have been compromised at slow scan rates.

4.1.4. Acid Study at the Glassy Carbon Electrode

After examining the effect of increasing acid concentration on the cerium redox couple at both Au and Pt electrodes, comparison with the results at the non-metallic GC working electrode was sought. Data obtained for the acid study at the GC electrode are presented in Figure 4.7 and summarized in Table 4.3. Similar to the results obtained at the metal electrodes, a diminishing of the voltammetric response associated with cerium redox activity was observed as acid concentration was increased. This decrease in current magnitude was most marked for the transition from 0.1 to 1.0 M, a tenfold concentration increase. In addition to this decrease in peak magnitude and definition, a

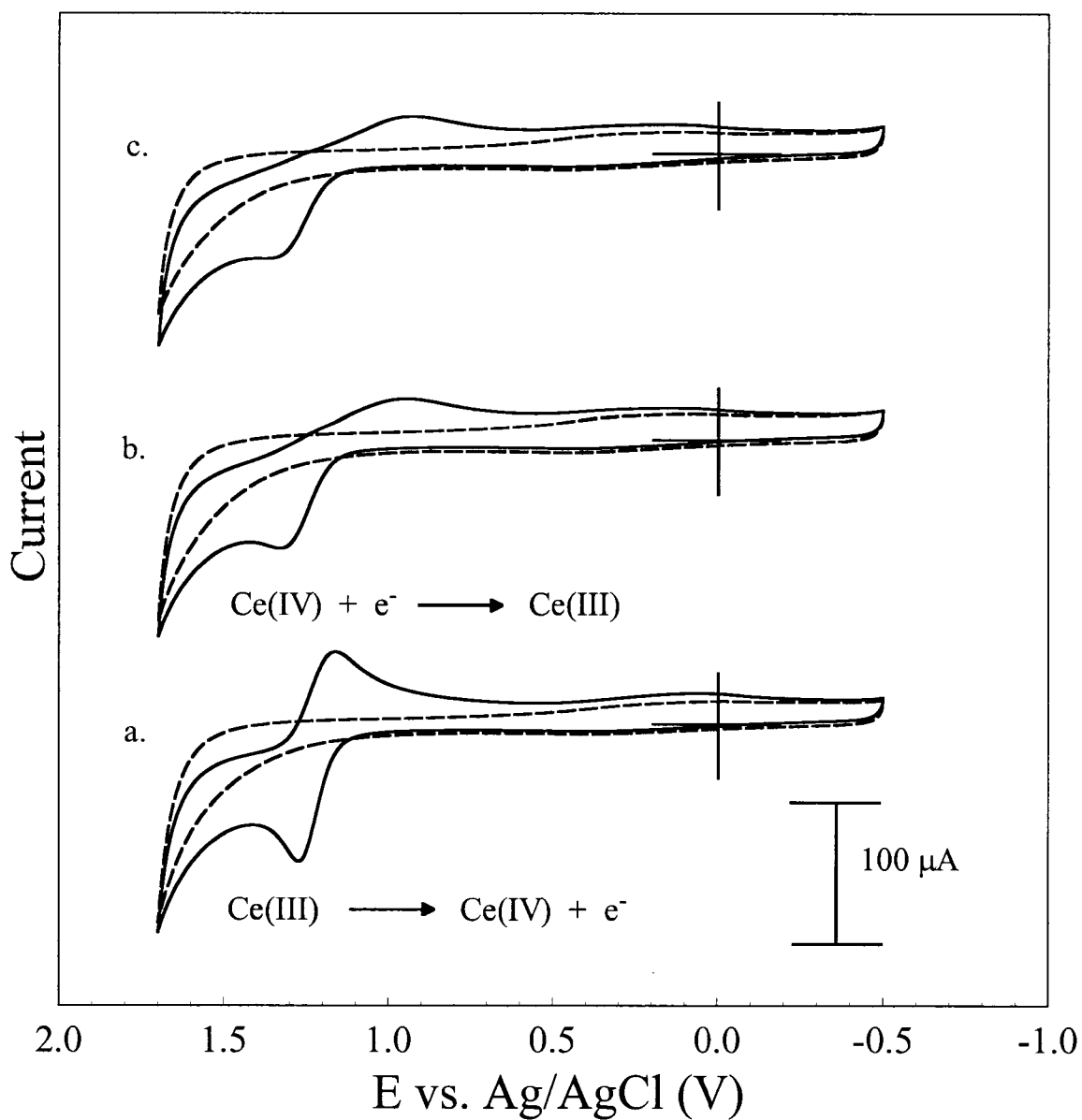


Figure 4.7. Steady-state voltammograms obtained at the GC working electrode for 6.0 mM $\text{Ce}(\text{NO}_3)_3 \cdot 6\text{H}_2\text{O}$ in *a.* 0.1 M H_2SO_4 *b.* 1.0 M H_2SO_4 and *c.* 2.0 M H_2SO_4 . ($\nu = 100$ mV/s, solid line = cerium solution, dashed line = background, no cerium).

widening of the peak potential separation from 0.112 V to 0.489 V was observed, concomitant with the rise in acid concentration from 0.1 to 2.0 M. These results support the conclusion that the electrochemical reversibility of the cerium system is hindered at more acidic conditions. The reduction in the magnitude of the voltammetric response observed with increasing acid concentration at GC has been ascribed to diminished diffusion coefficients with increasing solution viscosity (Fang *et al.*, 2002). The ΔE_p obtained at GC in 2.0 M H₂SO₄ was intermediate in value between those obtained at Au

Table 4.3. Electrochemical data obtained at the GC working electrode in increasing concentrations of H₂SO₄ ($\Delta E_p = E_{pa} - E_{pc}$ and $E_{1/2} = (E_{pa} + E_{pc})/2$). All peak current values (i_{pa} and i_{pc}) are net current values obtained through background subtraction.

	E_{pc} (V)	i_{pc} (μA)	E_{pa} (V)	i_{pa} (μA)	$E_{1/2}$ (V)	ΔE_p (V)	i_{pa}/i_{pc}
0.1 M H₂SO₄	1.162	48.21	1.274	-79.81	+1.218	0.112	1.66
1.0 M H₂SO₄	0.946	23.25	1.329	-53.94	+1.138	0.383	2.32
2.0 M H₂SO₄	0.928	22.86	1.417	-42.10	+1.173	0.489	1.84

and Pt. In other words, the redox couple at GC was more reversible at 2.0 M acid than that observed at Pt, and less reversible than the voltammetry at Au, which yielded the most Nernstian behavior of the three at the highest acid concentration implemented in the study. The GC electrode, however, was able to yield the nearest to Nernstian voltammetry among the three electrodes at 0.1 M sulfuric acid concentration (0.112 V

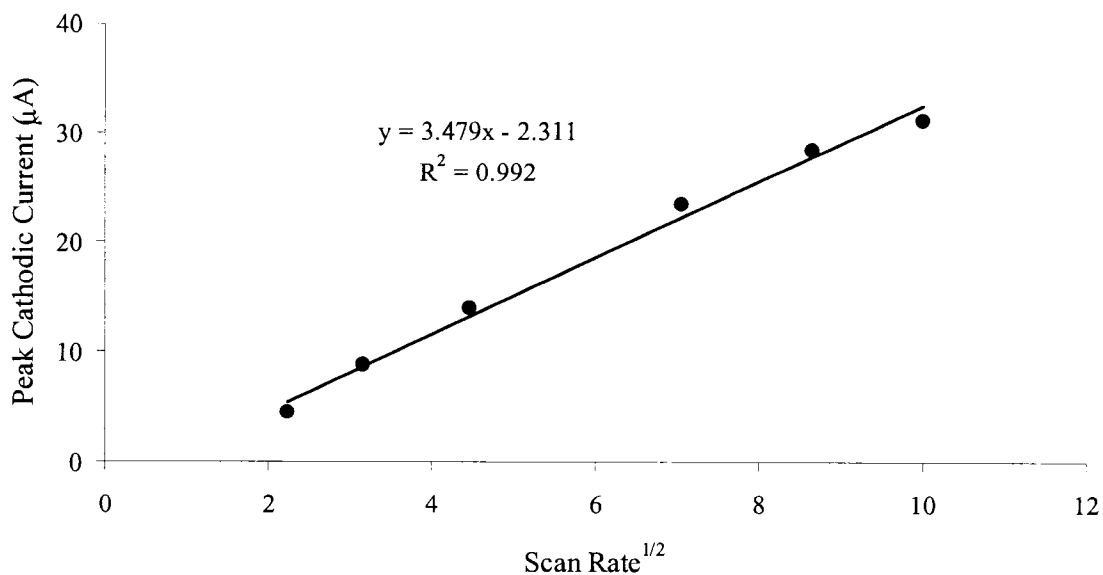


Figure 4.8. Peak Ce(IV) reduction current vs. $v^{1/2}$ at the GC disk working electrode in 0.1 M H_2SO_4 ($v = 5, 10, 20, 50, 75,$ and 100 mV/s, $[Ce(III)] = 6.0$ mM).

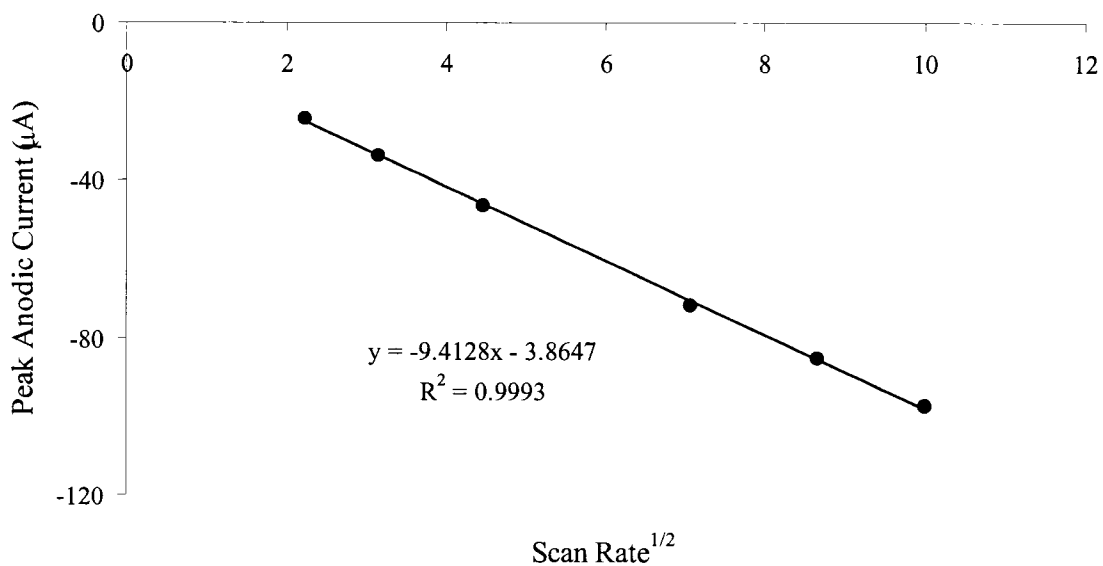


Figure 4.9. Peak Ce(III) oxidation current vs. $v^{1/2}$ at the GC disk working electrode in 0.1 M H_2SO_4 ($v = 5, 10, 20, 50, 75,$ and 100 mV/s, $[Ce(III)] = 6.0$ mM).

compared to 0.187 V and 0.202 V for Au and Pt, respectively). Data from scan rate experiments conducted at the GC electrode in 0.1 M H₂SO₄ are presented in Figures 4.8 and 4.9. While the significance of the linear correlation between peak reduction current and the square root of the scan rate is comparable ($R^2 = 0.992$) to that demonstrated by the metal electrodes, the anodic peak/scan rate relationship is much more linear at the glassy carbon electrode ($R^2 = 0.9993$). This may demonstrate the nature of the redox process at GC to be strictly diffusion controlled, without adsorption processes placing limitations on the flux of species to and from the electrode surface. Less linear results for the Ce(III) oxidation current at Au and Pt may indicate the effects of adsorption on the diffusion of electroactive species.

Interestingly, as shown in Figure 4.7, the experiment at the GC electrode yielded good resolution of the redox couple at even the highest acid concentration used, although the Ce(III) oxidation peak was still somewhat close to the positive limit of the potential window. While the Au electrode offered the best resolution from the O₂ evolution current, interference with the observation of Ce(IV) reduction was encountered from the Au oxide reduction peak at high acid concentrations. Pt was also not a good choice at more acidic conditions, yielding the least reversible behavior of the three electrodes in the 2.0 M H₂SO₄ solution. Optimum conditions for all three electrodes, however, were realized at 0.1 M sulfuric acid concentration.

4.1.5. Ce(IV)/Ce(III) Electrochemistry in Nitric Acid

The determination in the sulfuric acid experiments of the favorable effect of lower acid concentrations on the resolution of Ce(IV)/Ce(III) electrochemistry suggested the possibility of comparison with the same concentration of an alternate acid. For this

reason, cyclic voltammetry was carried out on the cerium redox couple in 0.1 M HNO₃, and the results obtained at the three electrodes are shown in Figure 4.10. The corresponding data is summarized in Table 4.4.

Table 4.4. Electrochemical data obtained at the GC, Au, and Pt working electrodes in 0.1 M nitric acid ($\Delta E_p = E_{pa} - E_{pc}$ and $E_{1/2} = (E_{pa} + E_{pc})/2$). All peak current values (i_{pa} and i_{pc}) are net current values obtained through background subtraction.

	E_{pc} (V)	i_{pc} (μ A)	E_{pa} (V)	i_{pa} (μ A)	$E_{1/2}$ (V)	ΔE_p (V)	i_{pa}/i_{pc}
0.1 M HNO₃ (GC)	1.239	45.97	1.412	-46.79	+1.326	0.173	1.02
0.1 M HNO₃ (Au)	1.190	63.28	1.408	-91.18	+1.299	0.218	1.44
0.1 M HNO₃ (Pt)	1.273	208.04	1.435	-195.00	+1.354	0.162	0.94

Electrochemical investigations performed on the Ce(IV)/Ce(III) system in 0.1 M HNO₃ yielded comparable results to those obtained in 0.1 M H₂SO₄. As depicted in Figure 4.10, satisfactory redox peak resolution was observed using all three working electrodes in nitric acid medium (note the variation in scale for the three voltammograms). Voltammetry obtained at the Pt and GC electrodes, in particular, showed good reversibility with ΔE_p values of 0.162 V and 0.173 V, respectively. Peak current ratios obtained for these electrodes were also approximately equal to unity, showing a near-Nernstian redox process. A positive shift, on the order of ~100 mV relative to peak positions in 0.1 M H₂SO₄, was observed for the redox couple at the three

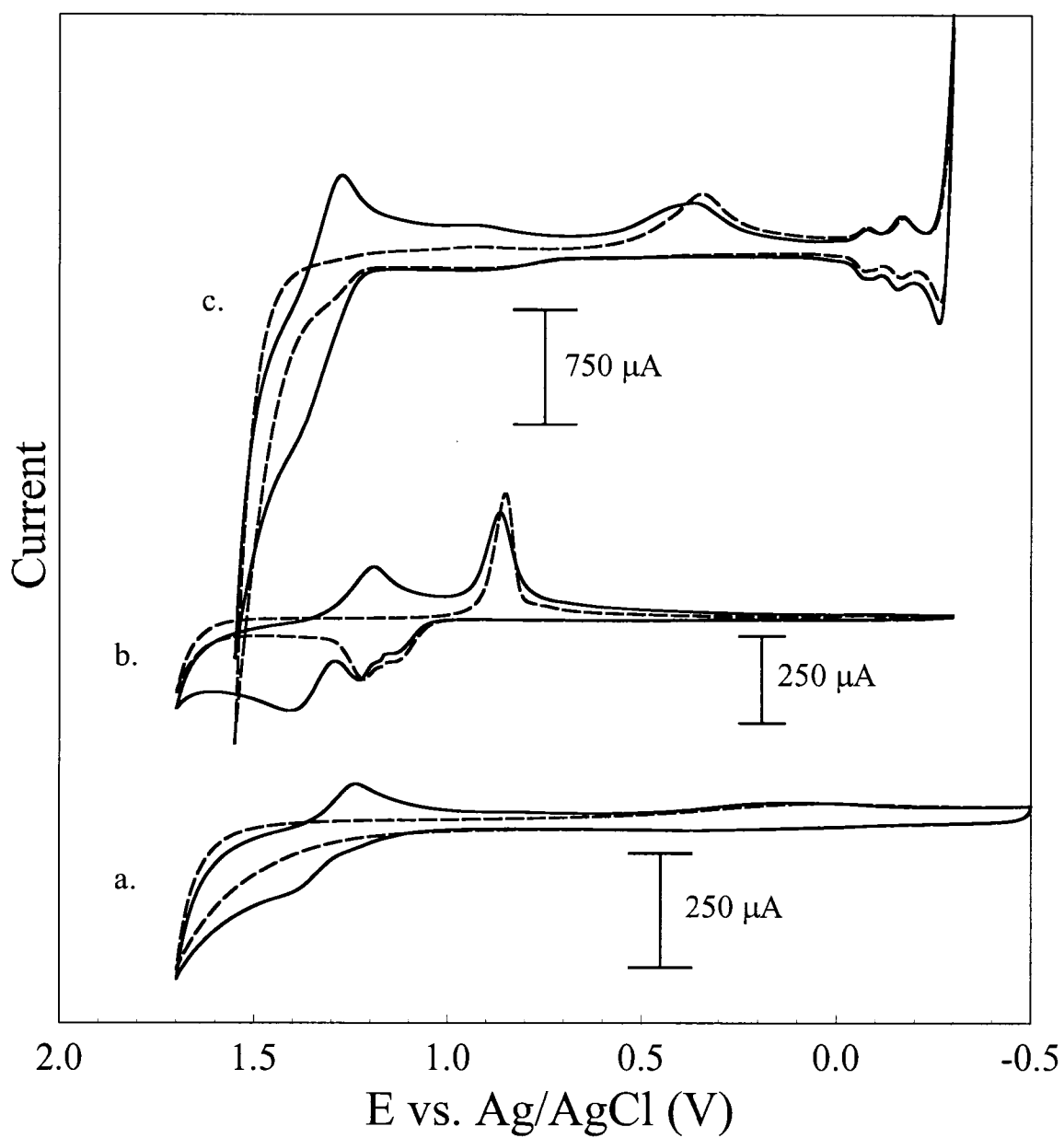


Figure 4.10. Steady-state voltammograms obtained for 6.0 mM $\text{Ce}(\text{NO}_3)_3 \cdot 6\text{H}_2\text{O}$ in 0.1 M HNO_3 at the *a.* GC *b.* Au and *c.* Pt working electrode ($v = 100 \text{ mV/s}$, solid line = cerium solution, dashed line = background, no cerium).

electrodes involved in the nitric acid experiment, resulting in an experimental $E_{1/2}$ of approximately +1.3 V compared to the $\sim +1.2$ V obtained in 0.1 M H_2SO_4 . This anodic shift is perhaps the greatest drawback to the use of aqueous nitric acid as the electrolytic medium for investigations of Ce electrochemistry, since the redox couple is not sufficiently separated from the background oxidation currents, and this was one of the most important requirements of optimum conditions. The observation of Ce(IV)/Ce(III) redox behavior at slightly less positive potentials in H_2SO_4 than in other acids, such as HNO_3 , has been ascribed to more stable sulfate complexation of both the Ce(III) and Ce(IV) cations (Kunz, 1931; Noyes and Garner, 1936; Smith and Getz, 1938; Connick and Mayer, 1951; Hardwick and Robertson, 1951). Other than this positive potential shift, the results of the HNO_3 experiments revealed that the substitution of nitrate for bisulfate/sulfate anions did not significantly alter the cerium redox behavior observed in the presence of a comparable proton concentration.

The optimum results in the acid study (most reversible redox couple, peak current ratios nearest to unity, and best resolution from background currents) were obtained at 0.1 M sulfuric acid concentration at all working electrodes examined. One of the advantages associated with the use of the GC electrode in this application was its higher overpotential for oxygen evolution, resulting in a wider potential window through which to observe cerium redox behavior. These favorable results at GC are at variance with previous work claiming the inefficiency of GC for electrochemical investigations of the cerium system (Sacchetto *et al.*, 1992). There is concurrence, however, with the work of other researchers who observed that background currents hindered the observation of Ce(III) oxidation at noble metal electrodes such as Pt and Au, possibly due to oxide

formation at their surfaces, or their catalysis of the water oxidation reaction (Bishop and Cofré, 1981; Kiekens *et al.*, 1981). Thus, cerium redox behavior may be successfully monitored at more highly acidic conditions than those generally employed, using the glassy carbon working electrode in place of Au or Pt. These observations illustrate the profound effect of working electrode composition on the observed electrochemistry of the cerium redox system.

4.2. pH Study

4.2.1. Introduction

The information gleaned from the acid study demonstrated that resolution of the Ce(IV)/Ce(III) redox couple was favored at 0.1 M acid concentration, with H₂SO₄ being the preferred acid medium. These optimum solution conditions correspond to a pH of 1.0 and an ionic strength (μ) of 0.3. The question raised by this study regarded the exact nature of the effect we observed as acid concentration was increased. In other words, as we increased the concentration of acid in the working electrolyte, we were actually making three simultaneous changes to the solution environment. These changes included the lowering of the solution pH, increasing its ionic strength, and increasing the concentration of sulfate anions in solution. A way of experimentally isolating the pH variable was sought, and found in the form of K₂SO₄. To this end, cerium electrochemistry was investigated at all three electrodes in a 0.1 M solution of K₂SO₄ at the same ionic strength and SO₄²⁻ concentration as the optimum conditions determined by the acid study. Since the acid study showed the gradual disappearance of the voltammetric response for cerium at pH values lower than 1, the second part of the pH

study was designed to investigate the electrochemical behavior of Ce(IV)/Ce(III) at the higher end of the pH scale. To accomplish this, the effects of increasing solution pH were examined in sulfate solutions of fixed pH at a constant ionic strength, so that pH would be the only variable in the experiment. The ionic strength solution parameter has not come under particular scrutiny in the literature.

4.2.2. Ce(IV)/Ce(III) Electrochemistry in 0.1 M K₂SO₄

Cyclic voltammetric experiments conducted on the cerium redox couple in 0.1 M K₂SO₄ ($\mu = 0.3$, [SO₄²⁻] = 0.1 M, pH = 6.1) are depicted in Figure 4.11 and illustrate the absence of any observable voltammetric response for cerium at either the Au or Pt working electrodes (Figure 4.11 b and c, respectively). Although a visible attenuation of the Pt and Au oxide reduction currents from those of the backgrounds (less pronounced for Au) was observed in the presence of cerium, there are no peak currents clearly attributable to cerium. However, as the figure interestingly reveals, resolution of the Ce(IV)/Ce(III) redox couple was possible at the GC electrode, although with an extremely large peak potential separation of 1.23 V, indicating a very irreversible redox process. This increase in the value of ΔE_p was mostly due to the significant shift of the Ce(IV) reduction peak in the negative potential direction ($E_{pc} = -0.146$ V compared to +1.162 V at GC in 0.1 M H₂SO₄). The peak current ratio, however, was very close to unity ($i_{pa}/i_{pc} = 1.38$), showing a near-equal occurrence of the two electrode processes despite significant kinetic limitations on electron transfer from the electrode to the Ce(IV) solution species.

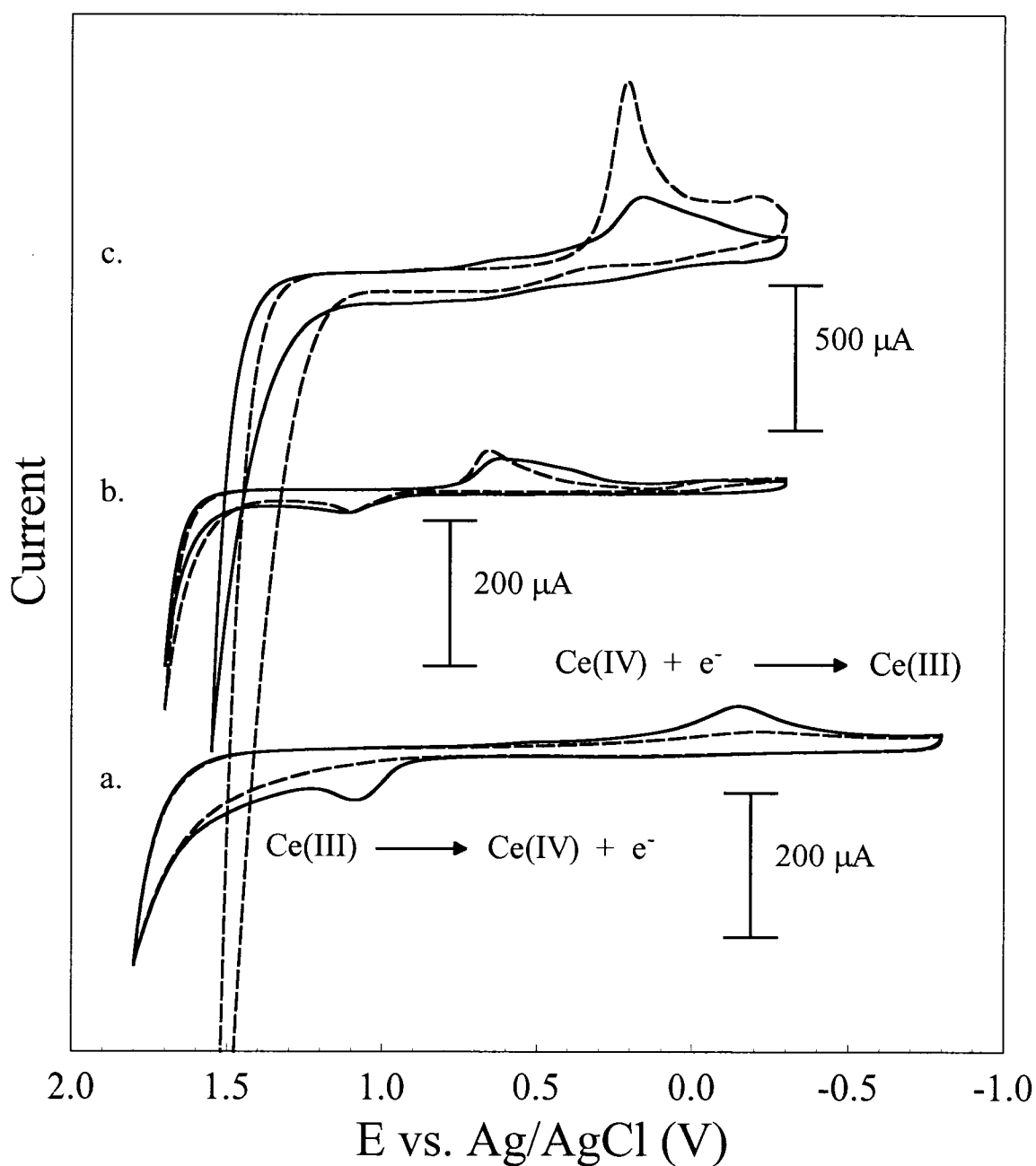


Figure 4.11. Steady-state voltammograms obtained for 6.0 mM $\text{Ce}(\text{NO}_3)_3 \cdot 6\text{H}_2\text{O}$ in 0.1 M K_2SO_4 at a. GC b. Au and c. Pt working electrodes ($\nu = 100 \text{ mV/s}$, solid line = cerium solution, dashed line = background, no cerium).

4.2.3. pH Study at the Au, Pt, and GC Electrodes

In summary, the results obtained from experiments in 0.1 M K_2SO_4 showed that the solution pH, and not the ionic strength, truly was the key to successfully resolving the Ce(IV)/Ce(III) redox couple. Since the acid study revealed that a solution pH below 1 (acid concentrations higher than 0.1 M) was detrimental to the observation of cerium electrochemistry, and the K_2SO_4 study showed that a pH of ~ 6 was too high, a question was raised as to the pH range available for observing Ce redox chemistry at each of the three electrodes. A pH study was therefore outlined utilizing HSO_4^-/SO_4^{2-} solutions of constant ionic strength (0.3) and increasing pH (3.4 and 4.7), to determine the effect of solution pH, as an isolated variable, on cerium electrochemistry. Cyclic voltammetry was used to compare cerium redox behavior in these solutions to that observed in the 0.1 M sulfuric acid medium (pH = 1.0). The results of the pH study at the Au electrode are shown in Figure 4.12 and reveal the damaging effects of increasing solution pH on redox couple resolution, with the complete absence of observable redox activity at pH 4.7. At the intermediate pH value of 3.4, cerium electrochemistry at this electrode was no longer clearly discernible and definitely not reversible, with what appeared to be a current for Ce(IV) reduction appearing at $\sim +0.35$ V.

With the use of Pt as the working electrode (Figure 4.13), the increase in solution pH had an even more pronounced effect, eliminating observable redox activity at a pH of only 3.4. Again, the voltammetry in the figure corresponding to pH 1.0 was that obtained in the acid study at 0.1 M sulfuric acid concentration. Interestingly, the presence of cerium in solution resulted in reduced Pt oxide reduction currents, especially at higher pH. This may indicate an inhibition effect of cerium on the formation of surface oxides.

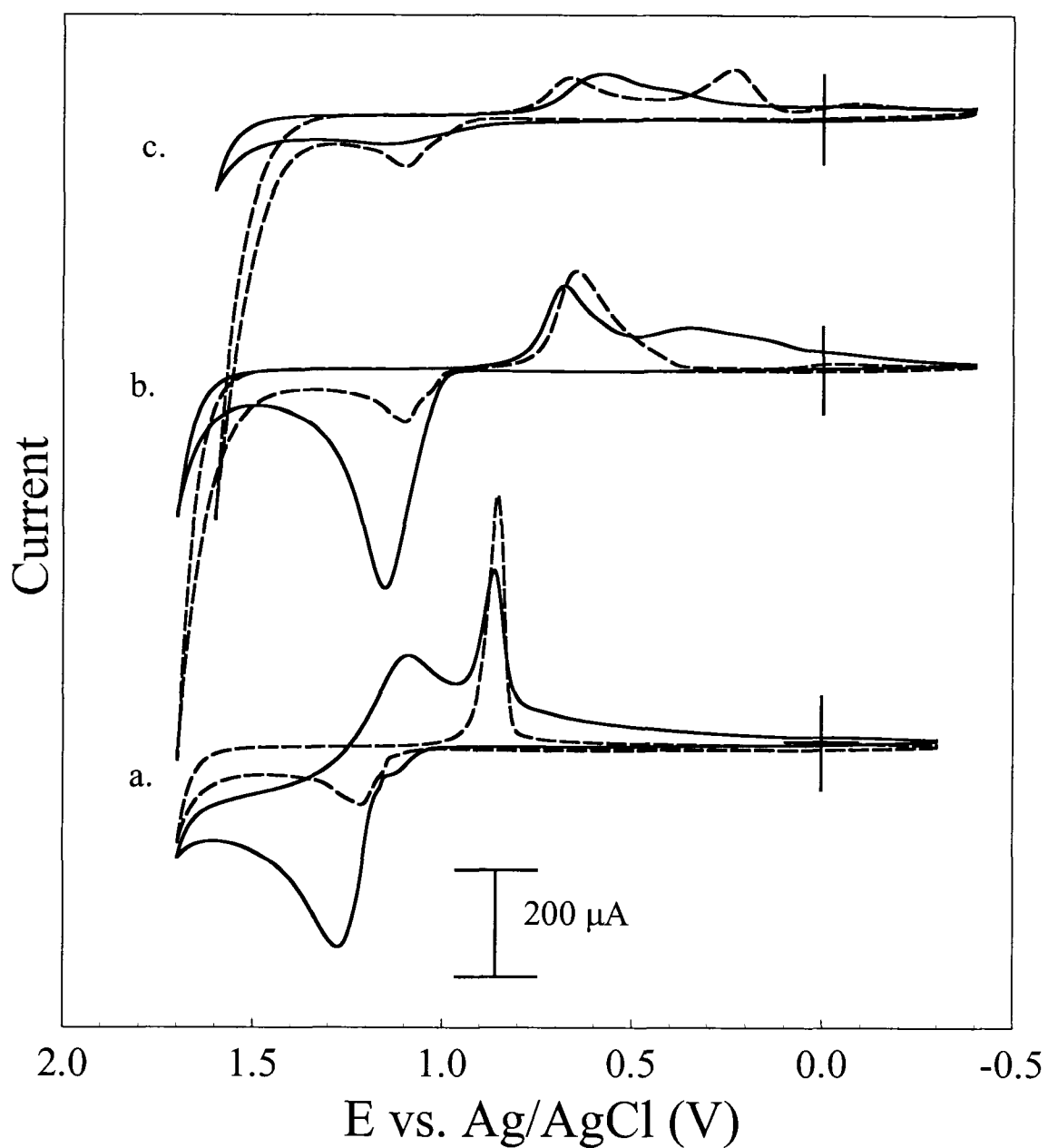


Figure 4.12. Steady-state voltammograms obtained at the Au working electrode for 6.0 mM $\text{Ce}(\text{NO}_3)_3 \cdot 6\text{H}_2\text{O}$ at *a.* pH = 1.0 *b.* pH = 3.4 and *c.* pH = 4.7 ($v = 100 \text{ mV/s}$, solid line = cerium solution, dashed line = background, no cerium).

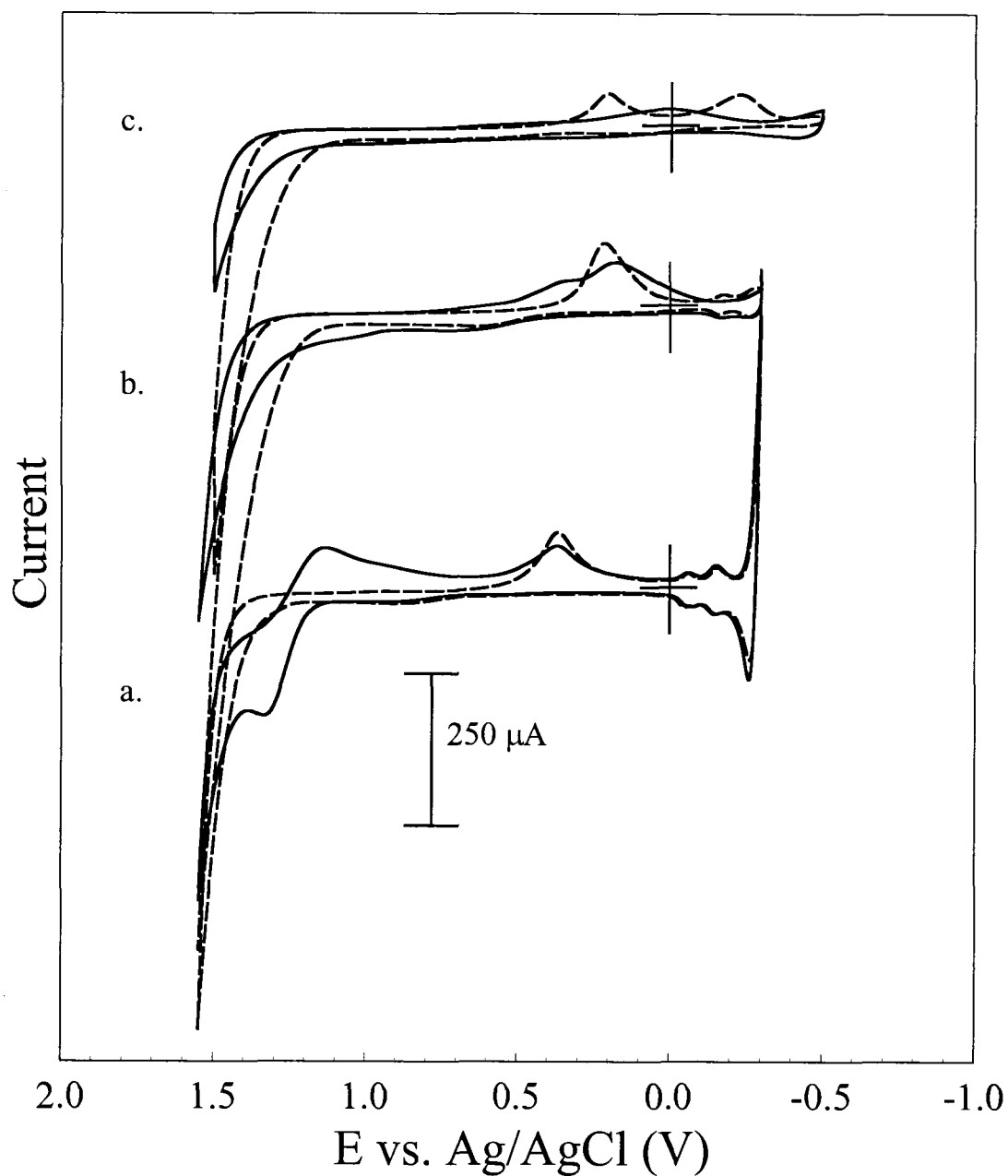


Figure 4.13. Steady-state voltammograms obtained at the Pt working electrode for 6.0 mM $\text{Ce}(\text{NO}_3)_3 \cdot 6\text{H}_2\text{O}$ at *a.* pH = 1.0 *b.* pH = 3.4 and *c.* pH = 4.7 ($v = 100 \text{ mV/s}$, solid line = cerium solution, dashed line = background, no cerium).

Profoundly different results were obtained when glassy carbon was used as the electrode material. These observations, summarized in Figure 4.14, revealed that despite an increase in redox peak separation (decreased reversibility) compared to that obtained at optimum conditions, cerium redox activity was nevertheless observable using the GC electrode. This was true even at a pH of 4.7, the highest solution pH employed in the study. Once again, just as shown by the acid study, it was possible to resolve the Ce(IV)/Ce(III) redox couple using the GC electrode in solution environments that precluded any such observation at either of the metal electrodes.

There are several possible factors which may play a role in the inability to observe Ce redox activity at either Au or Pt at higher pH. It has been suggested that metal electrodes may require acid activation before electron transfer to and from cerium species can occur (Greef and Aulich, 1968). Additionally, it has been proposed that oxide formation may hinder the electronic interaction of cerium with the metal electrode surface (Kiekens *et al.*, 1981). There are, however, several inconsistencies encountered in the attempt to reconcile these hypotheses with our experimental results. First, if acid activation enhances electron transfer at the metal electrodes, then higher, more defined redox peak currents for cerium should have been observed at the higher acid concentrations examined in the acid study (1.0 and 2.0 M). This was not the case, since redox activity was no longer clearly observable at acid concentrations higher than 0.1 M and reduced peak currents were observed even at the GC electrode. A pH of 1 did, however, yield profoundly better results than the less acidic values (pH 3.4 and 4.7) investigated in the pH study. These data indicate that, while acidic conditions appear to be necessary for successful resolution of the cerium redox couple, there is some optimum pH value

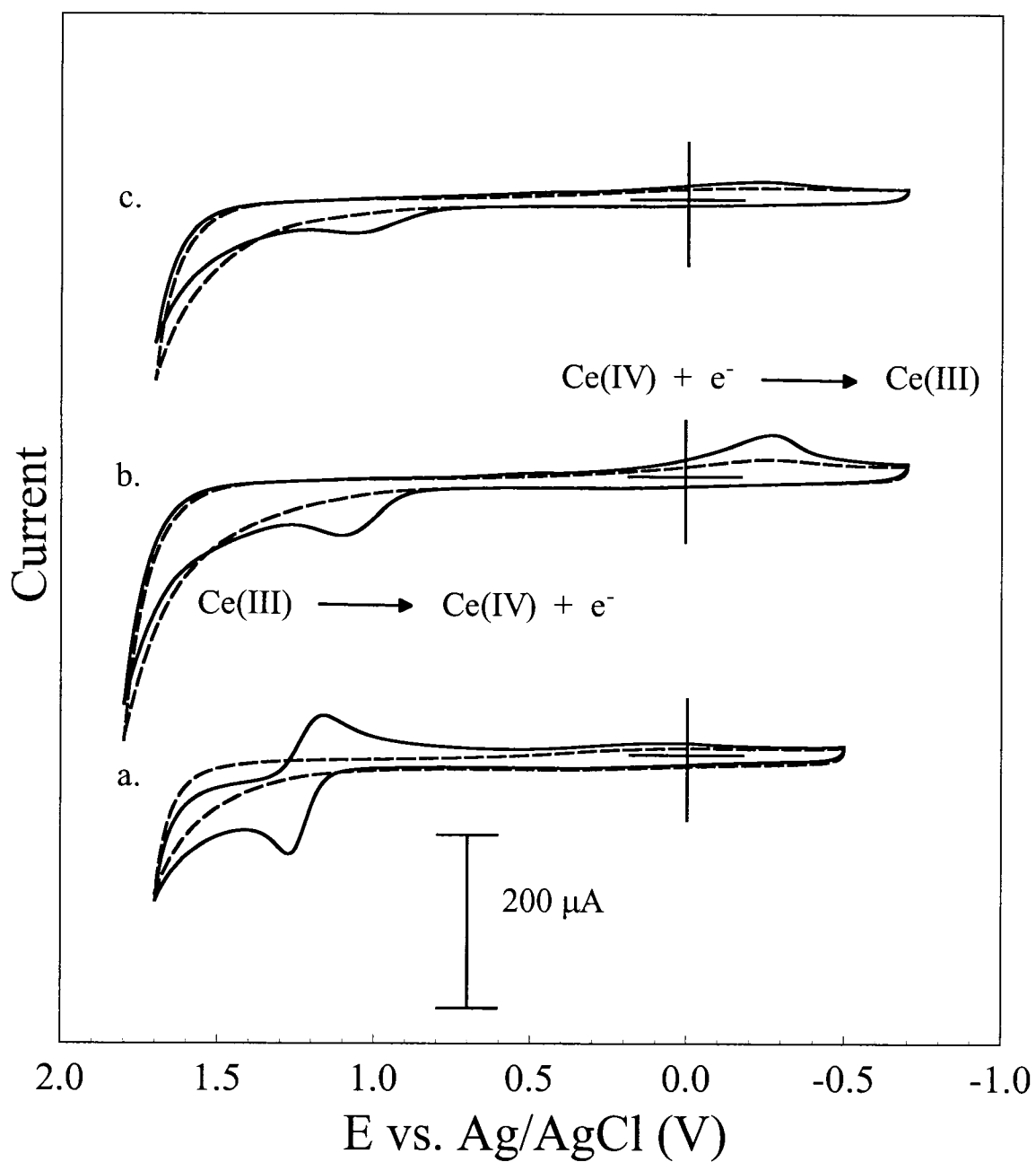


Figure 4.14. Steady-state voltammograms obtained at the GC working electrode for 6.0 mM $\text{Ce(NO}_3)_3 \cdot 6\text{H}_2\text{O}$ at *a.* pH = 1.0 *b.* pH = 3.4 and *c.* pH = 4.7 ($\nu = 100$ mV/s, solid line = cerium solution, dashed line = background, no cerium).

beyond which any increase in acidity leads to detrimental effects on the ability to observe Ce electrochemistry.

The possibility of Pt surface oxides interfering with electron transfer processes gives rise to another contradiction. Strongly acidic solution conditions, such as those at pH 1, lead to extensive oxidation of the Pt electrode surface. Indeed, the oxide peak currents in Figure 4.13 are higher at pH 1 than at pH 4.7, indicating enhanced oxidation of Pt in more acidic solution environments. Thus, we see optimum resolution of the redox couple in solution conditions favoring oxide formation. This utterly contradicts the suggestion of Pt oxide interference. The problem here may lie in the general treatment of Pt surface oxide as a single compound when, in reality, it has been shown to exist as either one of two possible compounds, depending on solution pH, with $\text{Pt}(\text{OH})_4$ forming in acidic media and $\text{PtO}(\text{OH})_2$ in basic (Benziger *et al.*, 1986). The $\text{Pt}(\text{OH})_4$ formed at low pH may act as a catalyst for electron transfer to and from the cerium solution species, while the basic form of the oxide may have a significant inhibition effect on the redox processes. If this is true, and the acidic oxide form exerts this favorable effect on the redox reactions of $\text{Ce}(\text{IV})/\text{Ce}(\text{III})$, it may be that this is only the case when the oxide layer remains relatively thin. This importance of oxide thickness may be the reason behind the poor results obtained at pH values lower than 1, as acid concentration was increased to 1.0 and 2.0 M. An examination of Figure 4.4 reveals that the thickness of the oxide layer increased (higher oxide reduction peak currents) as acid concentration went up. Thus, a thin layer of the $\text{Pt}(\text{OH})_4$ formed at low pH may facilitate electron transfer to and from the cerium system, while a thicker layer may have an insulating effect, retarding the electrochemical reaction of Ce. Similar results allow for the same

interpretation of oxide effects at the Au electrode, since the stoichiometry of Au oxide is also dependent on the pH conditions prevailing during its formation, with Au(OH)₃ formed on electrodes in acidic solution environments and Au₂O₃ in basic (Juodkazis *et al.*, 1999).

The results of increasing solution pH at the GC electrode are remarkable for two reasons in particular. Most importantly, the cerium redox couple was observed at the GC electrode at even the highest pH values examined in the studies (4.7 and 6.1). What is interesting about these results is not only the observation of a redox couple throughout such a wide range of solution pH, but that the redox couple observed at and above the pH value of 3.4 shows a significant increase in peak potential separation, due mostly to the shift of the Ce(IV) reduction peak by ~1.3 V in the cathodic direction. The reason for this difference in the redox couple voltammetry at pH 3.4 compared to pH 1.0 may be found in Figure 4.15, which demonstrates that the speciation and ratio of SO₄²⁻ to HSO₄⁻ are strongly pH-dependent and would be very different in these two solution environments. It is known that while Ce(III) forms only the CeSO₄⁺ complex with the sulfate anion (Connick and Mayer, 1951; Newton and Arcand, 1953; Spedding and Jaffe, 1954), Ce(IV) is capable of successively forming CeSO₄²⁺, Ce(SO₄)₂, and Ce(SO₄)₃²⁻ as sulfate concentration is increased (Hardwick and Robertson, 1951b). It is important to note that these researchers found no evidence for the existence of cerium/bisulfate complexes. The stability constant of the cerous/sulfate complex CeSO₄⁺ has been estimated at 10^{1.25} in 1 M NaClO₄ and the stability constants of the Ce(IV) complexes CeSO₄²⁺, Ce(SO₄)₂, and Ce(SO₄)₃²⁻ have been estimated at 10^{3.54}, 10^{2.30}, and 10^{1.30}, respectively, in the same medium (Sillén and Martell, 1964). With this information, we

can speculate that in the 0.1 M H_2SO_4 solution environment, with its low SO_4^{2-} concentration (shown in Figure 4.15 at pH 1.0), each cerium cation is, in general, complexed to one sulfate anion. At a pH of 3.4, we can assume a SO_4^{2-} concentration of approximately 0.1 M, more than ten times the concentration of Ce(III) in this solution. The Ce(IV) concentration is obviously vastly exceeded by that of SO_4^{2-} since the ceric cation is formed only at the electrode surface as potential cycling proceeds. It can therefore be proposed that in the pH 3.4 solution, Ce(III) is present as CeSO_4^+ and Ce(IV) as $\text{Ce}(\text{SO}_4)_3^{2-}$. This explains the experimental observation of very little variation in the Ce(III) oxidation peak potential going from pH 1.0 to 3.4, since the identity of the

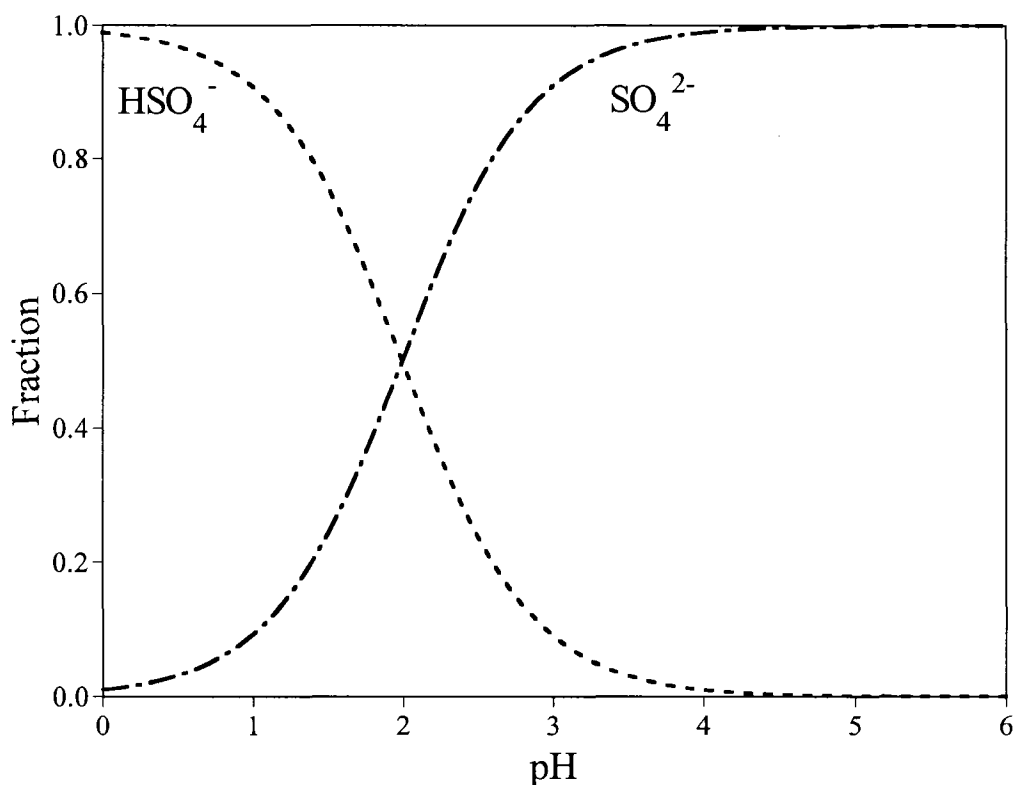


Figure 4.15. Speciation of sulfuric acid as a function of pH.

electroactive complex has not changed. Conversely, the large shift of the peak arising from Ce(IV) reduction to much more negative potentials at pH 3.4 than at pH 1.0 may be explained by the fact that the $\text{Ce}(\text{SO}_4)_3^{2-}$ complex present at higher pH has a very different stoichiometry, and likely very different reduction potential, than the CeSO_4^{2+} complex present at pH 1.0. The triply-complexed Ce(IV) cation may simply require more extremely negative potentials to displace the three sulfate anions instead of just one.

Interestingly, a close examination of Figures 4.12 and 4.13 reveals cathodic peaks that may arise from the reduction of this extensively complexed ceric cation, but the reduction of surface oxides at both the Au and Pt electrodes was such a considerable interference in this potential region that it was impossible either to clearly discern or to ascribe these voltammetric responses to the reduction of Ce(IV). The use of the GC working electrode thus allowed for the electrochemical investigation of the Ce(IV)/Ce(III) redox couple in solution environments of more extremely acidic or basic pH that precluded its observation at either of the metal electrodes. The higher overpotential for both oxidation and reduction of the aqueous medium resulted in access to a wider potential window using the GC electrode. Additionally, the relative inertness of glassy carbon compared to either Au or Pt resulted in a background free from the interferences of the redox reactions of the electrode itself.

4.3. Complexation Study

4.3.1. Introduction

As discussed in Chapter 1, the shift of redox couples to less positive potentials as a result of complexation with stabilizing ligands is a known phenomenon in electrochemical investigations. The advantages offered by the use of aqueous sulfuric acid solutions over those of other acids such as nitric and hydrochloric have been widely observed and exploited in the literature, and were also confirmed in the acid study described in section 4.1 of this work. It is also known that lanthanides such as cerium form their most stable complexes with the polydentate aminopolycarboxylate ligands such as EDTA and NTA (Aspinall, 2001). From this information, it follows that the stable complexation of Ce cations with such strongly-binding ligands should result in a shift toward even less positive potentials than those afforded by SO_4^{2-} complexation.

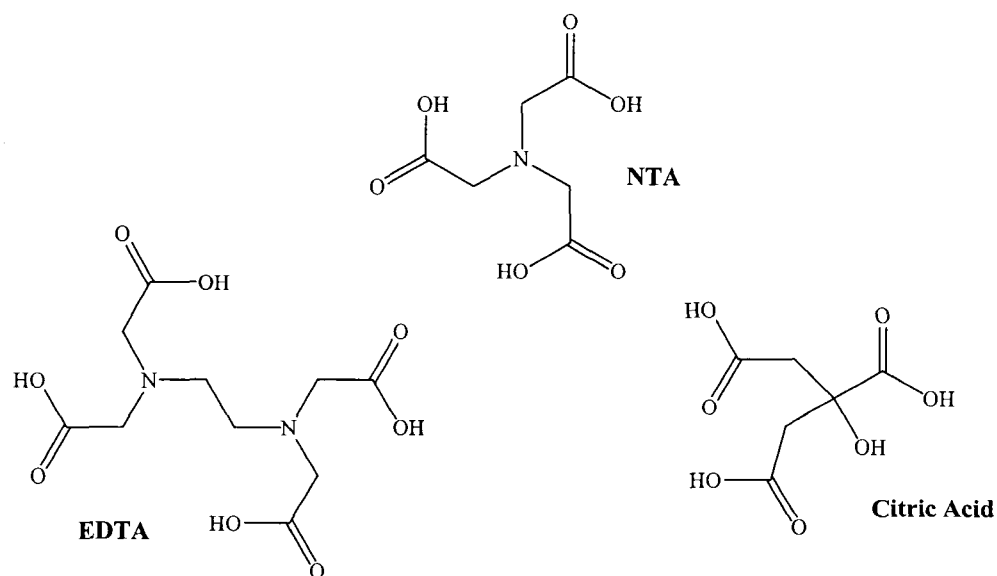


Figure 4.16. Structures of EDTA, NTA, and citric acid.

The manipulation of redox potentials through the effects of stable complexation could, therefore, offer improved resolution from O₂ evolution currents arising at the positive limit of each electrode's working potential window. In order to investigate the efficacy of such solution effects on the ability to resolve Ce(IV)/Ce(III) electrochemistry, a complexation study was designed and carried out. The polydentate ligands chosen to examine in this study were NTA, citrate, and EDTA. The structures of these compounds in their neutral form are shown in Figure 4.16.

Since they are polyprotic acids, citric acid ($pK_1 = 3.128$, $pK_2 = 4.761$, $pK_3 = 6.369$), EDTA ($pK_1 = 0.0$, $pK_2 = 1.5$, $pK_3 = 2.0$, $pK_4 = 2.66$, $pK_5 = 6.16$ (NH), $pK_6 = 10.24$ (NH)) and NTA ($pK_1 = 1.1$, $pK_2 = 1.650$, $pK_3 = 2.940$, $pK_4 = 10.334$ (NH)) can exist in several forms depending on the pH of the medium (Harris, 1999). For this reason, studies of the three different ligands were conducted in the form of pH titrations, in which pH was gradually increased and cyclic voltammograms obtained at each pH increment. This was done to identify the optimum pH range for each ligand at each electrode, through the electrochemical observation of emerging or disappearing redox peaks as the titration progressed. Since speciation and complexation are also affected by the ratio at which the metal and ligand are present in solution, further electrochemical experiments were carried out by varying the ratio of Ce to EDTA in solution and examining the resulting voltammetry at each of these values. All titration and varying ratio experiments were carried out at all three working electrodes (Au, GC, and Pt) for comparison, since previous results from the acid and pH studies demonstrated the importance of the role played by the working electrode.

4.3.2. Complexation Study in NTA

The results of the cerium complexation study using NTA at the Au and GC working electrodes are presented in Figures 4.17 and 4.18, respectively. Disappointingly, no observations of cerium electrochemistry could be made at either electrode in this solution. For the Au electrode, the only prominent features visible in the voltammograms were a single cathodic peak in the region of +0.4 to +0.6 V and a large anodic current in the range of +1.0 to +1.5 V. These current peaks, however, were also present in the voltammetry of the NTA background solution, and their relation to the redox activity of Ce could be ruled out. These peaks can most likely be ascribed to the oxidation/reduction reactions of the Au electrode itself, since they occur in the region where such reactions typically occur for Au. Although it was not possible to assign it confidently, the most noteworthy observation that can be made from Figure 4.17 is perhaps the second cathodic peak appearing at ~ -0.25 V in the voltammogram obtained at pH 10. In general, however, the results obtained in the Ce/NTA system at the Au electrode were poor, showing very little change in comparison to the background at each pH value.

Similarly unsuccessful results were obtained at the GC electrode (Figure 4.18), where a comparison of cerium solutions with their appropriate backgrounds revealed little difference except for a cathodic peak appearing in the range of +0.3 to +0.6 V at pH values of 2, 4, and 6, which may possibly arise from the reduction of Ce(IV). This peak was no longer observable at pH 8 and 10, at which values the sample and background voltammograms corresponded quite closely. If nothing else, investigations of the Ce/NTA system at the Au and GC electrodes demonstrated the importance of obtaining background voltammograms for each solution system, since the redox of both the

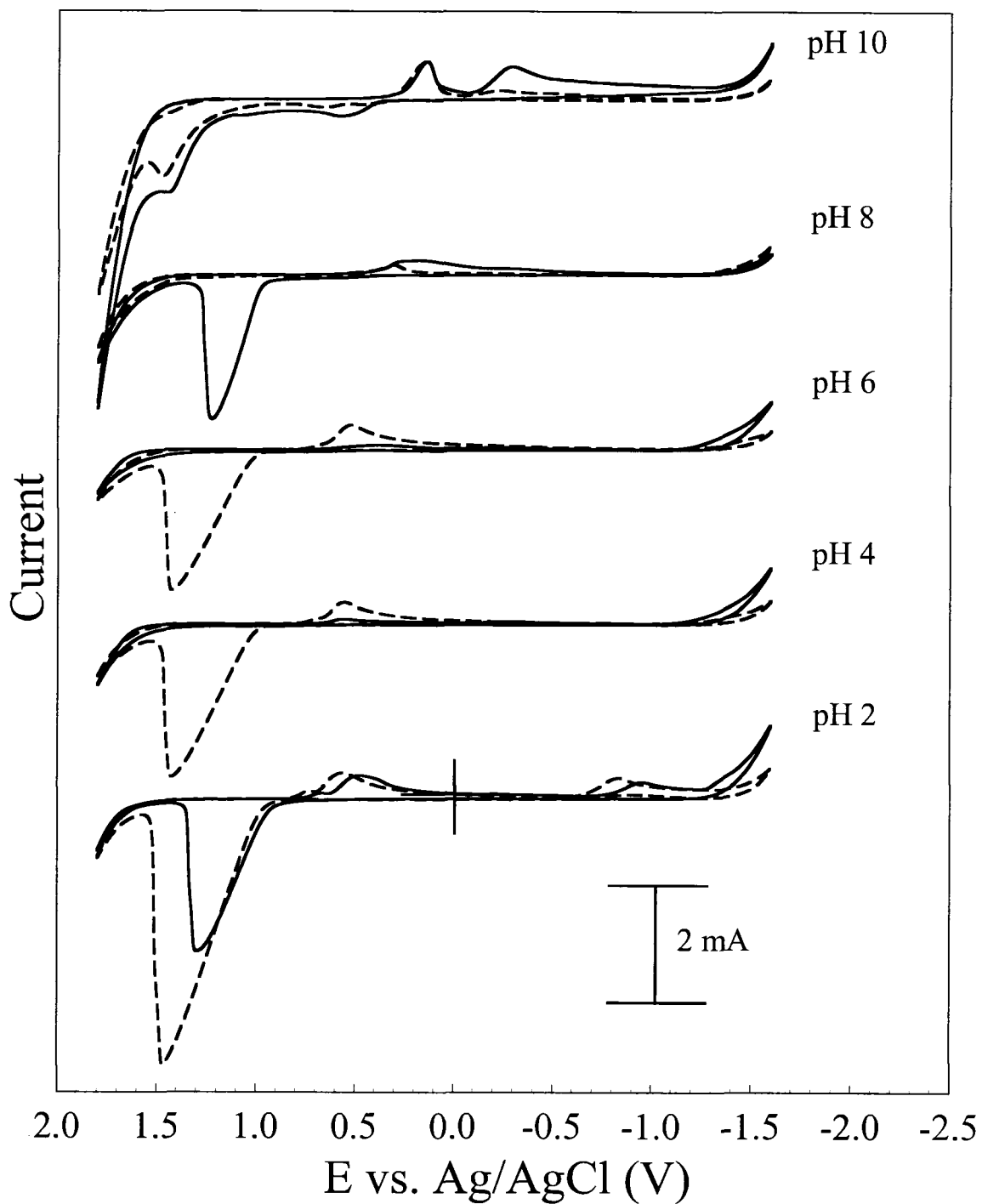


Figure 4.17. Steady-state voltammograms obtained at the Au working electrode for 6.0 mM $\text{Ce}(\text{NO}_3)_3 \cdot 6\text{H}_2\text{O}$ in 12.0 mM Na_2NTA at pH values of 2, 4, 6, 8, and 10 ($\nu = 100$ mV/s, solid line = cerium solution, dashed line = background, no cerium).

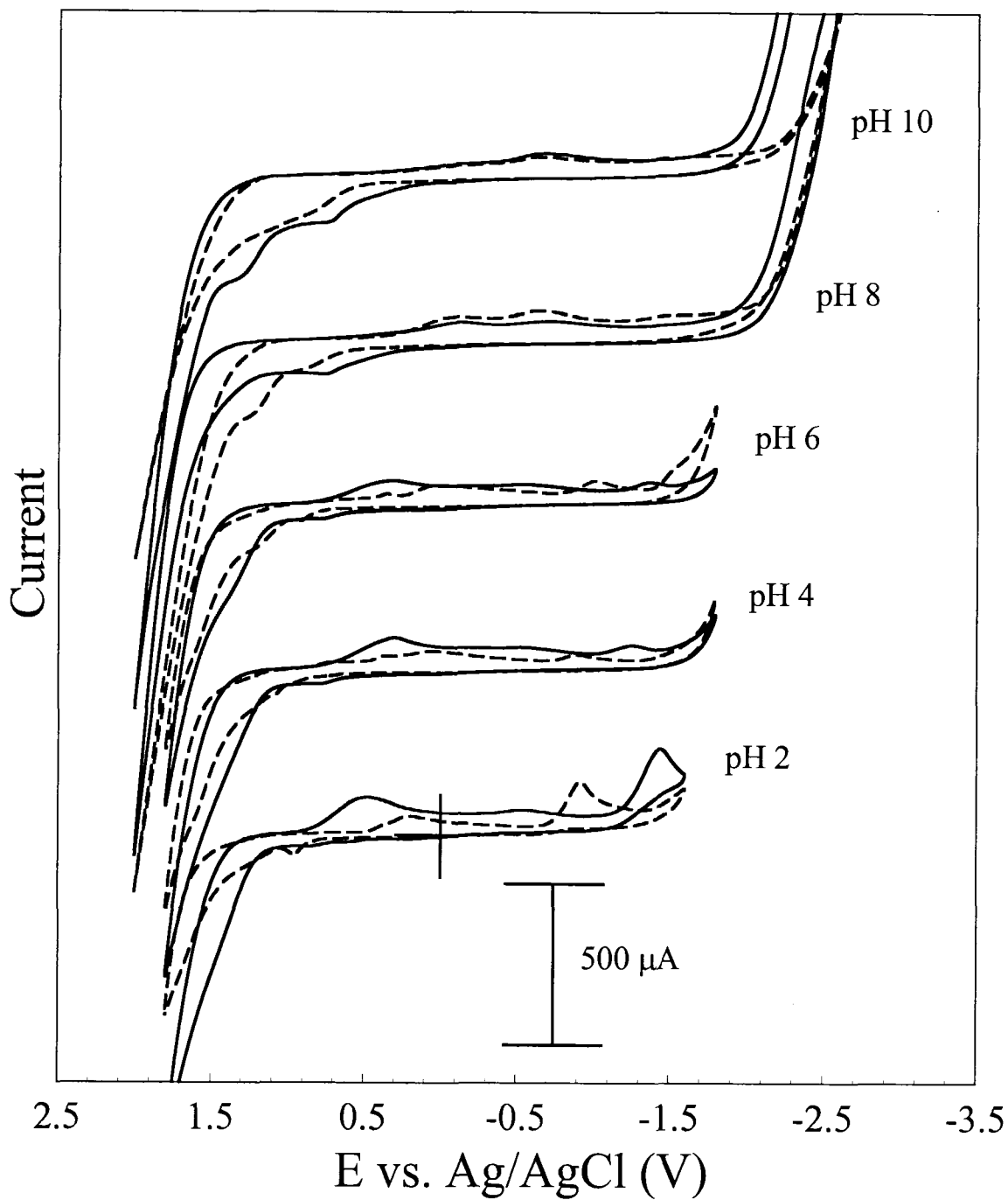


Figure 4.18. Steady-state voltammograms obtained at the GC working electrode for 6.0 mM $\text{Ce}(\text{NO}_3)_3 \cdot 6\text{H}_2\text{O}$ in 12.0 mM Na_2NTA at pH values of 2, 4, 6, 8, and 10 ($v = 100$ mV/s, solid line = cerium solution, dashed line = background, no cerium).

electrode and the aqueous medium itself could otherwise easily be mistaken for cerium electrochemical activity.

Experiments on the Ce/NTA system at the Pt working electrode (Figure 4.19) were also unsuccessful at resolving cerium electrochemistry. A reduction peak was observed in the potential range of +0.4 to +0.9 V, which may be due to the reduction of the ceric cation. However, the current values are indicative of very low reaction of Ce(IV) at the electrode surface. The occurrence of this voltammetric response was in a comparable range to the cathodic peak observed at the GC electrode (Figure 4.18) and was again no longer present at pH 8 and 10. Perhaps the most remarkable feature in Figure 4.19 is the distinct redox couple occurring at an $E_{1/2}$ of approximately -0.5 V. When looking at this couple, it is initially tempting to ascribe it to the redox activity of some Ce/NTA complex, but an examination of the corresponding background reveals a very similar current for the NTA solution alone. Interestingly, this feature disappeared when the solution pH was increased to 4. An examination of the speciation of NTA as a function of pH is presented in Figure 4.20 and reveals the differences in the solution species at pH 2 compared to those present at pH 4. Thus, this redox couple may arise from the redox of either the H_3NTA or H_2NTA^- in solution at pH 2. For the rest of the pH range probed in the study (4 to 10), there is predominantly only the HNTA^{2-} solution species. The interaction of this ligand with cerium cations may result in the formation of a solution complex with electrochemical activity that is not observable within the potential range available to the Au, GC, and Pt working electrodes.

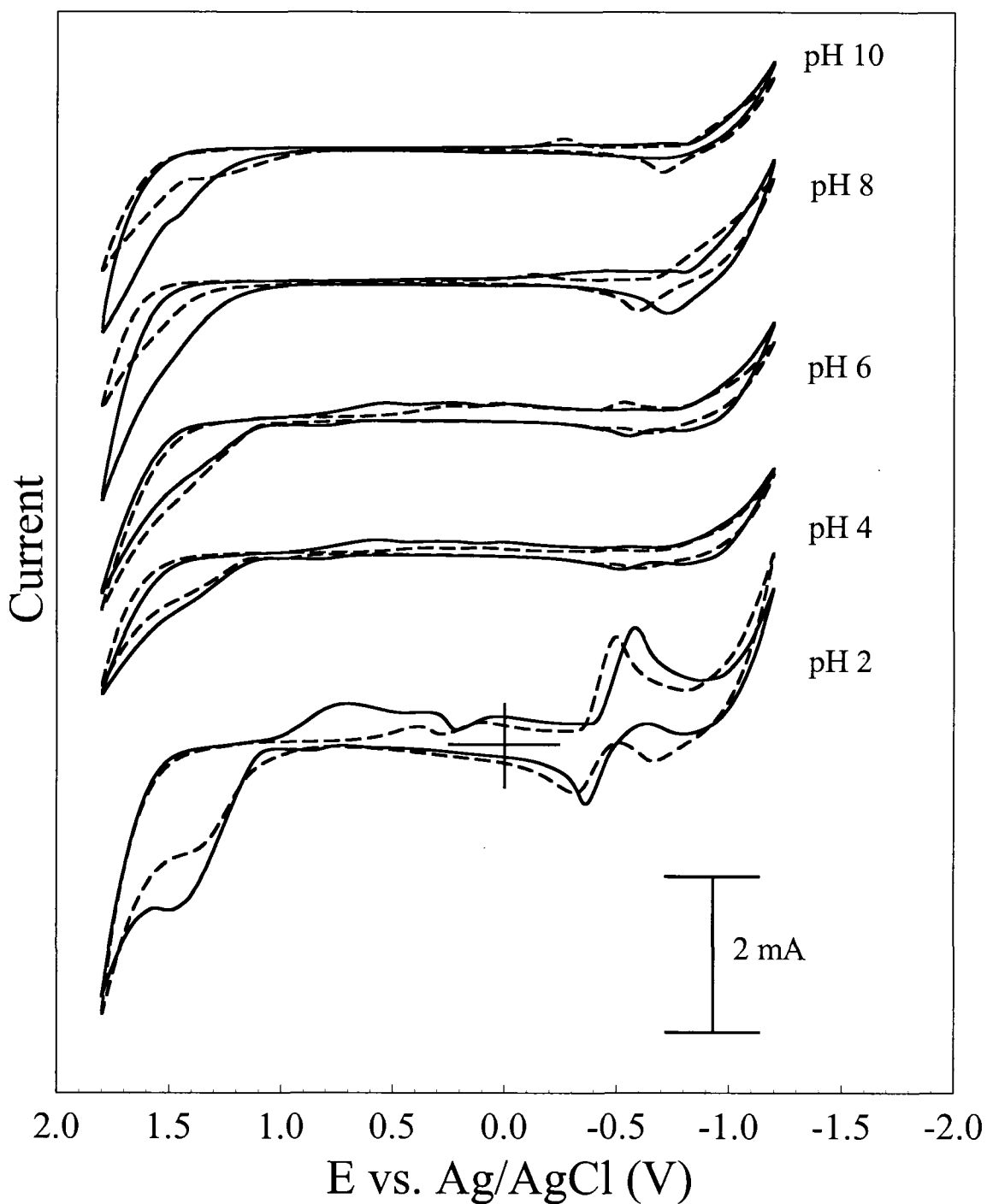


Figure 4.19. Steady-state voltammograms obtained at the Pt working electrode for 6.0 mM $\text{Ce}(\text{NO}_3)_3 \cdot 6\text{H}_2\text{O}$ in 12.0 mM Na_2NTA at pH values of 2, 4, 6, 8, and 10 ($\nu = 100$ mV/s, solid line = cerium solution, dashed line = background, no cerium).

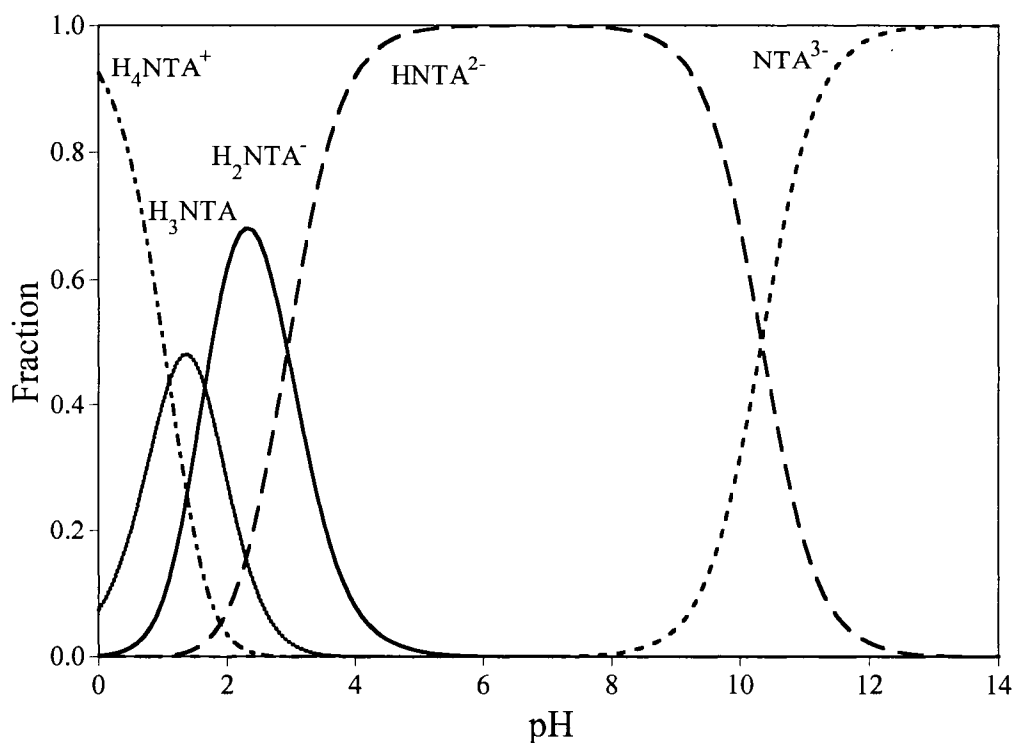


Figure 4.20. Speciation of NTA as a function of pH.

4.3.3. Complexation Study in Citrate

The results of the complexation study using the citrate ligand at the Pt electrode are shown in Figure 4.21. Only the voltammograms obtained at pH 2 and 4 yielded any observable cerium redox behavior that could be distinguished from background currents. This experiment yielded the somewhat surprising observation that complexation with citrate resulted in a redox couple which was clearly not resolved from the O_2 evolution current. The $E_{1/2}$ value of $\sim +0.75$ V obtained in this medium was, however, significantly shifted in the positive potential direction relative to the $E_{1/2}$ values of approximately +1.2 V observed in the acid study at optimum conditions. This desirable result was counteracted by the concurrent shift of the oxidation of water to less positive potentials. The same interferences between Ce(III) and water oxidation were simply moved to a less

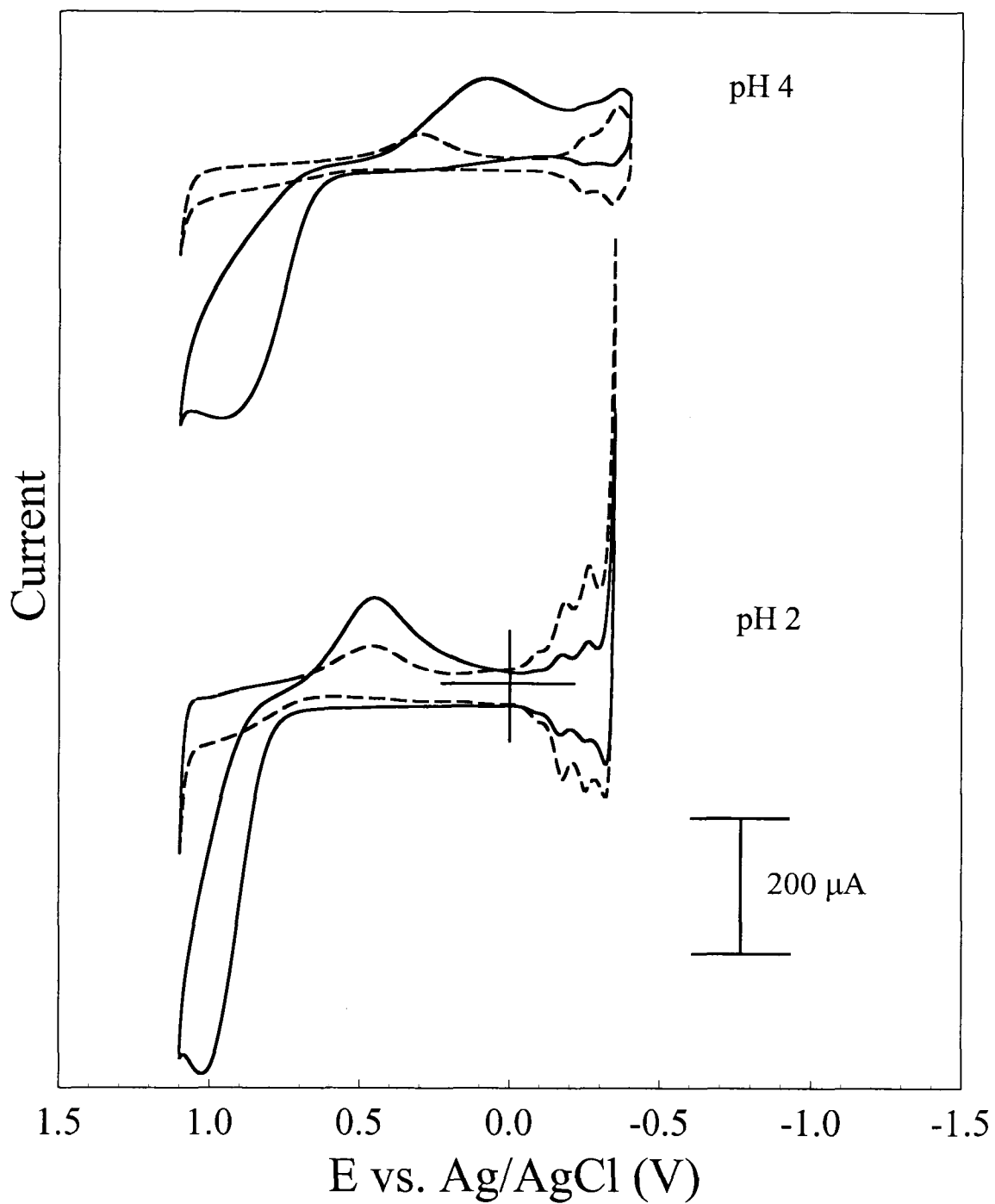


Figure 4.21. Steady-state voltammograms obtained at the Pt working electrode for 6.0 mM $\text{Ce}(\text{NO}_3)_3 \cdot 6\text{H}_2\text{O}$ in 12.0 mM citric acid monohydrate at pH values of 2 and 4 ($\nu = 100 \text{ mV/s}$, solid line = cerium solution, dashed line = background, no cerium).

positive potential regime without any resolution of the original problem. The reduction of Pt surface oxide occurred at a similar potential to Ce(IV) reduction at the Pt electrode in this medium, which presented a further drawback to the use of citrate as a solution environment for studies of the cerium redox system. Unlike the Ce/NTA study at the Pt electrode, observation of the redox couple was possible using citrate as the complexing ligand, although far better resolution was obtained in the acid study using aqueous sulfuric acid. Results for the citrate system at the Au electrode were so poor that no significant conclusions could be drawn. In the interest of completeness, these results are included in Figure 4.22.

The citrate study at the GC working electrode (Figure 4.23) yielded very different results from those obtained at the two metal electrodes. At pH 2, the Ce(IV)/Ce(III) redox couple was clearly discernible and adequately resolved from the water oxidation current. Compared to the $E_{1/2}$ value of +1.218 V obtained at GC in 0.1 M H₂SO₄, the use of the citrate system afforded a redox potential of +0.773 V at the same electrode. This was a negative potential shift of nearly 0.5 V accomplished through manipulation of the solution environment. There was, however, a loss of reversibility, going from a ΔE_p of 0.112 V in 0.1 M sulfuric acid to 0.283 V in citrate solution. The favorable effects of citrate complexation also proved to be strongly pH dependent, with reduced peak currents and reversibility as pH was increased to 6 and a total disappearance of redox couple activity by pH 8. In summary, although citrate complexation did shift the Ce(IV)/Ce(III) redox couple to less positive potentials, resolution was possible at the GC electrode only. Additionally, a limited pH range and poor reversibility demonstrated the considerable disadvantages associated with citrate as a complexing ligand in this application.

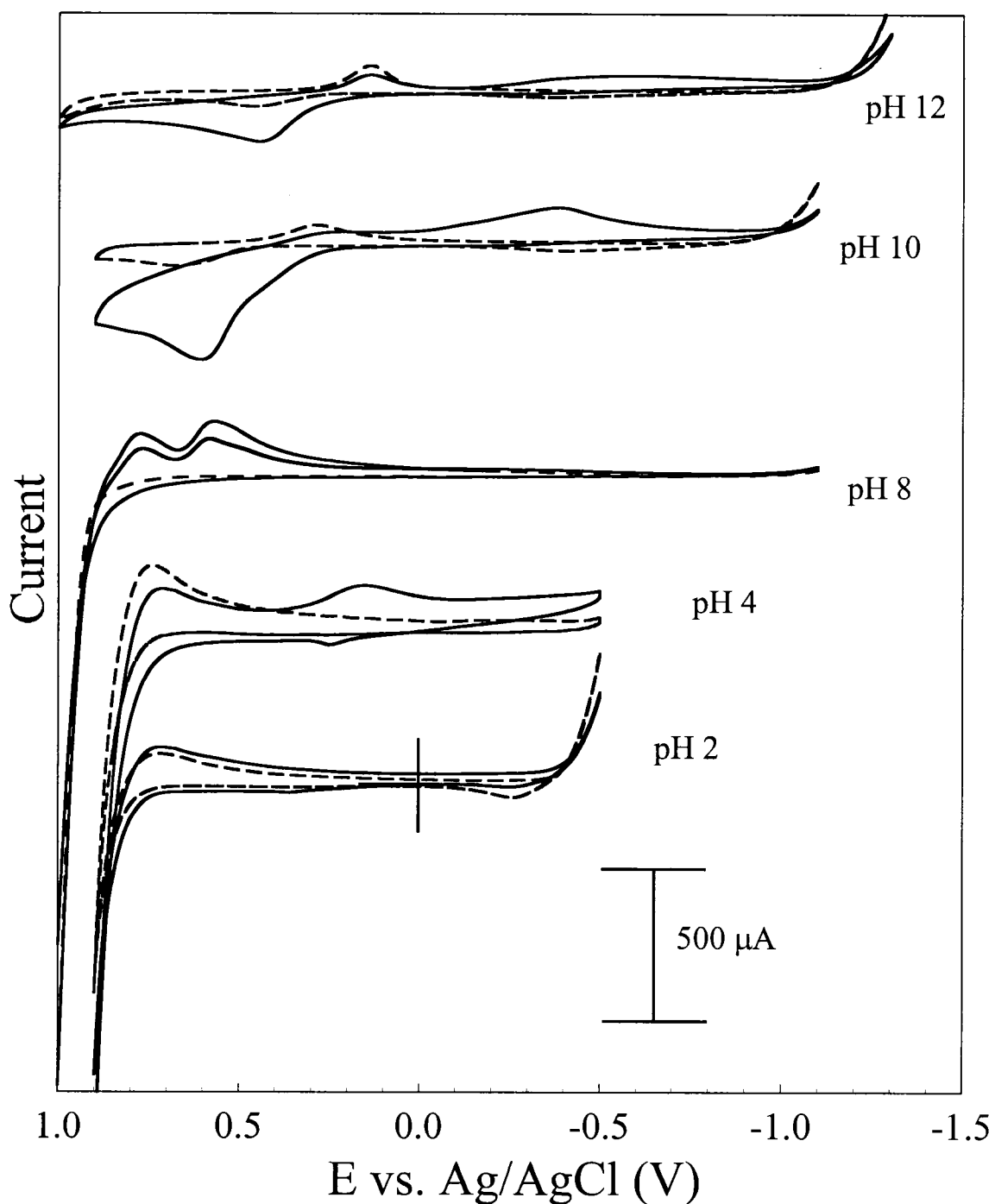


Figure 4.22. Steady-state voltammograms obtained at the Au working electrode for 6.0 mM $\text{Ce}(\text{NO}_3)_3 \cdot 6\text{H}_2\text{O}$ in 12.0 mM citric acid monohydrate at pH values of 2, 4, 8, 10, and 12 ($\nu = 100 \text{ mV/s}$, solid line = cerium solution, dashed line = background, no cerium).

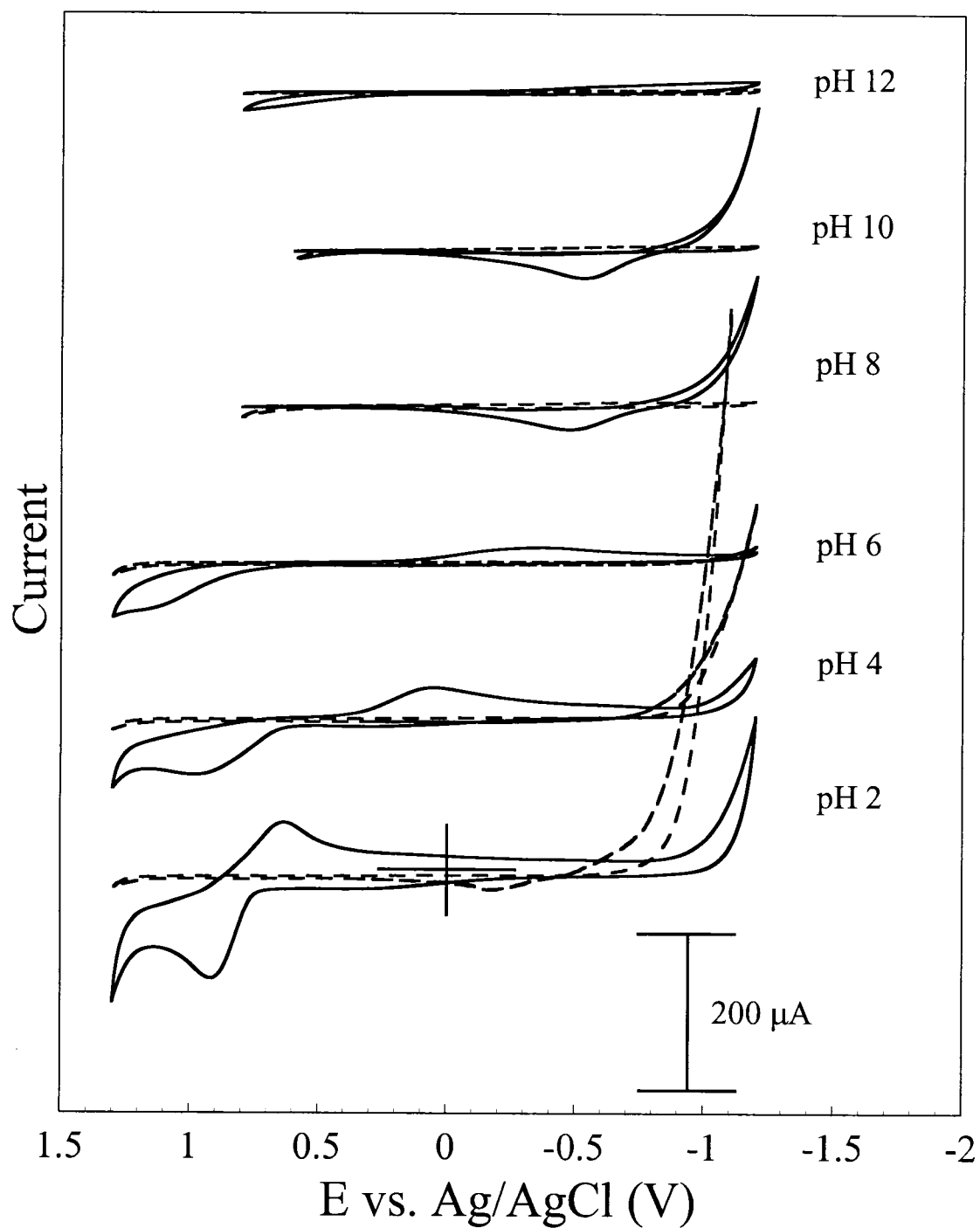


Figure 4.23. Steady-state voltammograms obtained at the GC working electrode for 6.0 mM $\text{Ce}(\text{NO}_3)_3 \cdot 6\text{H}_2\text{O}$ in 12.0 mM citric acid monohydrate at pH values of 2, 4, 6, 8, 10, and 12 ($\nu = 100 \text{ mV/s}$, solid line = cerium solution, dashed line = background, no cerium).

4.3.4. Complexation Study in EDTA

Of the three complexing ligands examined in this study, it is EDTA which forms the most stable complexes with cerium cations in solution. The stability constant for the CeEDTA^- complex has been estimated at $10^{16.01}$, compared to the values of $10^{3.2}$ for $\text{CeH}_3\text{citrate}^{2+}$ and $10^{10.71}$ for the formation of CeNTA . For this reason, cyclic voltammetry on cerium solutions in EDTA as the working electrolyte were expected to yield the best resolution of the Ce(IV)/Ce(III) redox couple. However, voltammograms obtained at the Au and GC working electrodes in EDTA were unsatisfactory, showing no defined redox couple attributable to cerium. Experimental results at the GC electrode as a function of pH are presented in Figure 4.24 as an example of the problems encountered using EDTA as the aqueous medium. Both the reduction and oxidation peaks for cerium were observed at approximately -0.8 V and +0.9 V, respectively. This redox couple was quite irreversible, however, and the redox activity of the EDTA medium was a significant interference at this electrode. Significantly irreversible redox couples often indicate the presence of some non-diffusion mechanism, such as adsorption, inhibiting the flux of electroactive species to and from the electrode surface. Adsorption effects may well play a role at the GC electrode since the Ce-EDTA redox complex is largely organic in nature and may have an increased affinity for the carbon electrode surface.

The most successful results using aqueous EDTA medium were those obtained at the Pt electrode. In fact, the use of the Pt electrode in conjunction with EDTA yielded the best results of all the experimental systems evaluated in the complexation study. These voltammograms are presented in Figure 4.25 and revealed several major points of interest that demonstrated the advantages of the Pt/EDTA combination over the Pt/ H_2SO_4 system

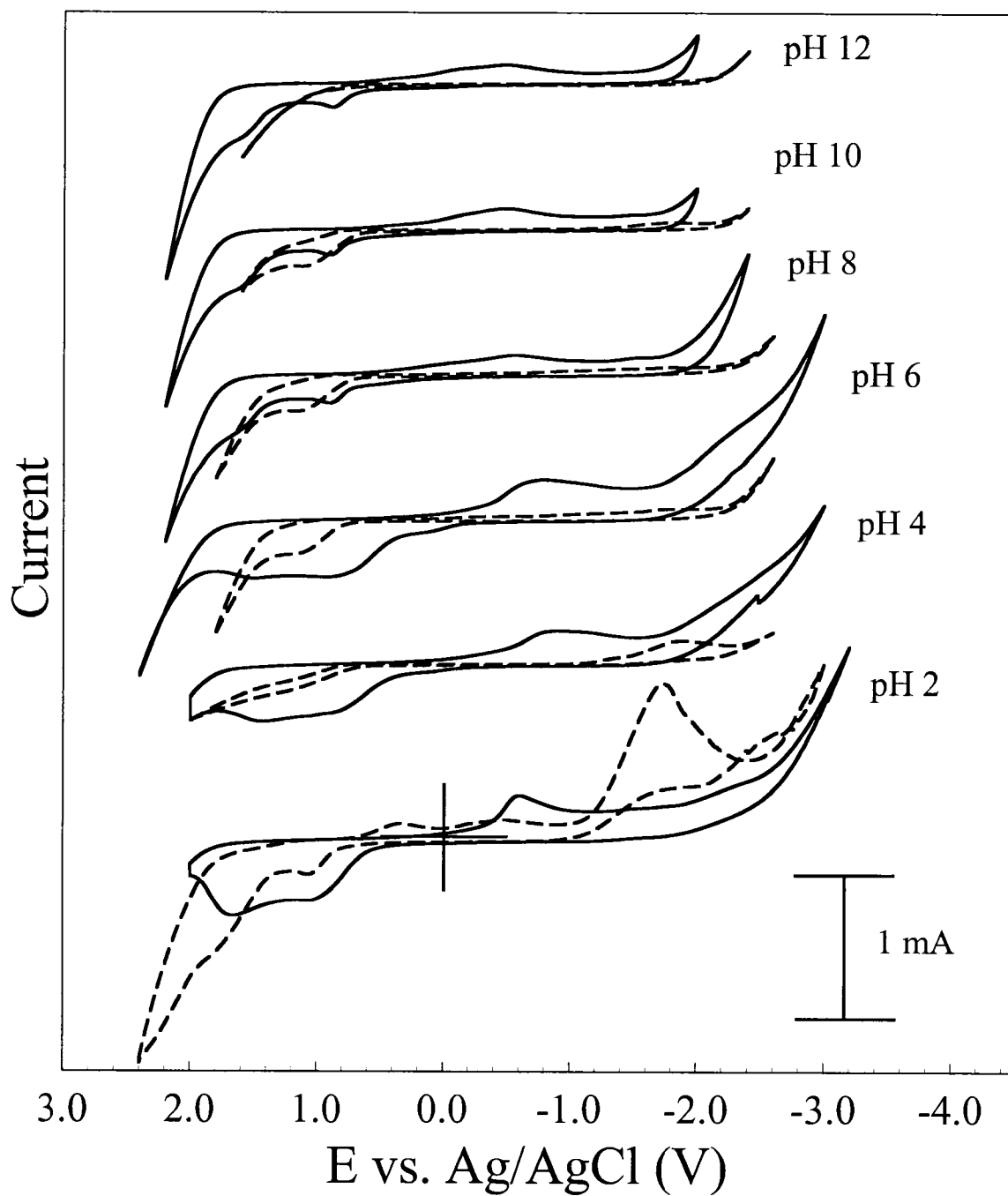


Figure 4.24. Steady-state voltammograms obtained at the GC working electrode for 6.0 mM $\text{Ce}(\text{NO}_3)_3 \cdot 6\text{H}_2\text{O}$ in 12.0 mM $\text{Na}_2\text{EDTA} \cdot 2\text{H}_2\text{O}$ at pH values of 2, 4, 6, 8, 10, and 12 ($\nu = 100$ mV/s, solid line = cerium solution, dashed line = background, no cerium).

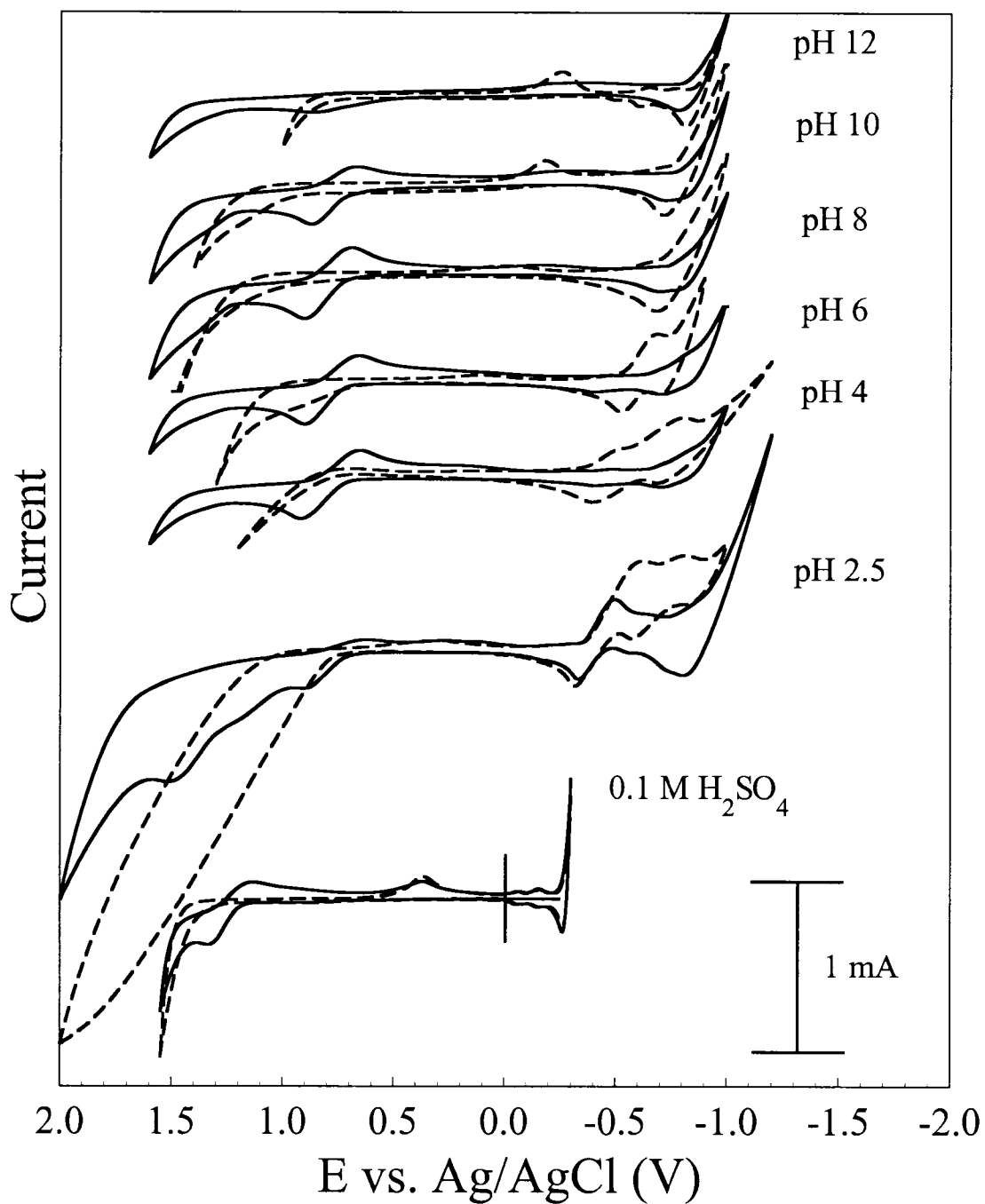


Figure 4.25. Steady-state voltammograms at the Pt working electrode for 6.0 mM $Ce(NO_3)_3 \cdot 6H_2O$ in 12.0 mM $Na_2EDTA \cdot 2H_2O$ at pH values of 2.5, 4, 6, 8, 10, and 12 compared to results obtained at Pt in 0.1 M H_2SO_4 ($v = 100$ mV/s, solid line = cerium solution, dashed line = background, no cerium).

determined as optimum in the acid and pH studies. First, and most importantly, the Ce(IV)/Ce(III) redox couple was not only clearly discernible but was also shifted by ~0.4 V in the negative potential direction compared to the redox potential obtained in 0.1 M H₂SO₄. The calculated values for the EDTA experiments are given in Table 4.5.

Unlike the results at Pt in NTA and citrate, and at the GC electrode in citrate, the redox couple at Pt in EDTA was very well resolved from the O₂ evolution background currents. The Pt/EDTA system thus ideally moved the cerium redox couple to a more easily accessed potential regime, while displaying a high overpotential for water oxidation. The data in Table 4.5 reveal a redox couple with an only slightly less Nernstian ΔE_p value than that observed in 0.1 M sulfuric acid. The peak current ratios in EDTA showed even better reversibility, maintaining a value near unity throughout an

Table 4.5. Electrochemical data obtained at the Pt working electrode in EDTA solutions of increasing pH ($\Delta E_p = E_{pa} - E_{pc}$ and $E_{1/2} = (E_{pa} + E_{pc})/2$). All peak currents presented (i_{pa} and i_{pc}) are net current values obtained through background subtraction.

	E_{pc} (V)	E_{pa} (V)	$E_{1/2}$ (V)	ΔE_p (V)	i_{pa}/i_{pc}
EDTA pH 2	0.632	0.910	+0.771	0.278	1.29
EDTA pH 4	0.654	0.922	+0.788	0.268	1.00
EDTA pH 6	0.660	0.902	+0.781	0.242	0.73
EDTA pH 8	0.686	0.908	+0.797	0.222	0.80
EDTA pH 10	0.669	0.874	+0.772	0.205	0.98

experimental pH range of 2 through 10. Indeed, the good reversibility and near-constant redox potential in EDTA showed an excellent resistance to changes in pH; something that could not be said for sulfate as the complexing medium. The strong affinity of cerium for the EDTA ligand clearly plays a major role; however, the electrode material was shown to possess at least an equal importance since experiments in EDTA at Au and GC did not meet with similar success. It is actually significant to note that none of the other complexing ligand/electrode combinations returned results that were even as good as those obtained in 0.1 M H₂SO₄. In fact, the electrochemical study of Ce(IV)/Ce(III) using the Pt/EDTA system alone yielded all of the characteristics hoped for when the complexation study was outlined.

Since the employment of the Pt/EDTA system yielded the best results of all the electrochemical experiments in the complexation study, clarification of the effects of altering the metal:ligand ratio was sought. For this purpose, cyclic voltammetry was carried out on solutions of increasing cerium concentration, while that of EDTA was held constant (Figure 4.26). The solution pH was also maintained at a value of 2.0, since Figure 4.25 reveals noticeable variations in the background currents in response to changes in pH. There were several features of interest in the voltammograms in Figure 4.26. First, the Ce(IV)/Ce(III) redox couple observed in the previous study, and centered at around +0.8 V, was visible throughout the entire concentration range. A reduction peak at ~ +0.1 V began to emerge as oxidation of the Pt electrode became more extensive. Interestingly, the voltammograms for 14 and 24 mM Ce(III) revealed a reduction peak at around -0.9 V, just before the evolution of hydrogen. It is significant that this reduction peak appeared only after the concentration of cerium in solution

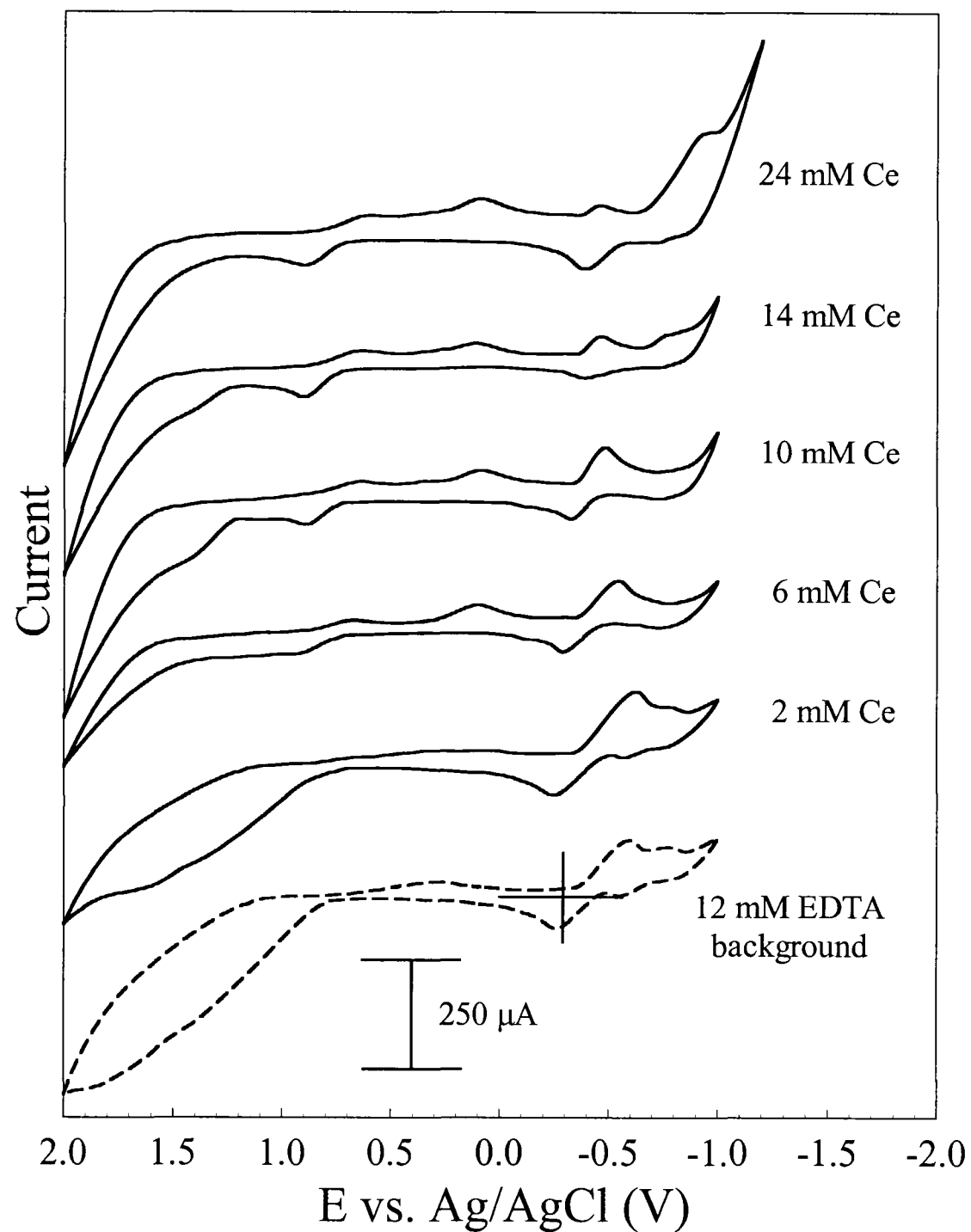


Figure 4.26. Steady-state voltammograms at the Pt disk working electrode for 2, 6, 10, 14, and 24 mM $\text{Ce}(\text{NO}_3)_3 \cdot 6\text{H}_2\text{O}$ in 12.0 mM $\text{Na}_2\text{EDTA} \cdot 2\text{H}_2\text{O}$ at a pH of 2.0 ($\nu = 100$ mV/s, solid line = cerium solution, dashed line = background, no cerium).

exceeded that of EDTA. This peak may represent the reduction either of free Ce(IV), since hydrolysis would not occur to a significant extent at a pH of 2, or perhaps that of an EDTA complex with more than one ceric cation, although the literature indicates that only the 1:1 complex forms (Bhat and Radhamma, 1965; Malinina *et al.*, 1969). What was especially interesting to note in this study was the presence of a second redox *couple* clearly observable at an $E_{1/2}$ of approximately -0.45 V. It was tempting, initially, to attribute this peak to a possible second redox process of cerium such as $\text{Ce(III)} \leftrightarrow \text{Ce(II)}$, or to the redox activity of a second Ce-EDTA complex, although the Ce(III) cation also has been shown to form a single 1:1 complex with EDTA (Vickery, 1952; Wheelwright *et al.*, 1953). If this couple represented some redox process of cerium, then its peak currents should have increased as a function of cerium concentration and Figure 4.26 shows that this was not the case. An examination of the EDTA background voltammetry revealed similar redox activity occurring in the same potential range. However, as cerium concentration was increased to 14 and 24 mM, and exceeded the concentration of EDTA, this redox couple should have disappeared if it was related to the electrochemistry of free EDTA alone. The strong pH dependence of this redox couple was marked and clearly demonstrated in Figure 4.27, where an increase in solution pH from 2.5 to 3.0 resulted in the disappearance of this redox couple. If EDTA is the electroactive species, this electrochemical pH dependence may reflect the difference in the EDTA species present as a function of pH (Figure 4.28). At pH values of 2.0 and 2.5, the predominant EDTA species is the neutral H_4EDTA . This species is almost completely converted to H_3EDTA^- and $\text{H}_2\text{EDTA}^{2-}$ by the time a pH of 3.0 is reached. Thus, it may be that H_4EDTA is the electroactive form, or at least the species that may affect some intrinsic

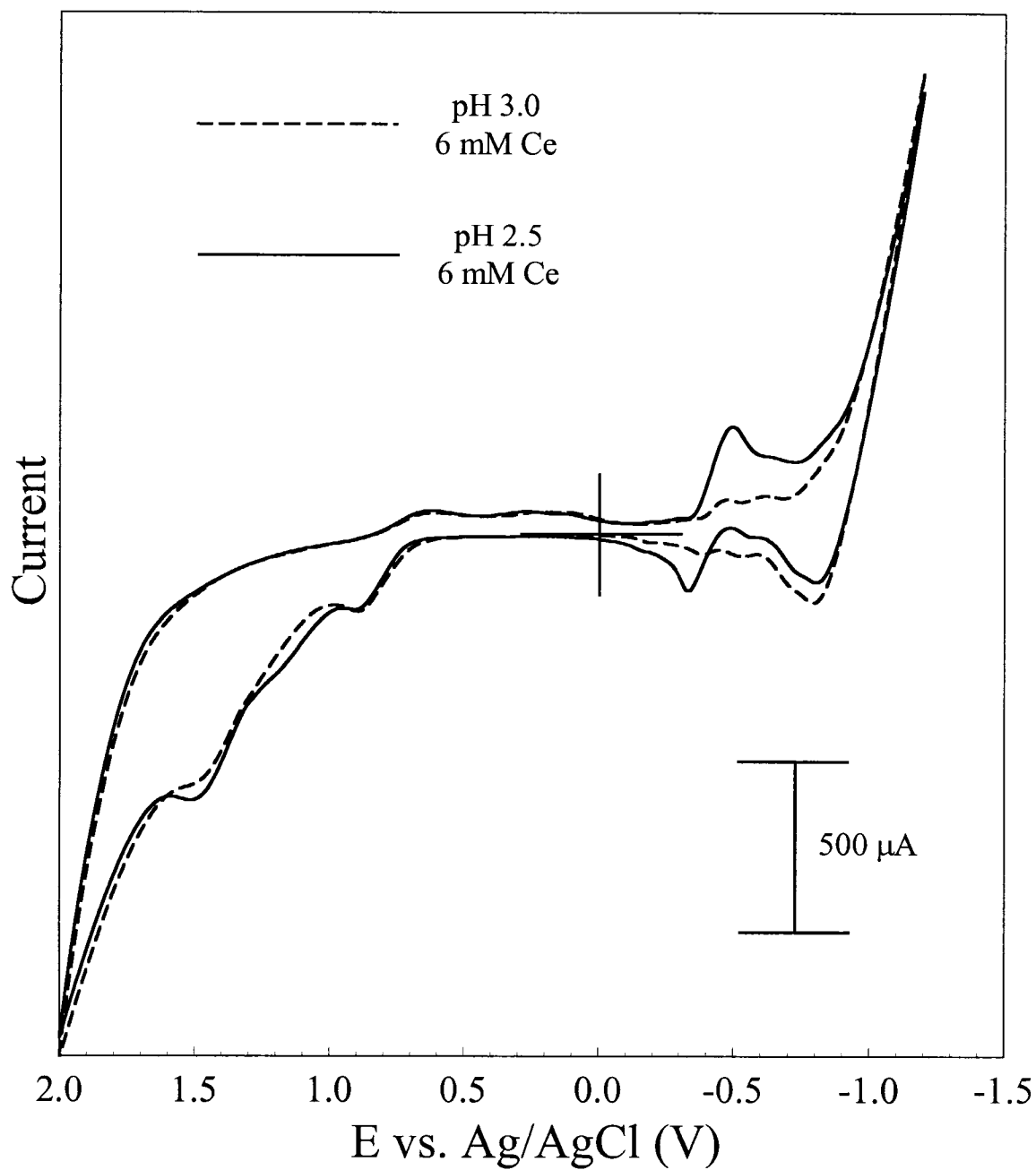


Figure 4.27. Steady-state voltammograms at the Pt working electrode showing the effect of increasing pH from 2.5 to 3.0 on the redox couple at ~ -0.5 V. ($[\text{Ce}(\text{NO}_3)_3 \cdot 6\text{H}_2\text{O}] = 6.0$ mM, $[\text{Na}_2\text{EDTA} \cdot 2\text{H}_2\text{O}] = 12.0$ mM, $v = 100$ mV/s).

electrode reaction such as hydrogen adsorption/desorption at Pt. However, this conclusion was not supported by our observation of the redox couple at cerium concentrations that precluded the existence of fully protonated, uncomplexed EDTA (Figure 4.26, 14 and 24 mM Ce). It should be noted that the cerium redox couple at +0.8 V was unaffected by the change in pH, which is to be expected if only the 1:1 Ce-EDTA

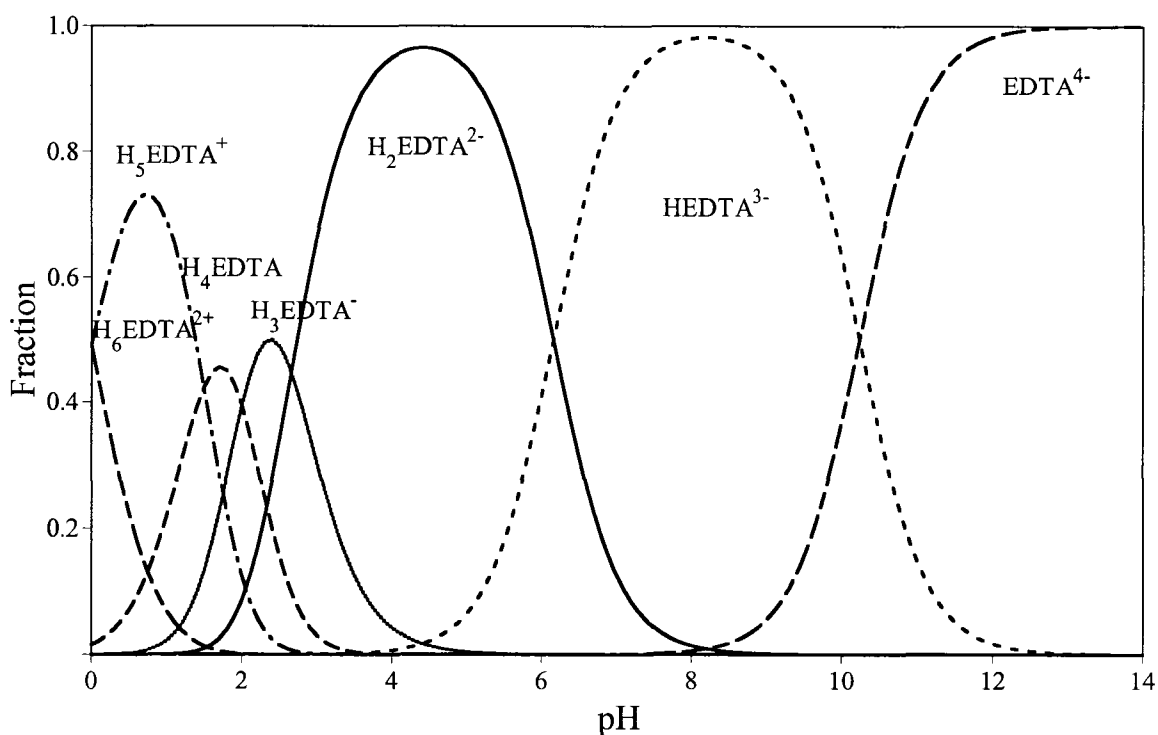


Figure 4.28. Speciation of EDTA as a function of pH.

complex forms. The solution pH, and the pH-dependent speciation of EDTA, would not be expected to affect such a complex since cerium cations are able to displace any protons from the ligand to form complexes with free EDTA⁴⁻ (Wheelwright *et al.*, 1953).

In a further effort to determine the identity of this second redox couple, an experiment was conducted comparing solutions of Ce, Sm, and Eu in EDTA with an EDTA

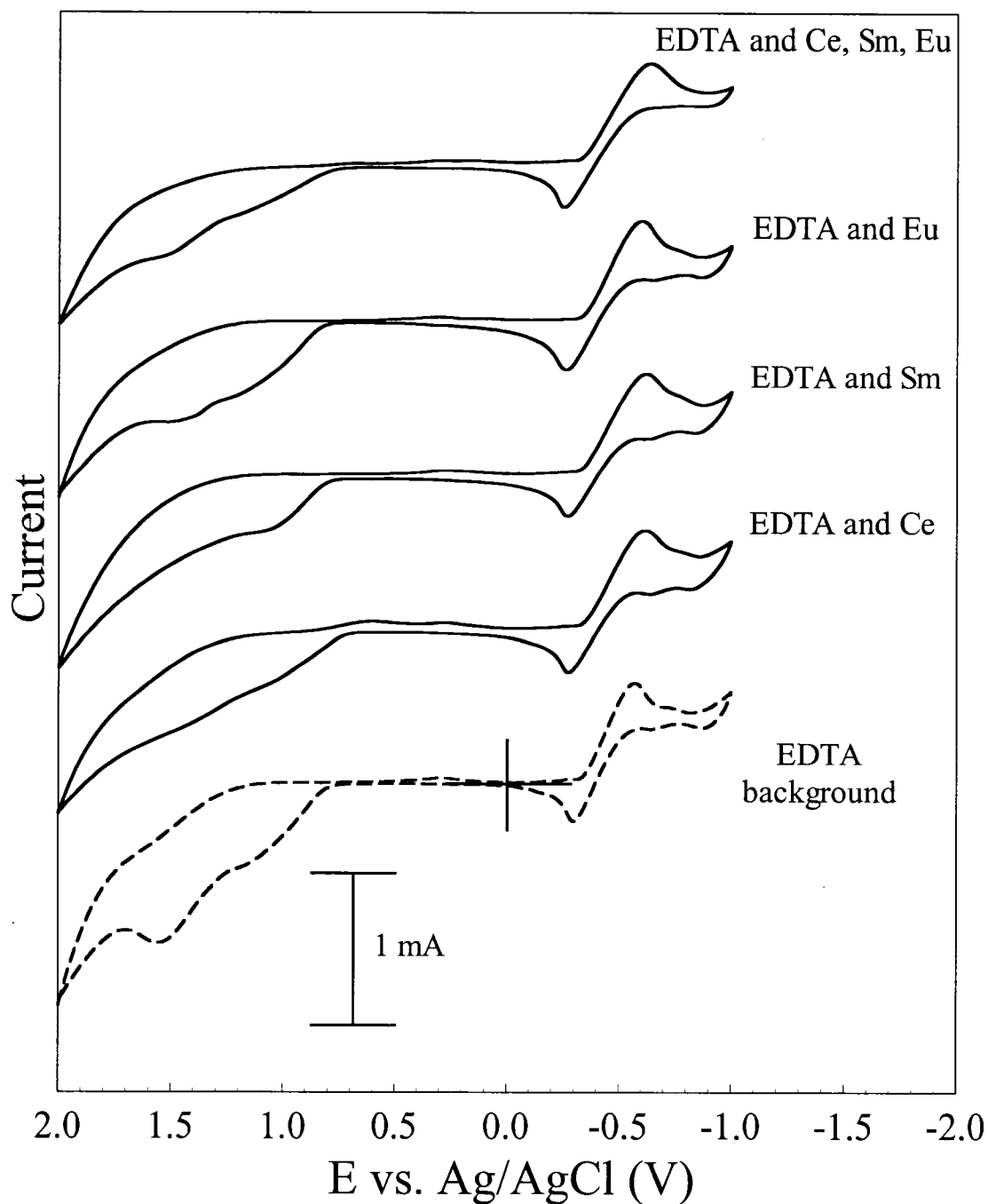
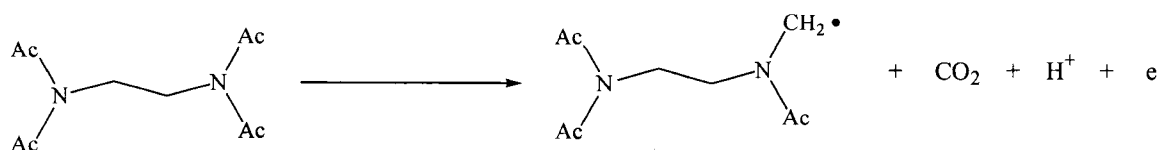


Figure 4.29. Steady-state voltammograms at the Pt working electrode comparing the redox couple at ~ -0.5 V in EDTA, EDTA/Ce, EDTA/Sm, EDTA/Eu, and EDTA/Ce, Sm, Eu solutions at pH 1.4. ($[\text{lanthanide(III)}] = 2.0$ mM, $[\text{Na}_2\text{EDTA}\cdot 2\text{H}_2\text{O}] = 12.0$ mM, $v = 100$ mV/s, solid line = lanthanide solution, dashed line = background, no lanthanides).

background, as well as with a mixed solution of all three of these rare earth cations (Figure 4.29). The redox couple observed in all of these solutions was very similar and the mixed lanthanide solution did not yield multiple peaks. This would be expected if some lanthanide-EDTA complex was responsible for the couple, since the likelihood of all three peaks coinciding in redox potential is extremely low. A review of the literature concerning the electrochemistry of EDTA yielded conflicting information regarding this redox couple that has apparently remained an unexplained phenomenon throughout years of electrochemical research in EDTA solutions. Recent investigators of the electrochemistry of niobium in EDTA medium noted this second redox couple occurring at negative potentials and attributed it to the reduction of Nb(IV) \rightarrow Nb(III), although the linear increase in peak currents as a function of EDTA concentration was remarked upon (Das Graças Gomes and Franco, 1995). Unfortunately, background voltammograms were not obtained in this study. Similar conclusions were reached by Gomathi (2002), this time looking at the electrochemistry of Fe(III) in EDTA medium. Again, the second redox couple was assigned to the redox of an Fe-EDTA complex, without any comment on the appearance of the EDTA background itself. Other workers studying chromium electrochemistry in EDTA did not observe this redox couple, although this may have been due to the higher pH value of 5.7 at which their experiments were conducted (Bae *et al.*, 2002).

It is the earlier literature which provides the more painstaking investigations of the electrochemical reaction observed in EDTA. One such study suggested that EDTA molecules themselves underwent irreversible oxidation to a radical form within the

potential range in question (Johnson *et al.*, 1972). This process was proposed to occur according to the following reaction scheme:



This proposal, however, does not explain the presence of a redox *couple*, since the evolution of CO₂ makes this an irreversible oxidation process. Also, our observation of the redox couple at Ce concentrations far exceeding that of EDTA makes the redox of protonated EDTA molecules an unlikely explanation.

The hypothesis that perhaps best reconciles the conflicting evidence on this redox couple is one that was put forward by P. R. Rowland in 1968, which makes the suggestion that EDTA serves to depassivate and clean the Pt electrode surface, thus increasing the effective surface area and affecting the rates and reaction potentials of intrinsic electrode processes, such as hydrogen evolution. This phenomenon, which later came to be known as “Rowland’s Effect,” has been further investigated and found to greatly increase the rate of hydrogen evolution at Pt electrodes, and to cause its occurrence at significantly less negative potentials (Tunold *et al.*, 1995). This research further suggested that the mechanism of this effect was through the formation of stable adsorbed Pt-EDTA complexes, which formed preferentially to oxides at the Pt surface. The removal of surface oxides in this manner was suggested to increase the Pt surface area available for the reaction of hydrogen. It was further proposed that the presence of EDTA increased the amount of hydrogen that was weakly bonded to Pt, resulting in the decreased overpotentials observed. These researchers concluded that the EDTA thus adsorbed was not itself electroactive, in contradiction to the previous study discussed

above. What is interesting is that these researchers conducted their studies in basic solution, while the redox couple we observed only appeared at pH values lower than 3 (Figure 4.27). The observation of this couple at low pH values actually provides much stronger support for its suggested identity as a hydrogen redox phenomenon. Additionally, it is quite interesting to note that a similar redox couple, also centered at approximately -0.5 V, was observed at a pH of 2 at the Pt electrode in NTA medium (Figure 4.19). A similar observation was not made in the Pt/citrate experimental system (Figure 4.21). These data strongly suggest that the underlying redox process is one which involves hydrogen at a Pt electrode surface activated through stable interaction with adsorbed aminopolycarboxylate molecules. However, the diffusion-controlled currents observed for this redox couple in our experiments are not consistent with an adsorption/desorption process of hydrogen, where the redox peaks would be expected to appear at approximately equal potentials.

In conclusion, the observation of a redox couple occurring at similar potentials in both the EDTA backgrounds and the rare earth voltammograms seems to support its origin as a redox process of EDTA. However, these currents remained even when all of the EDTA in solution could be assumed to have bound to the Ce present at a metal:ligand ratio of 4:1. Also, a redox couple appeared in a very similar potential region in both the Ce/NTA and NTA background voltammograms at the Pt electrode in strongly acidic conditions. Thus, if the couple is due neither to the redox reaction of cerium nor to that of EDTA, it is possible that it arises from the enhanced adsorption/desorption of hydrogen at a Pt electrode surface rendered catalytically more active by adsorbed EDTA or a Ce-EDTA complex in a low pH version of "Rowland's Effect."

CHAPTER 5

CONCLUSIONS

The acid study utilized the technique of cyclic voltammetry to investigate the electrochemical behavior of the Ce(IV)/Ce(III) redox couple as a function of sulfuric acid concentration and the composition of the working electrode. In light of the disagreements found in the literature, the goal of this study was to clearly identify optimum conditions for observation of this redox couple by evaluating its reversibility and its adequate resolution from background currents. It was determined that solution conditions favoring a well-resolved, reversible Ce(IV)/Ce(III) system were optimized in the region of 0.1 M sulfuric acid concentration (pH = 1.0) for all three electrodes used in the study (Au, Pt, and GC). The most reversible redox couple in the study was that observed at the GC working electrode in 0.1 M H₂SO₄, with a peak potential separation of 112 mV. The relative inertness of the GC electrode also provided a potential window free from background currents due to electrode reactions. Both the oxidation and the reduction peak currents at the GC electrode showed a strong linear relationship with the square root of the experimental scan rate (R^2 values of 0.992 and 0.9993, respectively), indicating a diffusion-controlled redox process. An equally linear correlation was not observed at either of the metal electrodes, revealing some degree of kinetic limitation on the flux of reactive cerium species to and from their surfaces. This may be due to the

oxide layer present at the surface of the Au and Pt electrodes, and the possibility of adsorption effects on the diffusion of electroactive species. Although the cerium redox couple at the Au electrode in 0.1 M H₂SO₄ was less reversible than that obtained at GC, the reversibility at the Au electrode was least affected by the changes in acid concentration, with a small increase in ΔE_p from 0.187 to 0.248 V. The Au electrode also provided the best resolution from oxygen evolution currents, although this advantage was counteracted by the interference of the gold oxide reduction current with the reaction of Ce(IV) → Ce(III). Experiments conducted at both the Au and GC working electrodes yielded better results than those at Pt, which was the most negatively affected by the increase in acid concentration, provided the least separation from background currents, and demonstrated the poorest reversibility of all three electrodes at all acid concentrations investigated. These observations are interesting to note, since a majority of the literature on cerium electrochemistry describes experiments conducted at Pt working electrodes. Cyclic voltammetry in 0.1 M HNO₃ yielded comparable results to those obtained in 0.1 M H₂SO₄, but demonstrated an undesirable positive shift of the redox couple on the order of 100 mV. Thus, the acid study revealed that while acid concentration is a very significant experimental parameter, it is the choice of the working electrode that dictates the degree of influence exerted by the solution environment.

The pH study was designed to evaluate Ce(IV)/Ce(III) redox behavior as pH was increased from the optimum value of 1.0. Experiments carried out at all three working electrodes in 0.1 M K₂SO₄ revealed that pH, and not ionic strength, was the important solution variable in the electrochemical study of cerium. The purpose of the pH study was, therefore, to assess the pH range available for the observation of Ce

electrochemistry at each working electrode. The data obtained in this study indicated that while the increase of solution pH above 1.0 precluded the observation of Ce(IV)/Ce(III) electrochemistry at the Au and Pt working electrodes, resolution of the couple was possible at GC throughout the entire pH range investigated (1.0 to 6.1). Again, the relatively inert character of the GC surface provided a clear background with no interfering oxide currents. It was interesting to note that the redox peak potential separation at GC increased significantly as pH went up, due to the approximately 1.3 V shift of the Ce(IV) reduction peak in the negative potential direction. A hypothesis consistent with this observation is that the complexation of Ce(IV) with the increased concentrations of SO_4^{2-} present at higher pH leads to the formation of the $\text{Ce}(\text{SO}_4)_3^{2-}$ complex, which may require more negative potentials to displace the three sulfate anions from the metal prior to its reduction.

The complexation study was an attempt to exploit the stabilizing abilities of strongly complexing ligands to shift the Ce(IV)/Ce(III) redox couple to a potential range more readily accessible to the Au, Pt, and GC working electrodes, where the interferences of aqueous oxidation currents would be minimized. Cyclic voltammetry on the cerium system in NTA and citrate at all three electrodes met with varying degrees of failure, since no clear redox couple could be discerned from background currents in these media. The Pt/citrate experiment was the only exception, although observation of the redox couple was limited to pH values below 6, with a significant decrease in reversibility above pH 2. Experiments in EDTA as the complexing medium were similarly unsuccessful at both the Au and GC working electrodes.

It was the use of the Pt electrode in conjunction with EDTA that yielded the best results of all the experimental solution/electrode systems evaluated in the complexation study. The advantages of the Pt/EDTA combination over the Pt/H₂SO₄ system were clearly demonstrated in the approximately 0.4 V negative potential shift of the Ce(IV)/Ce(III) redox couple in EDTA. Most importantly, this shift of the redox couple was not accompanied by a similar negative shift of the water oxidation reaction. Thus, the EDTA solution system at Pt accomplished the goal of moving cerium redox chemistry to a more easily-accessed potential range while retaining a high overpotential for O₂ evolution. The redox couple was also well-defined and was only slightly less reversible than the couples observed in 0.1 M H₂SO₄ at the various electrodes. Perhaps the most significant observation made in this study was the resistance of redox couple reversibility to changes in the pH of the EDTA medium at the Pt electrode. A clearly discernible, reversible redox couple was observed throughout an experimental pH range of ~3 through 10. The pH study conducted in bisulfate/sulfate medium demonstrated a requirement of low pH for the observation of cerium electrochemistry. In contrast, the use of EDTA removed this experimental pH constraint. This advantage of using EDTA solutions may arise from "Rowland's Effect," which is the ability of EDTA to hinder the formation of oxide layers on Pt electrodes. These oxides may have been the cause of cerium redox inhibition in the sulfate solutions of higher pH.

There are many possible paths that may be taken with regard to future work on this project. There are, for example, other complexing ligands (*e.g.* DTPA⁵⁻) which form stable complexes with cerium, with effects on Ce(IV)/Ce(III) electrochemistry that have yet to be evaluated. Ultimately, however, the limits of such experiments are already set

by the inevitable reaction of the aqueous medium itself at sufficiently positive or negative potentials. It is at this point that research into new electrolytic media, such as ionic liquids, becomes so valuable. Such future work may provide potential windows that have remained unattainable in aqueous solution, despite all efforts at optimizing the electrode and solution characteristics.

Since the ultimate application of these research results is the electrochemical separation of solution species by potential control and selective chelation, the modification of the working electrode surface with conductive polymer membranes may better achieve such objectives. If the electrode were further modified by the dispersion of metal particles (*e.g.* Au, Pt, Pd) throughout the polymer membrane, and metal-bound chelating ligands were then added to this electrode/polymer/metal construction, it may be possible to control potential and complexation even more effectively, resulting in enhanced separation of target solution species.

REFERENCES

- Abbaspour, A. and Mehrgardi, M. A. "Electrocatalytic Activity of Ce(III)-EDTA Complex Toward the Oxidation of Nitrite Ion" *Talanta* **2005**, *67*, 579-584.
- Aspinall, H. C. *Chemistry of the f-Block Elements*; Gordon and Breach Science: the Netherlands, 2001.
- Bae, C. -H.; Roberts, E. P. L.; Dryfe, R. A. W. "Chromium Redox Couples for Application to Redox Flow Batteries" *Electrochim. Acta* **2002**, *48*, 279-287.
- Baes, C. F. and Mesmer, R. E. *The Hydrolysis of Cations*; Wiley: New York, 1976.
- Bard, A. J. and Faulkner, L. R. *Electrochemical Methods: Fundamentals and Applications*; Wiley: New York, 2001.
- Bauer and Glaessner, "Über das Electromotorische Verhalten der Oxyde des Cers" *Z. Elektrochem.* **1903**, *9*, 534-539.
- Benziger, J. B.; Pascal, F. A.; Bernasek, S. L.; Soriaga, M. P.; Hubbard, A. T. "Characterization of Platinum Electrodes by Infrared Spectroscopy" *J. Electroanal. Chem.* **1986**, *198*, 65-80.
- Bhat, T. R. and Radhamma, D. "Studies on EDTA Complexes: Part III – Iron(III)-EDTA & Cerium(IV)-EDTA Systems" *Indian J. Chem.* **1965**, *3*, 151-154.
- Bilal, B. A. and Müller, E. "Thermodynamic Study of Ce^{4+}/Ce^{3+} Redox Reaction in Aqueous Solutions at Elevated Temperatures: 1. Reduction Potential and Hydrolysis Equilibria of Ce^{4+} in $HClO_4$ Solutions" *Z. Naturforsch.* **1992**, *47a*, 974-984.
- Bishop, E. and Cofré, P. "Anodic Generation of Cerium(IV). Charge-Transfer Kinetic Parameters and Conditional Potentials at Platinum, Gold and Glassy Carbon" *Analyst* **1981**, *106*, 316-322.
- Bonewitz, R. A. and Schmid, G. M. "Oxygen Adsorption on Gold and the Ce(III)/Ce(IV) Reaction" *J. Electrochem. Soc.* **1970**, *117*, 1367-1372.
- Bouissieres, G. and Legoux, Y. "Formation d'Amalgames d'Éléments *cis*- et *trans*-Uraniens" *B. Soc. Chim. Fr.* **1965**, *2*, 386-388.

Broeders, C. H. M.; Broeders, I.; Kessler, G.; Kiefhaber, E. Recent Neutron Physics Investigations for the Back End of the Nuclear Fuel Cycle. In *Nuclear Methods for Transmutation of Nuclear Waste*; Khankhasayev, M. K., Kurmanov, Z. B., Plendl, H.S., Eds.; World Scientific: Singapore, 1997; pp 50-59.

Chemical Pretreatment of Nuclear Waste for Disposal; Schulz, W. W., Horwitz, E. P., Eds.; Plenum: New York, 1994.

Chung, Y. H. and Park, S. - M. "Destruction of Aniline by Mediated Electrochemical Oxidation with Ce(IV) and Co(III) as Mediators" *J. Appl. Electrochem.* **2000**, *30*, 685-691.

Chuveleva, E. A.; Peshkov, A. S.; Kharitonov, O. V.; Firsova, L. A. "Separation of Curium and Americium Traces by Displacement Complexing Chromatography in the Presence of Separating Ions: 1. The Use of Nitrilotriacetic Acid Solution as Eluent" *Radiochemistry* **1999**, *41*, 465-467.

Chuveleva, E. A.; Peshkov, A. S.; Kharitonov, O. V.; Firsova, L. A. "Separation of Curium and Americium Traces by Displacement Complexing Chromatography in the Presence of Separating Ions: 2. Influence of the Amount of Cadmium Ions and Modes of their Introduction in the System on the Efficiency of Separation of Curium and Americium" *Radiochemistry* **1999**, *41*, 468-470.

Connick, R. E. and Mayer, S. W. "Ion Exchange Measurements of Activity Coefficients and Association Constants of Cerous Salts in Mixed Electrolytes" *J. Am. Chem. Soc.* **1951**, *73*, 1176-1179.

CRC Handbook of Chemistry and Physics; 82nd Ed. Lide, D. R., Ed.; CRC: Boca Raton, FL, 2001.

Das Graças Gomes, M. and Franco, D. W. "Electrochemical Behavior of Nb^V-EDTA and Nb^V-Citrate Systems in Aqueous Solutions" *Electroanal.* **1995**, *7*, 778-781.

David, F.; Peretrukin, V. F.; Maslennikov, A. G.; Fourest, B. "Separation of Californium from Actinides and Lanthanides in Aqueous Solution by Electrochemical Formation of Amalgams" *Radiochim. Acta* **1990**, *50*, 151-154.

Desideri, P. G. "The Polarographic Behavior of Cerium(IV) and Cerium(IV)-Cerium(III) System in Sulphuric Media. A Direct Determination of Cerium(IV)" *J. Electroanal. Chem.* **1961**, *2*, 39-45.

Duke, F. R. and Parchen, F. R. "The Kinetics of the Ce(IV)-Ce(III) Exchange Reaction in Perchloric Acid" *J. Am. Chem. Soc.* **1956**, *78*, 1540-1543.

Fang, B.; Iwasa, S.; Wei, Y.; Arai, T.; Kumagai, M. "A Study of the Ce(III)/Ce(IV) Redox Couple for Redox Flow Battery Application" *Electrochim. Acta* **2002**, *47*, 3971-3976.

Ferro, S. and De Battisti, A. "Electrochemistry of the Aqueous Ceric/Cerous Redox Couple at Conductive Diamond and Gold Electrodes" *Phys. Chem. Chem. Phys.* **2002**, *4*, 1915-1920.

Fronæus, S. and Östman, C. O. "The Mechanism of the Exchange Reaction between Cerium(III) and Cerium(IV) at Platinum Surfaces" *Acta Chem. Scand.* **1956**, *10*, 769-778.

Galus, Z. and Adams, R. N. "The Investigation of the Kinetics of Moderately Rapid Electrode Reactions Using Rotating Disk Electrodes" *J. Phys. Chem.* **1963**, *67*, 866-871.

Gilroy, D. "Oxide Formation in the Oxygen Evolution Region at Pt Electrodes in $M\text{H}_2\text{SO}_4$ " *J. Electroanal. Chem.* **1977**, *83*, 329-339.

Goffart, G. "Titrimetrie des Ions Cereux par le Permanganate" *Anal. Chim. Acta* **1948**, *2*, 140-145.

Gomathi, H. "Chemistry and Electrochemistry of Iron Complexes" *B. Electrochem.* **2000**, *16*, 459-465.

Greef, R. and Aulich, H. "The Kinetics of the Cerous-Ceric Redox Reaction at a Platinum Electrode" *J. Electroanal. Chem.* **1968**, *18*, 295-307.

Hale, W. H. and Lowe, J. T. "Rapid, Gram-Scale Separation of Curium from Americium and Lanthanides by Cation Exchange Chromatography" *Inorg. Nucl. Chem. Letters* **1969**, *5*, 363-368.

Hammond, J. S. and Winograd, N. "XPS Spectroscopic Study of Potentiostatic and Galvanostatic Oxidation of Pt Electrodes in H_2SO_4 and HClO_4 " *J. Electroanal. Chem.* **1977**, *78*, 55-69.

Hardwick, T. J. and Robertson, E. "Ionic Species in Ceric Perchlorate Solutions" *Can. J. Chem.* **1951**, *29*, 818-827.

Hardwick, T. J. and Robertson, E. "Association of Ceric Ions with Sulphate (A Spectral Study)" *Can. J. Chem.* **1951**, *29*, 828-837.

Harris, D. C. *Quantitative Chemical Analysis*; W. H. Freeman: New York, 1999.

Heidt, L. J. and Berestecki, J. "Optical Studies of Cerous Solutions" *J. Am. Chem. Soc.* **1955**, *77*, 2049-2054.

Hobart, D. E.; Samhoun, K.; Peterson, J. R. "Spectroelectrochemical Studies of the Actinides – Stabilization of Americium(IV) in Aqueous Carbonate Solution" *Radiochim. Acta* **1982**, *31*, 139-145.

Johnson, J. W.; Jiang, H. W.; Hanna, S. B.; James, W. J. "Anodic Oxidation of Ethylenediaminetetraacetic Acid on Pt in Acid Sulfate Solutions" *J. Electrochem. Soc.* **1972**, *119*, 574-580.

Juodkazis, K.; Juodkazytė, J.; Šebeka, B.; Lukinskas, A. "Cyclic Voltammetric Studies on the Reduction of a Gold Oxide Surface Layer" *Electrochem. Commun.* **1999**, *1*, 315-318.

Kiekens, P.; Steen, L.; Donche, H.; Temmerman, E. "Kinetics of Ce(IV) Reduction at Gold, Carbon and Iridium Electrodes" *Electrochim. Acta* **1981**, *26*, 841-845.

Kriksunov, L. B.; Bunakova, L. V.; Zabusova, S. E.; Krishtalik, L. I. "Anodic Oxygen Evolution Reaction at High Temperatures in Acid Solutions at Platinum" *Electrochim. Acta* **1994**, *39*, 137-142.

Kunz, A. H. "The Reduction Potential of the Ceric-Cerous Electrode" *J. Am. Chem. Soc.* **1931**, *53*, 98-102.

Liu, Y.; Xia, X.; Liu, H. "Studies on Cerium (Ce⁴⁺/Ce³⁺)-Vanadium(V²⁺/V³⁺) Redox Flow Cell – Cyclic Voltammogram Response of Ce⁴⁺/Ce³⁺ Redox Couple in H₂SO₄ Solution" *J. Power Sources* **2004**, *130*, 299-305.

Loo, B. H. and Furtak, T. E. "Intrinsic Heterogeneity in the Multiple States of Adsorbed Hydrogen on Polycrystalline Platinum" *Electrochim. Acta* **1980**, *25*, 505-508.

Maeda, Y.; Sato, K.; Ramaraj, R.; Rao, T. N.; Tryk, D. A.; Fujishima, A. "The Electrochemical Response of Highly Boron-Doped Conductive Diamond Electrodes to Ce³⁺ Ions in Aqueous Solution" *Electrochim. Acta* **1999**, *44*, 3441-3449.

Malinina, E. A.; Martynenko, L. I.; Pechurova, N. I.; Spitsyn, V. I. "The Reaction of Ce(IV) with Ethylenediaminetetraacetic Acid in the Presence of Nitrate" *Russ. Chem. B+* **1969**, *18*, 1935-1936.

Martell, A. E. and Smith, R. M. *Critical Stability Constants*, Vols. 1-6; Plenum: New York, 1974-1989.

Maverick, A. W. and Yao, Q. "The Cerium(IV)/Cerium(III) Electrode Potential in Hydrochloric Acid Solution" *Inorg. Chem.* **1993**, *32*, 5626-5628.

Miller, F. J. and Zittel, H. E. "Voltammetry of Ce(IV), Mn(VII), Cr(VI) and V(V) with the Pyrolytic Graphite Electrode" *J. Electroanal. Chem.* **1964**, *7*, 116-122.

Morita, M.; Kitamura, S.; Ishikawa, M.; Matsuda, Y. "Immobilization of a Cerium Redox Mediator on a Glassy Carbon Electrode for Electroorganic Reactions" *Electroanal.* **1996**, *8*, 826-830.

Morris, D. E. "Redox Energetics and Kinetics of Uranyl Coordination Complexes in Aqueous Solution" *Inorg. Chem.* **2002**, *41*, 3542-3547.

Morris, D. E. and Hobart, D. E. "Voltammetric Investigation of the Cerium(IV/III) Redox Couple in Aqueous Carbonate Media" *Lanthanide Actinide* **1987**, *2*, 91-103.

National Research Council. Nuclear Wastes: Technologies for Separations and Transmutation; National Academy: Washington, D.C., 1996.

Newton, T. W. and Arcand, G. M. "A Spectrophotometric Study of the Complex Formed between Cerous and Sulfate Ions" *J. Am. Chem. Soc.* **1953**, *75*, 2449-2453.

Noddak, W. and Bruckl, A. "Die Reduktionspotentiale der Dreiwertigen Erden" *Angew. Chem.* **1937**, *50*, 362-365.

Noyes, A. A. and Garner, C. S. "Strong Oxidizing Agents in Nitric Acid Solution. I. Oxidation Potential of Cerous-Ceric Salts" *J. Am. Chem. Soc.* **1936**, *58*, 1265-1268.

Nzikou, J. M.; Arousseau, M.; Lopicque, F. "Electrochemical Investigations of the Ce(III)/Ce(IV) Couple Related to a Ce(IV)-Assisted Process for SO₂/NO_x Abatement" *J. Appl. Electrochem.* **1995**, *25*, 967-972.

Paulenova, A.; Creager, S. E.; Navratil, J. D.; Wei, Y. "Redox Potentials and Kinetics of the Ce³⁺/Ce⁴⁺ Redox Reaction and Solubility of Cerium Sulfates in Sulfuric Acid Solutions" *J. Power Sources* **2002**, *109*, 431-438.

Penneman, R. A. and Keenan, T. K. The Radiochemistry of Americium and Curium; Subcommittee on Radiochemistry, National Academy of Sciences – National Research Council, 1960.

Randle, T. H. and Kuhn, A. T. "Kinetics and Mechanism of the Cerium(IV)/Cerium(III) Redox Reaction on a Platinum Electrode" *J. Chem. Soc., Faraday Trans. I* **1983**, *79*, 1741-1756.

Ross, P. N. Jr. "Hydrogen Chemisorption on Pt Single Crystal Surfaces in Acidic Solutions" *Surface Science* **1981**, *102*, 463-485.

Rowland, P. R. "Electrolytic Separation Factor of Protium and Deuterium" *Nature* **1968**, *218*, 945-946.

Sacchetto, G. A.; Pastore, P.; Favaro, G.; Fiorani, M. "Liquid Chromatographic Determination of Non-Volatile Nitrosamines by Post-Column Redox Reactions and Voltammetric Detection at Solid Electrodes. Behavior of the Ce(IV)-Ce(III) Couple at Gold, Platinum and Glassy Carbon Electrodes and Suitability of the Ce(IV) Reagent" *Anal. Chim. Acta* **1992**, *258*, 99-108.

Salvatore, F. and Vasca, E. "Oxidation of Cerium(III) in Aqueous Carbonate Solutions" *J. Coord. Chem.* **1990**, *21*, 237-246.

Sherrill, M. S.; King, C. B.; Spooner, R. C. "The Oxidation Potential of Cerous-Ceric Perchlorates" *J. Am. Chem. Soc.* **1943**, *65*, 170-179.

Shibata, S. and Sumino, M. P. "The Effect of Anions on the Electrochemical Reduction of Thick Oxide Films on Platinum Electrode in Acidic Aqueous Solutions" *Electrochim. Acta* **1981**, *26*, 517-523.

Sillén, L. G. and Martell, A. E. Stability Constants of Metal-Ion Complexes; The Chemical Society: London, 1964.

Smith, G. F. and Getz, C. A. "Cerate Oxidimetry. Theoretical Considerations and Determination of Approximate Electrode Reference Potentials" *Ind. Eng. Chem. Anal. Ed.* **1938**, *10*, 191-195.

Spedding, F. H. and Jaffe, S. "Conductances, Solubilities and Ionization Constants of Some Rare Earth Sulfates in Aqueous Solutions at 25°" *J. Am. Chem. Soc.* **1954**, *76*, 882-884.

Spedding, F. H. and Jaffe, S. "Conductances, Transference Numbers and Activity Coefficients of Some Rare Earth Perchlorates and Nitrates at 25°" *J. Am. Chem. Soc.* **1954**, *76*, 884-888.

Stokely, J. R.; Baybarz, R. D.; Peterson, J. R. "Formal Potential of Bk(IV)-Bk(III) Couple in Several Media" *J. Inorg. Nucl. Chem.* **1972**, *34*, 392-393.

Tunold, R.; Brun, J.; Johansen, B.; Jakšić, M. M. "Effect of Ethylenediaminetetraacetic Acid (Rowland's Effect) on Electrochemical Behavior of Transition Metals and Electrocatalysis of Hydrogen Evolution Reaction: Rowland's Effect on Noble Metals" *Russ. J. Electrochem+* **1995**, *31*, 638-648.

Vickery, R. C. "Lanthanone Complexes with Ethylenediaminetetra-acetic Acid. Part II" *J. Chem. Soc.* **1952**, *Feb*, 421-425.

Vijayarathi, T.; Srinivasan, R. K.; Noel, M. "A Comparative Study of Two Stage Electrochemical Oxidation of Anthracene, Naphthalene and Benzene Using Ce⁴⁺/Ce³⁺ Redox System" *B. Electrochem.* **1999**, *15*, 293-297.

Vijayarathi, T.; Velayutham, D.; Noel, M. "Influence of Aromatic Reactants and Products Involved in the Two Stage Electrochemical Oxidation on the Voltammetric Behaviour of Ce(IV)/Ce(III) Redox Couple" *J. Appl. Electrochem.* **2001**, *31*, 979-986.

Wadsworth, E.; Duke, F. R.; Goetz, C. A. "Present Status of Cerium(IV)-Cerium(III) Potentials" *Anal. Chem.* **1957**, *29*, 1824-1825.

Wheelwright, E. J.; Spedding, F. H.; Schwarzenbach, G. "The Stability of the Rare Earth Complexes with Ethylenediaminetetraacetic Acid" *J. Am. Chem. Soc.* **1953**, *75*, 4196-4201.

Wheelwright, E. J.; Roberts, F. P.; Bray, L. A.; Ritter, G. L.; Bolt, A. L. USAEC Report BNWL-SA-1492 1968.

Wiberg, K. B. and Ford, P. C. "Ceric Ion Equilibrium in Aqueous Acetic Acid" *Inorg. Chem.* **1968**, *7*, 369-373.

VITA

Graduate College
University of Nevada, Las Vegas

Sandra Elias Elkouz

Home Address:

3155 Mann St.
Las Vegas, Nevada 89146

Degrees:

Associate of Science, General Science, 2001
Community College of Southern Nevada

Bachelor of Science, Chemistry, 2004
University of Nevada, Las Vegas

Thesis Title: Complexation and Electrode Effects on the Electrochemical Behavior of the Cerium(IV)/Cerium(III) Redox Couple

Thesis Examination Committee:

Chairperson, Dr. David W. Hatchett, Ph. D.
Committee Member, Dr. Spencer Steinberg, Ph. D.
Committee Member, Dr. Kenneth Czerwinski, Ph. D.
Graduate College Representative, Dr. Shawn Gerstenberger, Ph. D.